Spring 2005

Application of self-assembled ultrathin film coatings to stabilize enzyme encapsulation and activity in alginate microspheres

Rohit Srivastava

APPLICATION OF SELF-ASSEMBLED ULTRATHIN FILM COATINGS TO STABILIZE ENZYME ENCAPSULATION AND ACTIVITY IN ALGINATE MICROSPHERES

By
Rohit Srivastava, BE

A Dissertation Presented in Partial Fulfillment
of the Requirements for the Degree
Doctor of Philosophy

COLLEGE OF ENGINEERING AND SCIENCE
LOUISIANA TECH UNIVERSITY

May 2005

LOUISIANA TECH UNIVERSITY

THE GRADUATE SCHOOL

4-1-05
Date

We hereby recommend that the dissertation prepared under our supervision by ROHIT SRIVASTAVA entitled APPLICATION OF SELF-ASSEMBLED ULTRATHIN FILM COATINGS TO STABILIZE ENZYME ENCAPSULATION AND ACTIVITY IN ALGINATE MICROSPHERES be accepted in partial fulfillment of the requirements for the Degree of DOCTOR OF PHILOSOPHY

Supervisor of Dissertation Research

Head of Department
Biomedical Engineering
Department

Recommendation concurred in:

Advisory Committee

Approved:
Director of Graduate Studies

Approved:
Dean of the Graduate School

Dean of the College

GS Form 13
(5/03)

ABSTRACT

Alginate-based hydrogels have been used for the encapsulation of a variety of materials, including enzymes, proteins, and cells for a wide range of applications from drug delivery to biosensors and bioreactors. However, due to the high porosity of the matrix, it has been increasingly difficult to retain macromolecules inside the alginate matrix, leading to loss in functionality over time. In an effort to improve the stability for long-term biosensor use, this work investigated layer-by-layer self-assembly as a potential technique to provide a diffusion barrier to an encapsulated macromolecule. Alginate microspheres (~2-50μm radius) were fabricated using an emulsification technique, and were ionically crosslinked with calcium ions and used for the encapsulation of macromolecules including dextran and the enzyme glucose oxidase. Stepwise-assembled polyelectrolyte nanofilm coatings of different composition and thickness were then formed on the microspheres, and the loss of enzyme was monitored over one week. The total loss of encapsulated material was reduced to less than 15% with the application of a single {PAH/PAA} coating, in comparison to ~50% loss observed with uncoated and {PDDA/PSS}-coated microspheres. The activity of the encapsulated enzyme was also tested over twelve weeks, and it was found that {PAH/PSS}-coated spheres retained more than 84% of their initial activity after twelve weeks, whereas uncoated and {PDDA/PSS}-coated microspheres retained less than 20% of initial activity after twelve weeks. The activity was further stabilized when a chemical conjugation technique with water soluble 1-ethyl-3-(3-dimethylaminopropyl) carbodiimide (EDC) immobilized the

enzyme in the alginate matrix. More than 90% activity retention was observed for all cases. Finally, novel biocompatible coating materials were used to coat the alginate microspheres to slow release and improve biocompatibility. The enzyme was crosslinked to the alginate matrix using EDC-NHSS conjugation techniques. The experimental results showed that the application of single layer thin films to the alginate microspheres was effective in reducing loss of the encapsulated enzyme from the microspheres with more than 80% enzyme retention reported for monolayer coatings and more than 95% enzyme retention for multilayer coatings. The encapsulated enzyme was also found to be highly active (>95% retention of activity) inside the uncoated microspheres and coated microspheres, and the activity results were compared over a period of three months. In vitro cytotoxicity tests were completed using 3T3 cells to determine the "optimum" coating material towards biosensor use. Of the coatings tested, chondroitin sulfate, humic acid, PEG bis(amine), and chitosan coatings were found to be suitable for in vivo testing. These results demonstrate that the simple application of ultrathin film coatings to functional micro-systems can be useful in prolonging the usability of the encapsulated material in those templates, thus leading to improved stability and increased longevity for biosensors and bioreactors.

APPROVAL FOR SCHOLARLY DISSEMINATION

The author grants to the Prescott Memorial Library of Louisiana Tech University the right to reproduce, by appropriate methods, upon request, any or all portions of this Dissertation. It is understood that "proper request" consists of the agreement, on the part of the requesting party, that said reproduction is for his personal use and that subsequent reproduction will not occur without written approval of the author of this Dissertation. Further, any portions of the Dissertation used in books, papers, and other works must be appropriately referenced to this Dissertation.

Finally, the author of this Dissertation reserves the right to publish freely, in the literature, at any time, any or all portions of this Dissertation.

Author 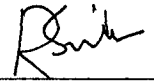

Date 5/10/05

GS Form 14
(5/03)

TABLE OF CONTENTS

LIST OF TABLES

LIST OF FIGURES

ACKNOWLEDGMENTS

I would like to take this opportunity to thank everyone who made this dissertation possible, especially my guide and advisor, Dr. Michael J. McShane, who supported me during all these years and pushed me ever so much to work harder and harder. Thanks are also due to Dr. James Palmer and Dr. David Mills for all their support and guidance. I would also like to thank my colleagues Jonathan Quincy Brown and Erich Stein for their valuable help during this project. Dr Huiguang Zhu is gratefully acknowledged for all the advice during the course of this project. The entire BioMINDS lab at IfM has been a source of inspiration for me during these five years at Tech. Finally, I would like to express my gratitude to my parents and brother for showing me the way to succeed in life.

I would like to dedicate this dissertation to the loving memory of my father, without whose dream, this achievement would never have been possible.

CHAPTER 1

INTRODUCTION

Diabetes mellitus is a debilitating disease that currently inflicts 18.2 million people in the United States (6.3% of the population), with 1.3 million new cases diagnosed each year in persons aged 20 and over.[1] The disease is also a major world health problem. It is estimated that there are over 170 million diabetics worldwide.[2] Worse still, incidence of this disease has risen by an alarming 11% of the last five years and a further doubling of the cases is predicted in the next 25 years. Glucose is the main circulating carbohydrate in the body and is the body's main energy source. In normal individuals, the concentration of glucose in blood is very tightly regulated, usually in the range between 80-120 mg/dL. Diabetes is a metabolic disorder in which insulin, the hormone that facilitates the uptake of glucose into the skeletal muscle and adipose tissue, cannot properly perform its role and consequently, blood glucose can elevate to abnormal concentrations ranging from 300-700 mg/dL (hyperglycaemia) or can fall below 45 mg/dL (hypoglycaemia). Much of the burden of the disease to the patient and to the health care providers is due to the long term tissue complications that affect both the small blood vessels (microangiopathy, causing eye, kidney and nerve damage) and the large blood vessels (causing accelerated atherosceloris, with increased rates of coronary heart disease, peripheral vascular disease and stroke).[3,4] There is good evidence that the

chronic complications of diabetes are related to the duration and severity of hyperglycaemia.[5] With careful management, these complications can be delayed and even prevented, although there is inadequate control of glycaemia with prescribed injections of insulin subcutaneously, and blood glucose levels can swing between high and low in an unpredictable manner (Figure 1.1).[3] This process is an example of an "open-loop" insulin delivery system, which is difficult to maintain. In addition, the recommendation of a minimum of four glucose measurements per day is not adhered to by most patients, and intermittent testing may miss episodes of hyper- and hypoglycaemia.[6] An alternate improved solution to this problem will be to devise a "closed-loop" system, which will use a self-adapting insulin infusion device with feedback from a continuously monitoring glucose biosensor that would sense the need for dispensing insulin at the correct rate and time.[7]

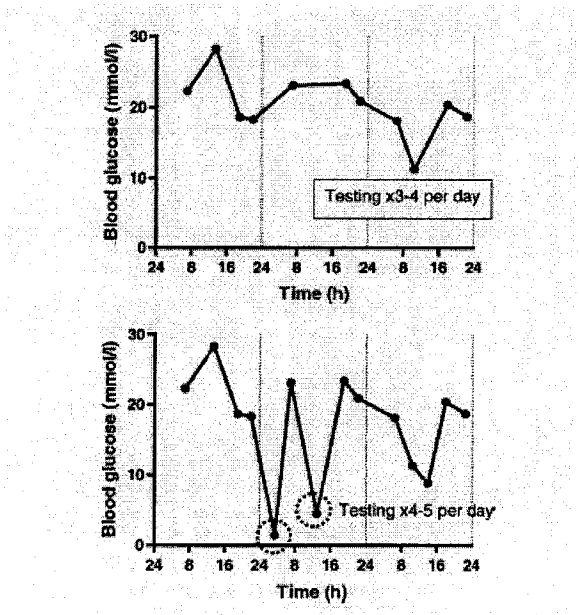

Figure 1.1. Intermittent glucose testing four or five times daily over a three day period in a type 1 diabetic patient demonstrates wide and unpredictable swings in blood glucose concentration (bottom panel). With reduced testing frequency, the episodes of hypoglycaemia are missed (circled).[3]

In this regard, two different types of glucose sensors need to be distinguished: the minimally-invasive and the non-invasive.[8] Minimally-invasive methods typically measure the glucose concentration in the interstitial fluid of the skin or in the subcutis. The sensor has to be either placed in the tissue to be exposed to interstitial fluid, or the fluid has to be transferred outside the body. The advantage of this approach is that glucose can be measured specifically and in absolute concentrations. The main disadvantage of minimally invasive glucose sensors is the necessity to break the skin barrier.[9] Penetration of the skin always carries the risk of local infection and inflammatory reaction. Therefore, such sensors have to be attached to a different skin location each time. On the other hand, most non-invasive approaches have been carried out using optical glucose sensors that are based on the absorption approach, the spectroscopic approach, or the scattering approach. The following section discusses some of the commercially available glucose monitoring sensors.

1.1 Commercial Glucose Monitoring Techniques

The ideal *in vivo* glucose monitoring technology should therefore be non-invasive (to improve compliance), or minimally invasive, and continuous (to capture all blood glycaemic variations at all times of the day). This technology will also provide the patients with the information required to optimize insulin therapy and metabolic control, which is known to drastically reduce the risk of chronic complications.[3] The most investigated technology for *in vivo* glucose monitoring is based on subcutaneously implanted amperometric enzyme electrodes, and a device is commercially available and used in clinical practice.[10] The continuous monitoring system (CGMS^{TM}) from Minimed (Northridge, CA) is based on the glucose oxidase enzyme platform. However, the current

version is an entirely retrospective device wherein only an authorized professional is permitted to use the collected data subsequent to sensor removal after three days. Although, this provides the patient with a delayed glucose profile, the major shortcoming is that it does not provide real-time feedback. Aside from that, the other problems with the device include unpredictable drift and impaired response *in vivo*, which requires repeated calibration using the finger prick method about four times a day. This problem has been attributed to the coating of these sensors with proteins and cells and a wound response, which causes alterations in blood flow and inflammatory cell consumption of glucose. In a recent study, the glucose measurements using the CGMS were compared to those using intermittent testing using the finger prick method (Figure 1.2).[10] It was observed there were many times when episodes of hyper- or hypoglycaemia in these patients were missed by intermittent testing but detected by continuous monitoring method, confirming the clinical utility of this device.

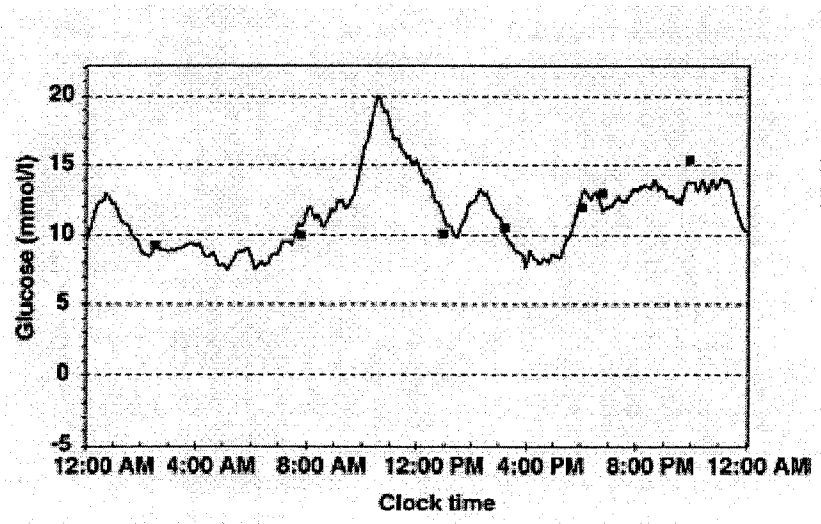

Figure 1.2. Comparison of glucose sensing using the CGMS and intermittent blood glucose monitoring.[3]

Another available technology for glucose sensing in diabetics is using reverse iontophoresis.[11] The GlucoWatch (Cygnus, Inc, San Francisco) uses a small current passed between two skin surface electrodes to draw ions and by electro-endosmosis, glucose-containing interstitial fluid is pulled to the surface into hydrogel pads incorporating a glucose oxidase biosensor. Readings can be taken every 10 minutes, with a single capillary blood calibration. In addition to real time read out, there is a provision to download the data to a computer for later analysis. There are three major difficulties with this sensor. The first is a skin rash due to continuous wearing of this sensor. The second is a long warm up time of three hours, and third is skipping of monitoring periods due to sweating and high activity of the user, and exposure of the unit to cold temperatures.[3] The principle of operation and *in vivo* blood glucose monitoring using the Cygnus GlucoWatch have been shown in Figure 1.3, which demonstrates how the hypoglycaemic glucose level activates the device alarm (starred points). The high and low alarm thresholds are indicated by dashed lines.

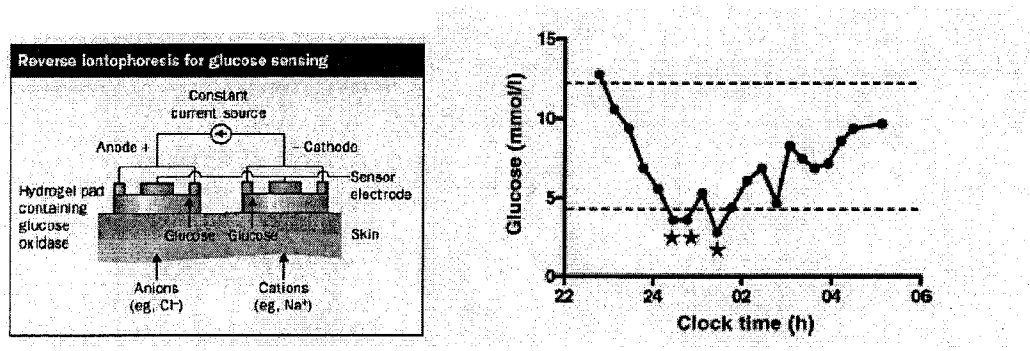

Figure 1.3. Left: Principle of operation of the GlucoWatch; Right: *In vivo* glucose monitoring using the GlucoWatch.[3]

The third commercial technology in current clinical use is the GlucoDay (Menarini Diagnostics, Italy). It is based on microdialysis system, where a fine hollow

dialysis fiber is implanted in the subcutaneous tissue and perfused with isotonic fluid. Glucose from the tissue diffuses into the fiber and is pumped outside of the body for measurements by an electrochemical sensor. More clinical trials are necessary to assess its clinical potential.[12] Despite considerable effort on the development of an implantable glucose sensor, currently there is no product that takes into account all the problems faced by these other sensors,[13] since there are many parameters that need to be met collectively for the development of an optimized glucose sensor. These parameters include sensor characteristics, such as accuracy, sensitivity, selectivity, linear range and response time. Other critical parameters are reproducibility and reversibility of signal, reproducibility of sensor fabrication, biocompatibility, operational lifetimes at body temperature, and storage stability of the sensor.[14] Thus new approaches to glucose sensing in diabetics are being explored, and fluorescence-based systems are receiving increasing attention, [15] which will be discussed in the next section.

1.2 Fluorescence-Based Glucose Monitoring

Fluorescence-based glucose sensing has the advantages of sensitivity, capability of non-invasive light detection, fast measurement, and the possibility of measuring both fluorescence intensity and lifetimes.[3,15,16] Recent advances in the development of fluorescence glucose sensors have been based on various receptor systems, including those that employ synthetic receptors (i.e., boronic acid derivatives), as well as naturally occurring ones (i.e., enzymes, the lectin concanavalin A (Con A), and sugar binding proteins), and those based on the rational design of genetically engineered proteins (i.e., GBP).[14] These techniques have been discussed in detail in the next chapter. This section presents a brief description of various techniques and their advantages and disadvantages.

Synthetic boronic acid derivatives have been used as receptors in the development of glucose sensing systems.[17] They are able to complex glucose rapidly and reversibly through covalent interactions, but boronic acid based fluorescence sensors are not suitable for glucose sensing in immobilized form, primarily due to the low water solubility of the system, and secondly due to the limited sensitivity achieved with such systems. In addition, the short excitation and emission wavelengths for most of these sensors make developing a final product to be used with biological tissues difficult. On the other hand, enzymes have been widely employed in glucose sensing primarily due to their high selectivity, although there is dependence on local oxygen levels and high costs associated with the cofactors required for some sensors.[18] Thus, intense efforts have been spent on the glucose- and mannose-specific binding protein Con A. The advantage of using Con A for glucose sensing is its independence of oxygen, but the main disadvantage includes it problems with aggregation.[19] The most recent methods of glucose sensing are based on fluorescence resonance energy transfer (FRET) and fluorescence intensity measurements.[14] However, problems remain in fabrication, leaching stability, and reversibility. Sugar binding proteins work on the principle of the protein conformational change upon binding to the corresponding target ligand. This process may involve incorporating reporter groups into the protein structure, which respond to the binding of the ligand. A disadvantage of this approach is that it reduces the solubility of the protein and makes *in vivo* measurements difficult.

Thus, there are still a number of limitations that need to be overcome for the development of an ideal glucose sensor.[14] Such a sensor should be able to monitor a wide range of glucose levels quickly and accurately, with a high signal response that is

reproducible and reversible. Its fabrication should be reproducible, and it should have extended lifetimes. In addition, the ideal sensor should also be biocompatible, utilizing nontoxic reagents that will not leach out of the system and be able to function at body temperature. The key parameter for the development of the ideal glucose sensor is the utilization of an advanced glucose recognition element, which would combine high selectivity with high operational and storage stability. Another parameter related to signal transduction is the increase of the detection wavelengths above the "optical window" of the skin to overcome the interference problems and to take advantage of transdermal glucose measurements. In addition, other parameters that need to be taken into account with the *in vivo* glucose monitoring are the issues of correlation of glucose levels in blood and interstitial fluid, sensor stability, selectivity, calibration, and biocompatibility. Techniques for encapsulation of *in vivo* fluorescent sensing assay are in their infancy, at least as far as testing in humans or animals in concerned.[15]

In this regard, efforts toward immobilizing such fluorescence sensing chemistry in a biocompatible polymeric matrix have been pursued to decrease concerns over cytotoxicity of the assay components, protein binding, and diffusion of dye from the area of interest, all of which affect the surrounding tissues as well as the experimental results.[20] However, an optical approach based on transdermally interrogated, intradermally implanted fluorescent glucose transducers with significant advantages over previous methods has been proposed: the "smart tattoo."[21,22,23] These transducers typically comprise hydrogel or polymeric microsphere carriers containing an appropriate fluorescent glucose assay, which are implanted in the skin and may be queried across the skin using light as shown in Figure 1.4 and Figure 1.5.[24,25]

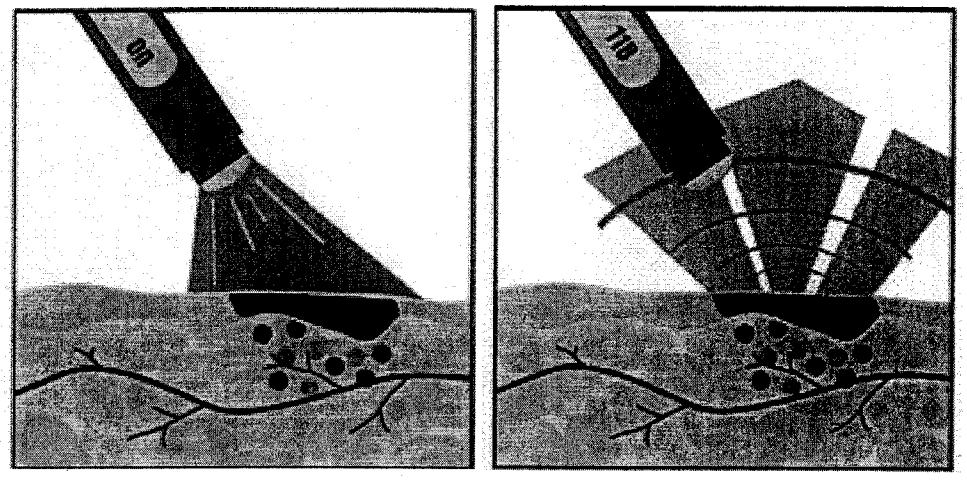

Figure 1.4. Illustration of "smart tattoo" concept.[24]

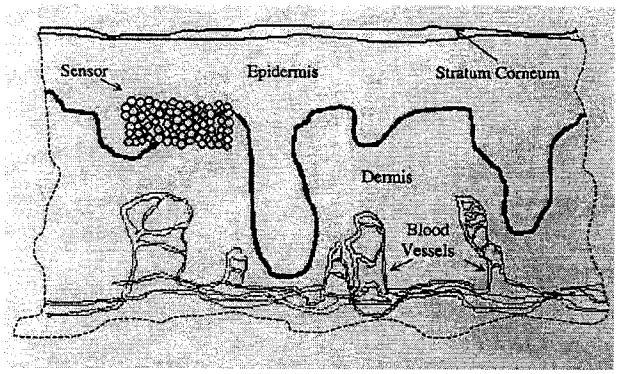

Figure 1.5. Crosssectional view of the human skin tissue. A layer of microspheres can be seen between the dermis and the epidermis.[25]

The first approach towards building these sensors involved immobilizing the sensor chemistry utilizing the resonance energy transfer transduction mechanism inside alginate microspheres.[26] However, there were two main problems with the immobilization technique, namely: 1) an appreciable amount of the encapsulated material was lost to the solution during gel bead formation, and 2) loss also occurred during storage and application of the microspheres due to diffusion into the surrounding solution. The resulting sensors were shown to be responsive to glucose increases up to 600mg/dL when tested in short term studies; however, reversal of glucose binding was

not achieved within a reasonable time. This work therefore tries to overcome the shortcomings of the previous approaches in attempting to build smart tattoo glucose sensors using the enzymatic transduction mechanism. The novel feature of this work is the immobilization and stabilization of the enzyme glucose oxidase inside small size alginate microspheres by modifying existing techniques. The novel aspect of this work also features application of self-assembled ultrathin film coatings including novel "biocompatible coatings" on alginate microspheres in order to modify the surface properties, to help stabilize the enzyme towards long term biosensor use as well as improve its biocompatibility, and to aid intradermal implantation. The major objectives of this project are, therefore, to develop stable entrapment procedures for enzymes using nanoengineered ultrathin coating technologies on alginate matrices towards implantable glucose sensors.

1.3 Organization of Chapters

The chapters in this dissertation are organized for clarity and continuity. Chapter 2 presents the techniques for fluorescence glucose sensing as well as the techniques for immobilization of enzymes. It also discusses the theory behind the approach taken in this work and reviews the work done in this field by various researchers, with an emphasis on identifying similarities and differences with the work presented here. Chapter 3 discusses the materials and methods used in this work. Chapter 4 covers the experiments conducted using FITC-dextran encapsulated inside alginate microspheres and compares their release over different molecular weights and coating materials. Chapter 5 and Chapter 6 discuss the encapsulation and stabilization of the enzyme glucose oxidase inside alginate microspheres using different polyelectrolyte coatings. Chapter 7 focuses on the chemical

conjugation technique used to stabilize the enzyme in alginate microspheres. Chapter 8 deals with the biocompatibility aspect of the sensors, including assembly of novel coatings used and *in-vitro* cytotoxicity tests. The final chapter summarizes the major findings of this work and discusses a suitable design for the glucose sensor.

CHAPTER 2

THEORY AND BACKGROUND

As already discussed in the previous chapter, the smart tattoo sensors will be implanted in the skin where they would be in contact with interstitial fluid and respond to local changes in glucose that can then be correlated to blood glucose levels.[27] Before we get into the discussion of fluorescence-based glucose sensors, it is appropriate to discuss the desirable features of these systems.[24] First and foremost, the materials used for making the sensors should be biocompatible. This biocompatibility is possible if the sensors do not lead to sustained long-term host response. The purity of the materials used in making the sensors can be a critical factor in determining the chronic response. Next is achieving a strong, sensitive, reversible, and fast response. This goal is discussed in the context that the fluorescence signal from these systems must be measurable, must change significantly over the range of interest, and must accurately reflect the current glucose levels. Ideally, a sensor response that produces a two-ten times change in the measurand (intensity ratio, wavelength, lifetime) over the 0-600 mg/dL glucose range in a sub minute time interval is expected. A third important characteristic is a stable assay response, which basically means that there is calibration required for changes due to denaturation of the protein elements over time, and if this happens, then the attractive feature of the smart tattoo sensors loses appeal. A stable assay response also means that the components used in the sensing assay must be maximally photostable, and the

environment must make sure that the enzyme is stabilized against irreversible conformational changes. Another important characteristic is specificity, which is possible if the glucose sensitivity is minimally affected by the presence of other sugars and competing analytes. Also, it should be easy to probe the sensors with low-cost instrumentation. Thus, the sensors should have optical properties that enable interrogation with reasonable signal-to-noise ratio. A final important characteristic for such systems is a reliable and repeatable fabrication method. It is important to have careful control over assembly to achieve the necessary configuration and dimensions. These "desired" characteristics will be discussed in more detail when we weigh the different available techniques. Before beginning the discussion of fluorescence-based glucose sensors, it is important to review some basic properties for enzymes and proteins.

Proteins do not always exist as long, extended chains of amino acids. Instead, they can be folded or coiled due to interactions between the amino acids, to give a specific three dimensional structure (conformation) as shown in Figure 2.1.[28]

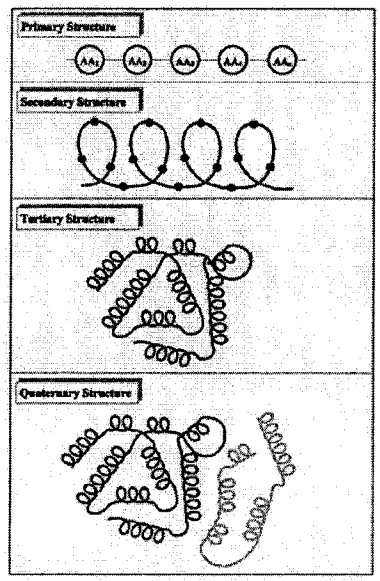

Figure 2.1. Schematic illustration of the four levels of protein conformation.[28]

The importance of a protein's conformation can be appreciated by considering enzymes, which are proteins that catalyze specific reactions. In these reactions, the enzyme binds a substrate molecule, and, consequently, a chemical reaction such as hydrolysis or phosphorylation occurs. The specificity of the reaction results from the binding of the substrate in a particular site of the molecule. This binding is possible because the enzyme structure is such that there is a region with the molecular dimension and arrangement of the functional group that reacts with the enzyme. Denaturation of the protein can result from changes in temperature, pH, and ionic strength, which interfere with the bonds that stabilize the enzyme structure, either by unfolding the enzyme structure or by exposing the active site to harsh solvents. Often, however, the reactions catalyzed by enzymes require the incorporation of additional chemical groups to facilitate rapid reaction. Thus, many enzymes incorporate non-protein chemical groups into the structures of their active sites, which are collectively referred to as enzyme cofactors or coenzymes. These may be bound to the enzyme through non-covalent interactions such as H-bonding, hydrophobic interactions, or covalent bonding. In such enzymes, requiring a cofactor for activity, the protein portion of the active species is referred to as the apoenzyme, and the active complex between the protein and cofactor is termed the holoenzyme.[28] These elements will again be addressed when we discuss the different enzyme and protein-based biosensors. The next section discusses the different fluorescence-based glucose sensing approaches starting with the boronic-acid based sensing.

2.1 Boronic Acid-Based Fluorescence Glucose Sensing

Fluorescent chemosensors have a high affinity to glucose. Such sensors generally consist of three components:[17] (a) proper functional groups that can have strong intermolecular attractions, (b) proper 'reporter' event, and (c) appropriate three dimensional scaffolds that provide the appropriate positioning for the relevant functional groups. Boronic acids have a strong functional group interaction with the diols that are present on glucose and other sugars. Boronic acids covalently react with 1,2- or 1,3-diols to form five or six membered cyclic esters in aqueous solution as shown in Figure 2.2. The cyclic esters formed from adjacent rigid *cis* diols of saccharides are stronger than simple acyclic diols such as ethylene glycol and *trans* diols.

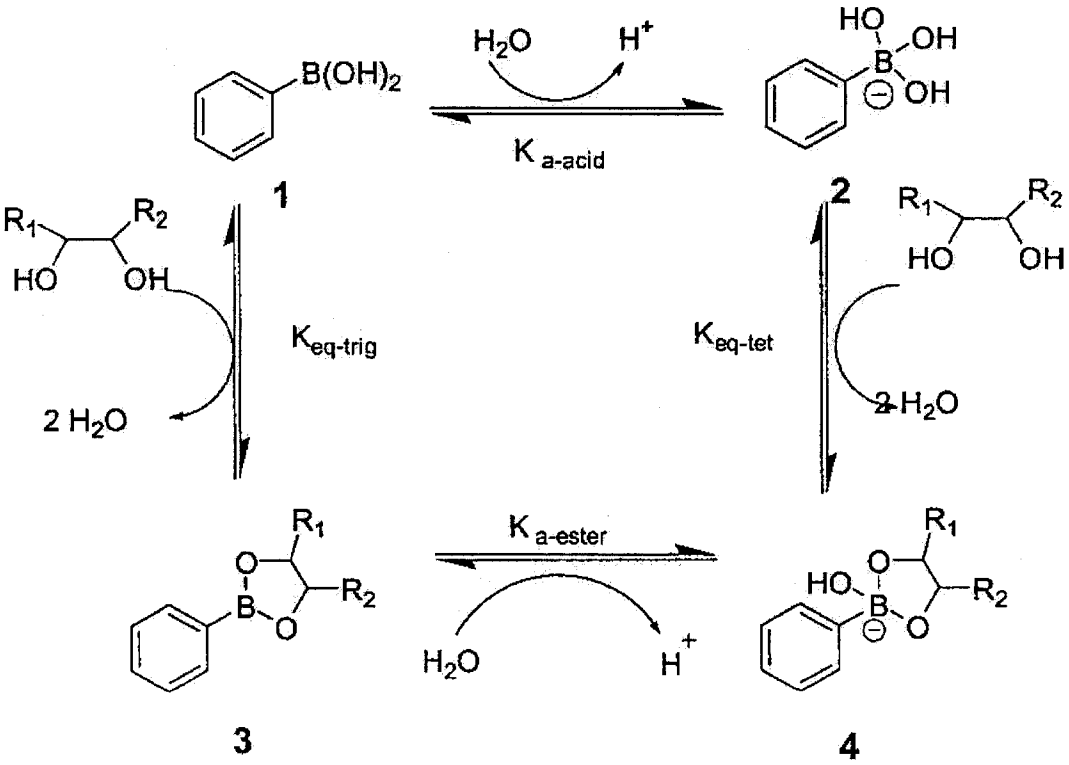

Figure 2.2. Binding process between phenylboronic acid and a diol.[17]

This mechanism of recognition can be used in a fluorescent sensing system,[14] but this is not a viable system, since it is limited to the analysis in basic media, as the pH of the sample needs to be higher than 8.8, the pKa of the boronic acid derivative used. Another disadvantages of this system is the poor selectivity achieved, which is in the order - D-fructose > D-allose = D-galactose > D-glucose. A diphenylboronic acid dianthrocene compound reported by Karnati et al., has very high selectivity to glucose – about 43-fold over fructose and 49-fold over galactose.[29] Addition of glucose causes an increase in fluorescence intensity (about sixfold at a saturating glucose concentration of 3mM; excitation wavelength (ex) 370nm, emission wavelength (em) 423nm for this compound). Another system overcame the limitations of the previously developed glucose sensing system by introducing a tertiary amine in the proximity of the boronic acid moiety.[30] This introduction reduced the pKa of the system to 4.8, making it usable for glucose determination in the physiological pH range. It also offered the ability to use photoinduced electron transfer as a tool for the transduction of the fluorescence signal (glucose concentration of 0.03-1mM; ex 370nm, em 423nm for this compound). The following selectivity was obtained with the binding constants in parenthesis: D-glucose (3981 M^{-1}) > D-allose (630 M^{-1}) > D-fructose (316 M^{-1}) > D-galactose (158 M^{-1}). In many such fluorescent sensors, the fluorophores are hydrophobic polyarene molecules such as anthracence that limit their water solubility. Therefore, the addition of an organic solvent as the co-solvent is usually required in order to study their binding with saccharides. The low water solubility thus makes their use in biological systems difficult. This problem was addressed by Norrild's group who developed the water soluble constrained diboronic acid that could bind to D-glucose with a binding constant of 2512

M^{-1} (Figure 2.3).[31] This boronic acid derivative has a low pKa of 4.0 due to the presence of the cationic pyridinium moieties, which helps to improve the binding with sugar in a neutral aqueous solution. In addition, the ionic nature of the two alkylated pyridine moieties helps to increase the water solubility of the system.

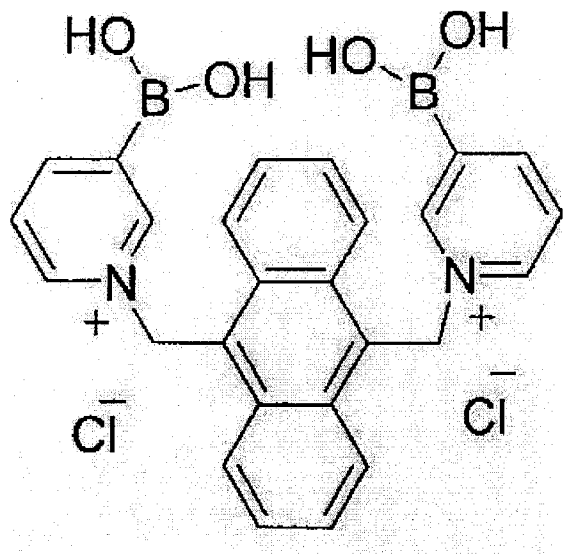

Figure 2.3. Structure for the water soluble boronic acid sensor.[17]

Another approach based on the lifetime based sensing of glucose employing phase-modulation methods was introduced by Lakowicz's group.[32] Upon interaction of the boronic acid receptor with glucose, there is a shift toward low-modulation frequencies, indicating longer mean lifetimes. The glucose detection range of this system was in the low millimolar range, well within the physiological concentrations of glucose. Tear glucose sensing using fluorescent sensors incorporated within contact lenses have also been pursued. Initial results indicate that such an approach offers the possibility of continuous monitoring of glucose concentration in the range of 50–1000 μM, which is

the normal physiological range in tears.[33] In conclusion, boronic acid based fluorescence sensors are not suitable for glucose sensing in immobilized form, primarily due to the short excitation and emission wavelengths used. Thus, efforts have focused on genetically engineered proteins with an affinity for glucose and other sugars, and these proteins are discussed in the next section.

2.2 GBP-Based Fluorescence Glucose Sensing

The periplasmic space of *E coli* and other bacteria contain a family of sugar- and other ligand-binding proteins of different molecular weights but similar structures, where there is a single polypeptide chain that folds into two domains connected by a hinge as shown in Figure 2.4.[15] Binding of a ligand at a site between the two domains is accompanied by a large conformational change with the domains closing around the ligand. Protein engineering techniques can be used to modify these molecules so that binding events are transduced by site-specifically attached fluorophores, either through changes in FRET between donor-acceptor pairs on the protein or by fluorescent changes in an environmentally sensitive single fluorophore.

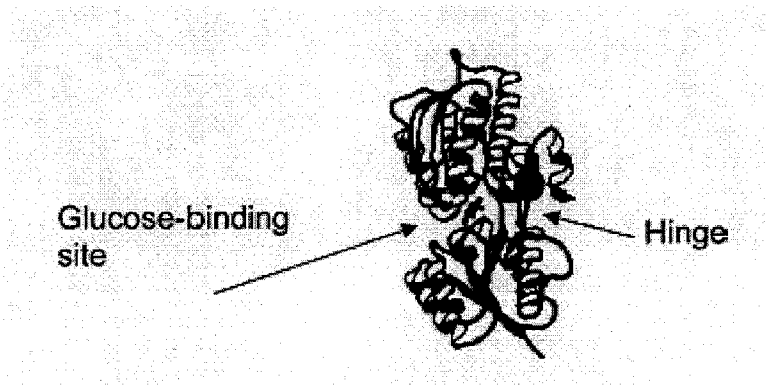

Figure 2.4. The structure of bacterial glucose-binding protein.[15]

The glucose/galactose-binding protein (GBP) has a binding affinity for glucose in the μM range.[34] Its structure consists of a single polypeptide chain folded into two domains connected by flexible hinge region typically 12-18 amino acids in length. The ligand binding site is located between the two domains. The protein has two conformations: an "open" conformation where the domains are far apart, and a "closed" conformation where they come together. Thus, biosensing involves monitoring conformational changes that occurs when proteins and ligands bind to each other. A 30% change in fluorescence was observed using the mutant GBP152 labeled with MDCC (Figure 2.5 A,B) with a detection limit of 1μM, while the mutant GBP148 yielded a detection limit of 0.05μM glucose, which is the lowest detection limit reported to date. Selectivity studies for mutant GBP148-MDCC showed that the interference from structurally similar sugars was insignificant. The labeled GBP mutant was found to be stable at 37°C for over three months, and the secondary structure of the protein was stable up to 64°C.[35]

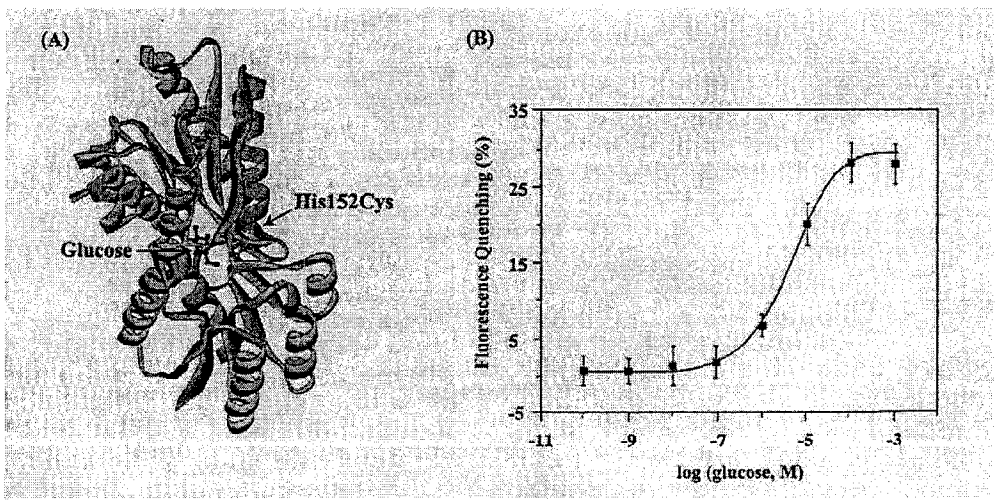

Figure 2.5. (A) X-ray crystal structure of GBP showing the mutation site His152Cys and mutant interaction with glucose, (B) Calibration curve of the fluorescence sensing system based on GBP152 for glucose.[35]

Similarly, Tolosa et al., worked with a mutant GBP26-IANNS, which yielded a binding constant of 1μM for a two-fold decrease in the fluorescence signal (ex 325nm, em 450nm), but no change in fluorescence lifetime at saturating glucose concentration (~8μM).[36] In addition, energy transfer based glucose sensors have been developed using GBP as the recognition element. Ye and Schultz fused the green fluorescent protein (GFP) (ex 395nm, em 510nm) and its mutant yellow fluorescent protein (YFP) (ex 513nm, em 527nm) at the *C*-terminus (the donor) and the *N*-terminus (the acceptor) of GBP.[37] Concentrations as low as 10μM could be accurately determined, and when incorporated in a dialysis hollow fiber, reversible detection of glucose with a response time of 100 seconds was achieved. Thus, with a suitable immobilization technique it may be possible to use some of the transduction methods described in this section for the construction of a fluorescence-based glucose sensor. The next section discusses different fluorescent glucose sensors based on enzymes.

2.3 Enzyme-Based Fluorescence Glucose Sensing

The most commonly used enzymes in the design of glucose biosensors contain redox groups that change redox state during the biochemical reaction.[38, 39] There are four types of enzymes that oxidize glucose as the primary substrate:[40] (a) glucose dehydrogenases (GDH), (b) quinoprotein glucose dehydrogenases (QGDH), (c) glucose 1-oxidases (GOx), and (d) glucose 2-oxidases (GOd). GDH and QGDH are both specific for β-D-glucose and have a high turnover. GDH from the thermoacidophilic archaeon *Thermoplasma acidophilum* is a tetramer of about 160kDa composed of four similar subunits of 40kDa each. The enzyme shows a K_d of 10mM for glucose and is resistant to

high temperatures and organic solvents. A mechanism that relies on NAD^+ acting as a cofactor, (rather than oxygen as a cosubstrate) produces NADH as shown in Eqt 2.1.

$$Glucose + NAD^+ \xrightarrow{GDH} Gluconolactone + NADH \qquad 2.1$$

To be useful as a glucose sensor, the GDH can be labeled to ANS, a polarity sensitive fluorophore which displays an increased quantum yield in low polarity environments.[41] Addition of glucose to ANS-GDH in the presence of 3% acetone resulted in an approximate 25% decrease in fluorescence intensity as shown in Figure 2.6.[34]

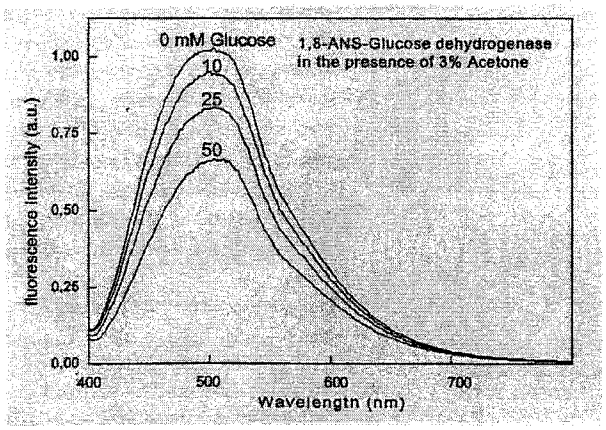

Figure 2.6. Effect of glucose on the emission spectra of 1,8-ANS-glucose dehydrogenase in the presence of 3% acetone.[34]

The polarization sensing mechanism can also be used for the measurement of glucose. Figure 2.7 shows the emission polarized spectra of ANS-GDH at various concentrations of glucose. The polarization decreases at higher glucose concentrations since the emission from the solution was observed through a horizontal polarizer. The wavelength dependent changes in polarization were then used to create a calibration curve for glucose, which showed that the system can detect glucose concentrations accurate to about 2.5mM at a glucose concentration near 20mM.[42]

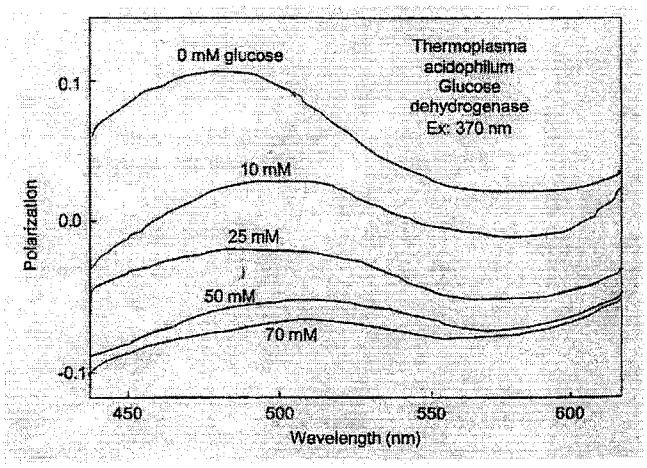

Figure 2.7. Emission polarization spectra of ANS-GDH in the presence of glucose.[42]

Another mechanism involves the use of QGDH which requires neither oxygen nor NAD^+. Quinoproteins form a class of enzymes, which require ortho-quinone cofactors to oxidize a wide variety of alcohols and amines to their corresponding aldehydes and ketones. The soluble QGDH uses pyrroloquinoline quinone (PQQ) as a cofactor as shown in Eqt 2.2. Similar mechanisms as described above may be used to detect glucose using QGDH.

$$Glucose + PQQ(ox) \xrightarrow{QGDH} Gluconolactone + PQQ(red) \qquad 2.2$$

Glucose 2-oxidases oxidize glucose to glucosone. In the presence of O_2, the other product is hydrogen peroxide. However, they also oxidize other carbohydrates like xylose and gluconolactone. This lack of specificity can rule out its widespread use in glucose sensors.[40] On the other hand, glucose 1-oxidase (GOx) is highly specific to β-D-glucose. In nature, oxidase enzymes such as GOx act by oxidizing their substrates, accepting electrons in the process, and thereby changing to an inactivated reduced state. These enzymes are normally returned to their active oxidized state by transferring these

electrons to molecular oxygen, resulting in the production of hydrogen peroxide (H_2O_2) as shown in Eqt 2.3.

$$Glucose + O_2 \xrightarrow{GOx} Gluconolactone + H_2O_2 \qquad 2.3$$

GOx is a slightly elongated globular protein with an axial ratio of 2.5:1, an average diameter of 8nm, a diffusion coefficient of 4.94×10^{-7} cm^2/sec in 0.1M sodium chloride, and a molecular mass in the range 151kDa and 186kDa.[40] The enzyme is a dimer composed of two identical subunits. The *N*-terminal region is similar to regions of *p*-hydroxybenzoate hydroxylase and glutathione reductase that are involved in binding the AMP moiety of FAD. This similarity suggests that the *N*-terminal region of GOx also has this function. The dimer contains two disulfide bridges, and it links the two subunits together. The dimer can be dissociated into its monomer by the detergent sodium dodecyl sulfate (SDS). There is also one free cysteine per monomer which is not involved in catalysis. GOx is a branched glycoprotein and contains 8-17% carbohydrates, and these differences account for variations in the isoelectric point between 3.9 and 4.3. Thus, at physiological pH, GOx is very anionic and so, polyamines like putrescine can inhibit it by altering its ionic environment of amino acids involved in catalysis. There are potentially eight sites on the protein where the protein and carbohydrate parts of the enzyme can be joined together. The carbohydrate component is in the form of a branched polysaccharide that envelopes the protein core. It is not involved in catalysis, but its partial removal with periodate can result in reduction of the enzyme's stability. GOx is very stable at pH 5, with rapid loss of catalytic activity below pH 2 and above pH 8. The rate of inactivation at high pH is reduced in the presence of glucose. Non-ionic detergents have little effect on its activity, but ionic detergents can inactivate GOx at low pH.[40]

Holo-GOx contains two molecules of the coenzyme flavin adenine dinucleotide (FAD). These two molecules of FAD are tightly bound ($K = 1\times10^{10}$) but not covalently linked to the enzyme. Thus, they can be removed without permanently denaturing the enzyme. The stability of apo-GOx can be enhanced by cross-linking of the active site with dimethyl-adipimidate. The reactivation of apo-GOx with FAD has been investigated with compounds that have a structure similar to FAD. The results indicated that the adenine amino groups, the ribose hydroxyl group, and the diphosphate bridge play an important role in the reactivation reaction. Phosphorylation of FAD to FADP abolishes its ability to reactivate GOx. Strong reductants like sodium dithionite reduce GOx, but the absorbance spectrum of enzyme reduced in this way is different from that of GOx reduced enzymatically. This could be because powerful reductants reduce not only the FAD but other parts of the enzyme as well. The first step in the reaction of GOx with glucose is the formation of an enzyme-substrate complex. This formation is followed by enzyme base catalysed reduction of FAD to yield the reduced form of the enzyme and the product gluconolactone, which rapidly hydrolyses to form gluconic acid and hydrogen peroxide.[40]

Thus, the glucose oxidase catalysed reaction can be monitored by fluorescence detection of oxygen consumption or hydrogen peroxide production. The ruthenium complex, tris(1,10-phenthrolene)ruthenium chloride (ex 447nm, em 604nm) is quenched by oxygen and has been used as an oxygen detector in the glucose oxidase-based glucose sensors by several groups.[15] An innovative technique towards the development of polyacrylamide-based ratiometric fluorescent glucose nanosensors was presented by Kopelmans's group.[43] The enzyme GOx and an oxygen sensitive fluorescent dye,

$(Ru[dpp(SO_3Na)_2]_3)Cl_2$ (4,7-diphenyl-1,10-phenanthroline disulfonic acid sodium salt), were immobilized in 45nm PEBBLEs ("probes encapsulated by biologically localized embedding"). The oxygen sensitive dye could detect changes in local oxygen depletion resulting from the enzymatic reaction. An oxygen insensitive fluorescent dye was used as a reference for ratiometric measurements. The nanosensors presented a linear range of 0.3-5 mM glucose with a response time of 150 seconds, reversibility, and good signal reproducibility, although they have some significant disadvantages. There is no guarantee of uniformity from sensor to sensor within the same batch and from batch to batch fabricated using the same process, due to the nature of the emulsion process. Another problem is leaching of the encapsulated chemistry over time. Since PEBBLEs are typically less 200nm in diameter, they are useful for intracellular monitoring but unsuitable for implantation since they are likely to be phagocytosed by macrophages. On the other hand, several methods are available for monitoring hydrogen peroxide production by fluorescence techniques. One of them uses the formation of a fluorescent oxidation product from the non-fluorescent *p*-hydroxyphenyl acetic acid (HPA) or homovanillic acid (HVA) in the presence of a second enzyme, peroxidase.[44] Since added reagents are necessary, these methods are not practical to implement *in vivo*.

Each of the above enzyme mechanisms can be utilized in glucose biosensors but feature different advantages and drawbacks. (a) The oxidase enzyme is inexpensive but requires oxygen as a cosubstrate. Consequently, as oxygen is depleted in the sample, performance decreases, whether one is monitoring oxygen depletion or hydrogen peroxide production. (b) The system NAD^+ dependent GDH, on the other hand, is oxygen independent and has the added attraction of being a well-established probe for monitoring

biochemical reactions. The drawback is that the cofactors are relatively expensive. (c) Finally, PQQ-GDH is a particularly efficient enzyme system, with a rapid electron transfer rate, but it, too, is comparatively costly.

Another simple scheme for the detection of glucose based on GOx takes advantage of the intrinsic fluorescence of the biomolecule.[14] GOx exhibits an intense fluorescence signal with excitation at 224nm and 278nm with emission at 334nm, mainly due to the tyrosine and tryptophan residue in the molecule. There is also another fluorescence band at 520nm due to the fluorescence of FAD. The visible fluorescence of FAD is quenched by adjacent amino acids, but the intrinsic fluorescence of GOx at 334nm can be used for the signal transduction in glucose determination. The disadvantage of using the intrinsic fluorescence of the enzyme is the short excitation and emission wavelengths used where there is interference from a large number of compounds. Scattering events take place in collagen fibers and cellular organelles, while skin contains melanin, which absorbs in the UV range. Also, pigments such as oxyhemoglobin, reduced hemoglobin, and bilirubin absorb the diffuse light. To overcome this drawback, a fluorophore that emits in the visible region was coupled to the glucose oxidase enzyme. GOx was labeled with a fluorescein derivative (GOx-FC, ex 489nm, em 520nm).[45] The mechanism of signal transduction was based on the inner filter effect between FAD and GOx-FC. The sensor had a linear range of 2.2-11mM glucose and a sensor lifetime of more than three months. The increase of the range of detection for glucose is desired for the measurement of blood glucose levels. Because glucose is consumed this enzyme cannot be used as a reversible sensor, which led to the

development of the sensors based on the enzyme inactivated by its inability to oxidize glucose, which is discussed in the next section.

2.4 Apo-Enzyme-Based Fluorescence Glucose Sensing

Another approach used apo-glucose oxidase (apo-GOx), resulting from the removal of FAD, which could still bind glucose with comparable affinity to that of the holoenzyme. The fluorescence emission spectrum of apo-GOx upon excitation at 298nm showed an emission maximum at 340nm, which is characteristic of partially shielded tryptophan residues. When 20mM glucose solution was added to the enzyme solution, there was an 18% quenching observed for the tryptophanyl fluorescence emission. Again, the intrinsic fluorescence from proteins is not useful as a sensing mechanism because of the need to work at lower wavelengths and the presence of numerous proteins in most biological samples.[34] The apo-GOx could then be coupled non-covalently to the fluorophore ANS (8-anilino-1-napthalene sulfonic acid), with excitation and emission wavelengths at 325nm and 480nm, respectively. ANS frequently binds with proteins with an increase in emission intensity. Thus, the addition of apo-GOx to an ANS solution resulted in an approximate 30-fold increase in ANS intensity. The fluorescence intensity and mean lifetime of ANS were found to decrease with the increase in glucose concentration in the sample. The intensity of ANS emission was sensitive to glucose, decreasing 25% upon addition of glucose (Figure 2.8). This decreased ANS intensity occurred with a glucose binding constant near 10mM, which is comparable to the K_d of the holoenzyme. Thus this sensor demonstrated reversibility without the consumption of glucose.[34] For *in vivo* sensing, the glucose detection range needs to be increased beyond

the available 5mM. A similar result was reported for ANS bound to apo-glucose dehydrogenase (i.e., without NAD[P] cofactor). However, 3% acetone was necessary to demonstrate any effect of glucose on the fluorescence of ANS-apo-GDH, which is not suitable for *in vivo* sensing.[42] The next section discusses the fluorescent glucose sensing based on lectins.

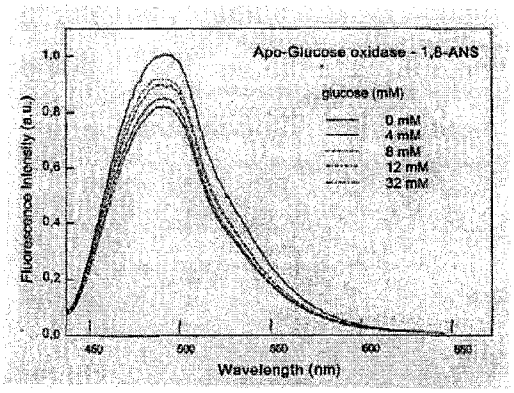

Figure 2.8. Emission spectra of 1,8-ANS-glucose oxidase in the presence of glucose.[34]

2.5 Lectin-Based Fluorescence Glucose Sensing

The interactions between a binding protein and its corresponding ligand have been utilized in a number of biomedical applications, such as drug design and development of biosensors.[14] One characteristic example is the plant sugar-binding protein Concanavalin A (Con A) isolated from Jack bean, which has four binding sites for glucose per molecule of the protein.[46] Glucose sensing methods involving Con A are based on competitive binding and fluorescence resonance energy transfer (RET). Schultz has shown that the FITC-dextran and TRITC-Con A association is sensitive to glucose concentration and has reported several variations of sensors based on this property, such that with the addition of glucose, dextran is displaced from Con A, resulting in measurable changes in energy transfer.[47-51] The linear range of the sensor was up to

11.1mM glucose. However, problems remain in fabrication, leaching stability, and reversibility. Also, the stability of the sensor is affected by the irreversible aggregation of Con A, which forms a precipitate over several hours.

Similarly, Lakowicz,[52-54] and Pickup[55] have investigated glucose assays based on affinity binding between Con A and dextran using fluorescence lifetime measurements. The sensitivity and detection range of the sensor were found to be dependent on the donor-acceptor pairs and their starting concentrations.[56] The attachment of ruthenium to Con A to form a metal-ligand complex (RuCon A) can also be used for the selective detection of glucose. This method of detection is based on FRET with RuCon A as the donor and maltose-insulin-malachite green (MIMG) complex as the acceptor. The maltose offers the affinity of an acceptor for ConA. This method utilizes the long lifetime of ruthenium, and changes in the decay time of the complex due to the presence of glucose can thus be measured.[52] Frequency domain intensity decays showed a decrease in the average lifetime of the RuCon A emission, which was attributed to energy transfer. Steady-state fluorescence measured for 2μM RuCon A and 4 μM MIMG demonstrated a consistent increase in the RuCon A emission signal as the glucose increased up to 150mM.

Rolinski et al., reported on the trasdermal sensing potential of the protein allophycocyanin (APC) (ex 650nm, em 670nm) while using it as a highly fluorescent donor in combination with malachite green as an acceptor in FRET studies.[57] Later, the APC/malachite green pair was incorporated in a Con A/dextran system for glucose sensing.[58] The time resolved NIR fluorescence assay for glucose based on APC-Con A and dextran-malachite green used a pulsed laser diode and time correlated single photon

counting for lifetime measurement. The measurements indicated a 20% decrease in mean fluorescence lifetime over a 30mM change in glucose. The issue of encapsulation of the Con A based FRET systems was addressed by Russel et al, who demonstrated the entrapment of the assay chemistry (TRITC-Con A and FITC-dextran) in 2 mm poly(ethylene glycol) (PEG) hydrogels towards a smart tattoo glucose sensor. They optimized the glucose response by varying the Con A to dextran ratio inside the hydrogel.[21,59] The response time for a step increase in glucose (0-11.1mM) was about 10-12 minutes and for a step decrease (55-0mM), about 20 minutes, although problems remained with leaching and stability of the sensor. Another report discusses encapsulating Con A and dextran molecules inside a microcapsule.[60] This system retains the advantages of the competitive binding approach: selectivity to the analyte of interest can be ensured, reaction byproducts are eliminated, and there is no consumption of the analyte during sensing process. Similarly, the use of apo-enzyme, which is highly selective to β-D-glucose as the lectin instead of the commonly used Con A eliminates the problems of toxicity, has also been demonstrated in microcapsules.[61] This work can be expanded by working with NIR fluorophores, which are potentially more suitable for interrogation through the skin. Some other techniques for fluorescent glucose sensing involves enzymes hexokinase, glucokinase and quantum dots, all of which have been discussed in the next section.

2.6 Other Techniques

The hexokinases catalyse the transfer of γ-phosphoryl group of ATP to the hydroxyl group at the C6 position of glucose. Mg^{+2} or some other divalent ion is required for activity. The structure of the hexokinase A from yeast has been determined using X-

ray diffraction measurements.[62] The polypeptide chain of 485 amino acid residues in the yeast protein is folded into two distinct domains, the *N*-terminal domain, and the larger *C*-terminal domain. The two domains are separated by a cleft in the absence of the ligand, which represents the enzyme active site. The binding of glucose causes the small lobe to rotate as much as 12° relative to the larger lobe, moving the polypeptide backbone as much as 8°, closing the gap between the two domains. This movement leads to the glucose molecule getting buried in the interior of the protein and the rearrangement of the side chains.[34] Hexokinase can be used as a fluorescent glucose sensor. It has four tryptophan residues of which two are surface residues, one glucose quenchable residue in the cleft, and one buried. The maximum quenching due to glucose was about 25%, and the concentration of glucose at half maximal quenching was 0.4mM for the monomeric form and 3.4mM for the dimeric form.[63] For use as a sensor, the protein should have long term stability.

Unfortunately, the yeast hexokinase and human hexokinase are unstable and lose activity at room temperature. Thus, glucose sensing based on the intrinsic fluorescence of sol-gel immobilized yeast hexokinase has been discussed.[64] The researchers put forth potential advantages of such a matrix, including immobilization of the enzyme, and protection from the biological medium. The sol-gel immobilized hexokinase showed an approximately 20% decrease in intrinsic fluorescence in response to saturating glucose concentrations. The maximal response of hexokinase in a monolithic sol-gel matrix was increased to about 40mM glucose (was 0.8mM glucose for enzyme in solution) and the Km to 12.5mM (was 0.3mM for free hexokinase) as shown in Figure 2.9. Application of an outer membrane consisting of 5% poly hydroxyethylmethacrylate extended the linear

range up to about 100mM and the Km to about 57mM glucose. A typical limitation of such a system is the increased response time in monoliths compared to that in solution.

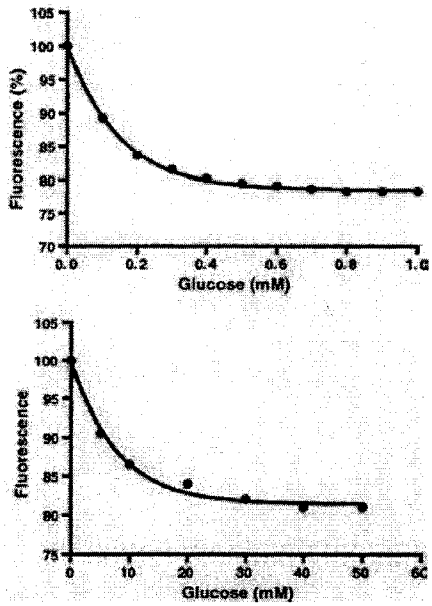

Figure 2.9. Upper: decrease in intrinsic fluorescence of hexokinase in solution on addition of glucose; Lower: hexokinase trapped in sol gel.[64]

Also, quantum dots have been used for glucose monitoring. Quantum dots typically have a CdSe core and a ZnS shell and exhibit size dependent emission. Their photostability and high quantum yield make them suitable for our applications.[65] Their glucose monitoring potential has been demonstrated with maltose-binding protein by tagging the quantum dots at specific points on the protein's structure and then using FRET for the measurement of glucose. Thus, various fluorescence glucose sensing techniques exist, each with their advantages and disadvantages. As discussed, a suitable immobilization method for the various sensing assays can make them potentially useful for transdermal measurements. This project attempts to build a smart tattoo glucose sensor based on the enzymatic transduction principle primarily because of the enzyme

glucose oxidase's high selectivity for β-D-glucose, and secondly because an oxygen sensor based on the transduction principle from photostable ruthenium complex can be easily integrated with the system. The challenge of course, lies in achieving immobilization of the enzyme glucose oxidase in a suitable matrix that will ensure that the enzyme's stability. The encapsulation method should ensure preservation of enzyme structure while also ensuring high encapsulation efficiency. These properties are essential for long term implantable glucose sensor and will be discussed in the next section, which discusses the various techniques available for immobilization of enzymes.

2.7 Techniques for Immobilization

A large number of techniques and supports are available for the immobilization of enzymes. The choice of the support as well as the technique depends on the nature of the enzyme and its ultimate application. Techniques for immobilization can be broadly classified into four categories: entrapment, covalent binding, cross-linking, and adsorption. A combination of one or more of these processes can be investigated to achieve the ultimate goal. These techniques will be addressed in the following section in more detail.

2.7.1 Entrapment

Entrapment has been extensively used for the immobilization of cells[66] and enzymes.[67] The major limitation for this technique for the immobilization of enzymes is the possible slow leakage during continuous use in view of the small molecular size compared to cells. Biocatalysts have been entrapped in natural polymers like agar, agarose, and gelatin through thermoreversal polymerization,[66] as well as in alginate and carageenan by iontotropic gelation.[66,68,69] Other hydrophilic polymers useful for the

process include chitosan, xanthans, emulsan, amylase, gellan, albumin, etc.[66,70] Still other widely used biodegradable materials used for protein/enzyme entrapment are microspheres made of poly(lactide-co-glycolide) (PLGA),[71] polylactide (PLA), and poly-DL-lactide-poly(ethylene glycol) (PELA).[72] Such systems offer numerous advantages compared to other techniques of immobilization including reduced toxicity and low cost. Other methods for enzyme encapsulation include the use of liposomes.[73] Liposomes are lipid vesicles containing a micro aqueous volume that is entirely enclosed by the lipid bilayer. There are some advantages to the use of liposomes to immobilize enzymes. Firstly, the enzyme is immobilized with no covalent binding and is therefore free of the conformational change induced by other techniques discussed later. Secondly, a biocompatible microenvironment is present for the enzyme, due to the characteristic of the liposome membrane that is similar to a biological cell membrane.

2.7.2 Covalent Binding

Covalent binding is an extensively used method for the immobilization of enzymes. Enzymes may be covalently linked to the support through the functional groups in the enzyme that are not essential to its catalytic activity. The functional groups extensively investigated are the amino, carboxyl, and the phenolic groups of tyrosine.[67] It is advisable to carry out the immobilization in the presence of its substrate or a competitive inhibitor so as to protect the active site. The covalent binding should also be optimized to ensure that there is no loss to the enzyme's conformational stability. Some of these problems can be obviated by covalent binding through the carbohydrate moiety when a glycoprotein is concerned. In general, functional aldehyde groups may be introduced in a glycoprotein by oxidizing the carbohydrate moiety by periodate oxidation

without significantly affecting the enzyme activity. The enzyme could then be covalently linked to the support through Schiffs base reaction.[74]

As an example, PMMA microbeads were prepared using dispersion polymerization of methylmethacrylate by using polyvinyl alcohol as a stabilizer. For this, the hydroxyl groups on the microbeads were first converted to aldehyde groups by periodate oxidation. Three amino compounds were then incorporated in the structure, and then the enzyme was linked to them using glutaraldehyde. The toxic nature of glutaraldehyde does not permit the use of such systems in biological environments. Similarly, microspheres with different functional groups may be used for the covalent immobilization of enzymes and proteins. Microspheres having aldehyde functional groups were obtained using radical emulsion copolymerization of styrene and acrolein and in sequential redox polymerization of pyrrole followed with free radical polymerization of acrolein.[67] Microspheres with hydroxyl groups were synthesized by radical emulsion copolymerization of styrene and α-t-butoxy-ω-vinylbenzyl-polyglycidol macromonomer. These microspheres were then used for the covalent immobilization of human serum albumin (HSA), gamma globulins, human fibrinogen, and enzymes including, glucose oxidase, and urease.

The problems when using such techniques of fabrication include protein unfolding, inactivation, and irreversible aggregation of the enzyme.[71] Mechanical forces employed towards the emulsion formation may also cause protein structural changes and thus, lead to protein inactivation. Since proteins may unfold at the oil-water interface, a stabilization technique would involve using a fairly high concentration of the protein in order to have a self-protecting effect. Using an amphiphatic excipient would also help by

sharing the interface with the protein. Yet another approach would involve addition of a polyol or sugar excipients. The sugar excipients can shield the proteins from organic solvents by preferential hydration of their surfaces, thus preventing protein-interface contacts.[71] Hence, a number of methods exist by which optimal covalent immobilization of enzymes can be achieved.

2.7.3 Crosslinking

Enzymes can also be immobilized through chemical crosslinking using homo as well as as heterobifunctional crosslinking agents. Among these, glutaraldehyde, which interacts with the amino groups through a base reaction, has been widely studied. It is believed that the aldehyde groups in the bifunctional glutaraldehyde molecule react with free amino groups between neighbouring amino acid residues to form covalent bonds that hold the structure together. Co-immobilization of glucose oxidase, invertase, and amyloglucosidase with concanavalin A (Con A) was studied by Hussain et al.[75] The enzymes were mixed separately with varying quantities of Con A and then crosslinked using glutaraldehyde before mixing with the alginate gel for immobilization. The Con A–glycoenzyme complexes retained large fraction of catalytic activity. The Con A–invertase complex exhibited a significant broadening of pH activity as well as temperature–activity profiles, indicating marked increase in stability. The alginate entrapped crosslinked Con A–invertase complex exhibited excellent capacity to hydrolyze sucrose over long durations. Enhancement of stability appeared to be an attractive feature of the Con A–enzyme complexes. The striking increase in thermostability of the Con A–enzyme conjugates would certainly be of great advantage since the enzyme reactors containing such conjugates could be efficiently operated at high temperatures and high durations.

Similar crosslinking using glutaraldehyde was described in a separate experiment, in which trypsin was microencapsulated in a calcium alginate matrix.[76] The purpose of this study was to explore the possibility of microencapsulating an enzyme and to determine the feasibility of recycling the entrapped enzyme over a period of time. The leaching of trypsin accounted for most of the loss of total enzymatic activity over time. The open structure of the matrix promoted free movement of the entrapped material out of the matrix. Also, the high concentration of the entrapped material favored diffusion across a concentration gradient. In addition, the solubility of the entrapped material in aqueous media favored easy access to the external environment. Thus, a covalent means for binding the enzyme to the matrix was devised for which glutaraldehyde was chosen as the crosslinking agent. Crosslinking may occur intermolecularly or intramolecularly, and the end result is a meshwork of closely knit proteinaceous material that precipitates out of solution. Then the protein can be harvested using centrifugation and used for further experiments. The crosslinking process stabilized the enzyme from the denaturing effect of solvents such as ethanol, isopropanol, etc. On the other hand, enzymatic activity was found to be inversely proportional to the concentration of glutaraldehyde used, due the fact that greater extent of crosslinking at higher glutaraldehyde concentration resulted in a distortion of the conformation of the active site for the enzyme. With this distortion, accessibility and accommodation of the substrate is not as favorable and, therefore, a decrease in enzymatic activity was observed.

2.7.4 Adsorption

This is perhaps the simplest of all techniques and one that does not grossly alter the activity of bound enzyme. In case of enzymes immobilized through ionic interactions,

there is adsorption and desorption of the enzyme based on ionic strength of the medium. Also, there have been various reports of alternate assembly of enzymes and polyions on matrices,[77] which involved changing the solution pH above or below the enzyme iso-electric point to facilitate adsorption. Immobilization of enzymes through hydrophobic interaction has also shown promise.[78] One of the important features of this technique, which is of great significance, is that, unlike ionic binding, hydrophobic interactions are usually stabilized by high ionic concentrations, thus enabling the use of high concentrations of substrates without the fear of desorption. A problem with this technique is that the matrix for immobilization needs to be oppositely charged to the enzyme for efficient encapsulation.

Most of the techniques described in the previous section have been used for the immobilization of enzymes for biosensor applications, but enzymes trapped in reverse micelles hold promise since they can be made out of commonly available natural polymers, which lead to low cost and high yield. In this regard, polysaccharides are the preferred water soluble polymers to be used; sodium alginate is on the top of the list because it is biocompatible and biodegradable in human tissues.[79] The following section discusses the properties of alginate that enable it to be used as a matrix for the immobilization of glucose oxidase.

2.8 Structure and Properties of Alginate

Alginate is a naturally occurring biopolymer that is finding increasing applications in the biotechnology industry. It has been successfully used as a thickening agent, a gelling agent, and a colloidal stabilizer in the food and beverage industry. Alginate has also been used as an immobilization matrix for the entrapment of cells,

proteins, drugs, and enzymes because of its non toxicity and its ability to form hydrogels under very mild conditions.

Alginates are linear chains of 1, 4'-linked monomers of β-D-mannuronic acid and α-L-guluronic acid extracted from seaweed. There are different sequences and compositions of these monomers in the various types of alginates. These monomers occur in the alginate chain in blocks. The regions are referred to as M blocks for the poly(mannuronic acid), G blocks for poly(guluronic acid), and MG blocks for poly(mannuronic-alt-guluronic acid). The differences in the nature of the linkage between M blocks and G blocks are reflected in the conformation of these sections in the polymer chain. The M block section is flat, while the G block section is buckled as shown in Figure 2.10. This nature of the alginate polymer confers different backbone chain flexibility to the polymers in solution. These differences in flexibility are not due to the differences in H-bonding, which is present to the same extent in each monomer. Rather, these differences in flexibility arise due to a greater restriction about the carbon-oxygen bonds joining the monomers. The α (1-4') linkage of the guluronic acid residues introduces greater stearic hindrance from the carboxyl groups and thus high M content alginate chains are more flexible in solution than high G content alginate chains. Also, the composition and extent of these sequences, and the molecular weight determine the physical properties of alginates. The viscosity of alginate solutions depends primarily on the molecular weight of the material. Light scattering has been used to determine the average molecular weights of several alginate samples, which have been shown to range from 80kDa to 290kDa.[68, 80]

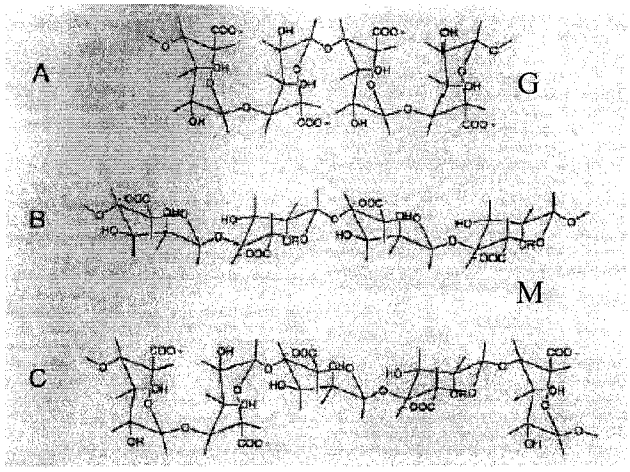

Figure 2.10. Alginate backbone structures. (A) poly(guluronic acid) sequence (GGGG); (B) poly(mannuronic acid) sequence (MMMM); (C) copolymer sequence (GGMMG).[68]

Alginate has several unique properties that have enabled it to be used as a matrix for the entrapment of a variety of enzymes, proteins, and cells, including a relatively inert aqueous environment within the matrix, a mild room temperature encapsulation process, high gel porosity allowing high diffusion rates of macromolecules,[81-82] the ability to control this porosity with simple coating procedures,[83-86] and dissolution and biodegradation of the system under normal physiological conditions. Alginate beads can be prepared by gelation using divalent crosslinkers. The gelation and crosslinking of alginate is mainly achieved by the exchange of sodium ions from the guluronic acids with the divalent cations, and the stacking of these guluronic groups to form the characteristic "egg-box" structure shown in Figure 2.11.

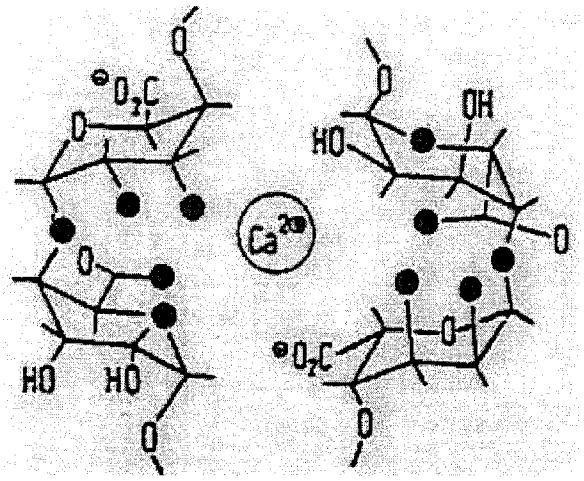

Figure 2.11. "Egg-box" model for gelation of sodium alginate with $CaCl_2$.[68]

The egg-box model is so named because of its appearance, as each calcium ion is surrounded by four guluronate residues, two from each chain. The divalent cations bind to the α-L-guluronic acid blocks in a highly cooperative manner, and the size of the cooperative unit is more than 20 monomers. Co-operativity requires the alignment of at least two chains such that the functional groups are aligned in a position to interact with the counter ion. Each alginate chain can dimerize to form junctions with many other chains and as a result, gel networks are formed rather than insoluble precipitates.

Degradation of Ca^{2+} crosslinked alginate gel can occur by removal of the Ca^{2+} ions. This removal can be accomplished by the use of a chelating agent such as ethylene glycol-bis (β-aminoethyl ether)-N,N,N′,N′-tetracetic acid (EGTA), ethylenediamine tetraacetic acid disodium salt dihydrate (EDTA), lactate, citrate, and phosphate, or by a high concentration of ions such as Na^{+}. As Ca^{+2} ions are removed, the crosslinking in the gel decreases and the gels are destabilized as shown in Figure 2.12.

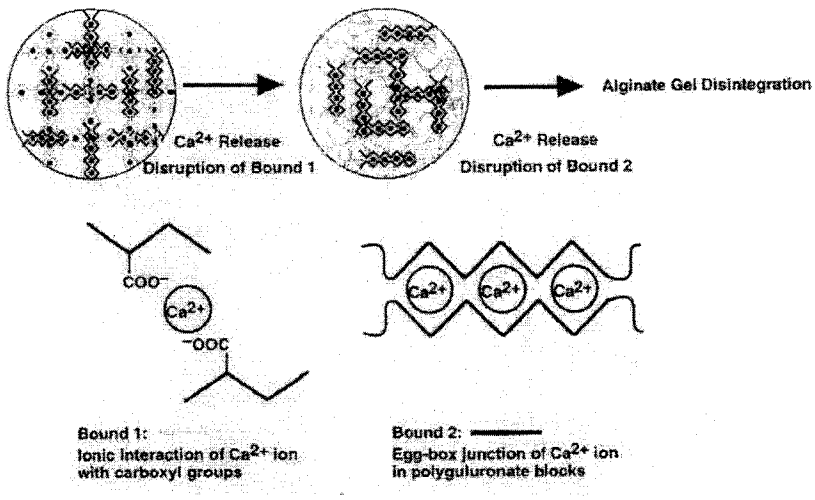

Figure 2.12. Disintegration of the "egg-box" junction upon chelation.[80]

This destabilization can then lead to leakage of the entrapped material and solubilization of the high molecular weight alginate polymers. Alginate gels have been observed to degrade and precipitate in a 0.1M phosphate buffer solution and completely dissolve in 0.1M sodium citrate at pH 7.8. Alginates are also known to form strong complexes with polycations, including chitosan, polypeptides such as poly-L-lysine (PLL), and synthetic polymers such as polyethyleneimine (PEI). These complexes do not dissolve in the presence of Ca^{+2} chelators and can be used to both stabilize the gel as well as reduce its porosity as discussed earlier. This is shown in Figure 2.13, which illustrates the formation of complexes between alginate and PLL.

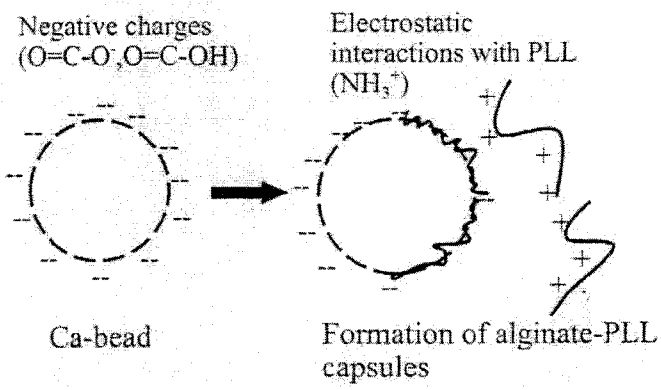

Figure 2.13. Formation of complex between alginate and PLL.[80]

Similarly, alginate gel beads can be coated with multiple coatings using the layer-by-layer (LbL) self-assembly technique that enables polyelectrolytes of opposite charge to be deposited onto charged templates, forming stable multilayers with each component layer being 1-10nm thick.[87,88] The LbL electrostatic adsorption process has been demonstrated as a robust method for depositing dense monolayers of charged molecules onto oppositely charged surfaces. The approach is extremely general, and materials employed in the assembly process range from the charged polymers to proteins to dyes to semiconductor nanoparticles. Each layer has a thickness on the order of a few nanometers, and the thickness and porosity are controllable through careful selection of materials and reaction parameters. Furthermore, the composition of films can be engineered through the sequential deposition of different materials; thus, complex film architecture may be achieved through a common process without need for complicated chemistry.[77] Thus, the LbL method provides a practical procedure for building precisely engineered nanocomposite films. The following section discusses the various available techniques for the fabrication of alginate gel beads.

2.9 Alginate Gel Bead Preparation

Alginate gel beads can be prepared using various techniques depending on the required size. In general, beads larger than 1mm in diameter can be prepared by using a syringe with a needle or a pipette.[89-91] Sodium alginate solution containing the encapsulant is transferred dropwise into a gently stirred crosslinking solution containing divalent ions as demonstrated in Figure 2.14. The diameter of beads formed is dependent on the size of the needle used and the viscosity of alginate solution. A larger diameter needle and a higher viscosity alginate solution will lead to larger diameter beads. The most important limitation of the syringe-droplet technique is that it is not suited for industrial scale up. In general, an alginate solution of greater than 5% (w/v) concentration is difficult to prepare because of the high viscosity. The beads that are formed are allowed to fully cure in the crosslinking solution before they are rinsed with deionized (DI) water. The composition of the alginate will also influence the bead size. Ca^{+2} alginate gels shrink during gel formation leading to a loss of water. The greatest shrinkage is found in the beads made of low-G alginate.[80]

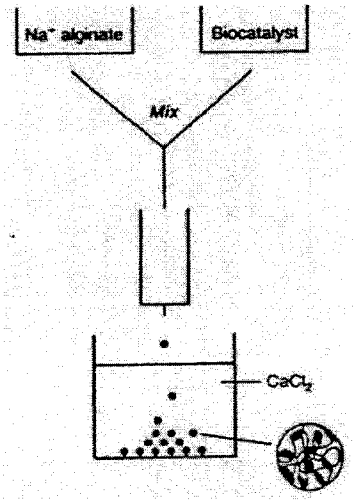

Figure 2.14. Syringe extrusion technique for alginate bead preparation.[89]

Alternative methods have been employed to produce smaller beads. The first method, known as the co-axial air flow method, employs a concentric air stream to shear the drop from the needle tip at a smaller size controlled essentially by the gas flow.[92] Beads in the 0.8-2 mm range can be produced. The size and sphericity of the beads also depends on the viscosity of the sodium alginate solution as well as the distance of the needle from the $CaCl_2$ solution (Figure 2.15).

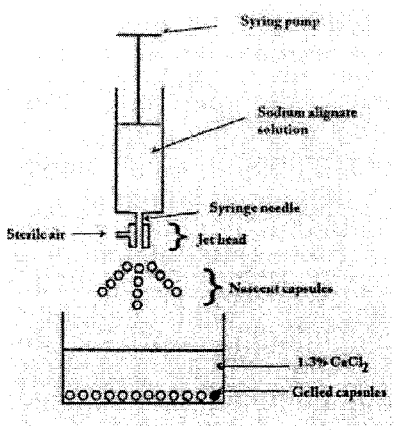

Figure 2.15. Co-axial air-flow method of making alginate beads.[92]

The second method uses vibration as a mechanical disturbance to induce the controlled breakup of a liquid capillary jet into uniformly sized droplets.[93] Beads can be produced in a range of 0.5-2 mm with a corresponding flow range of about 5-500mL/min. The third method uses electrostatic forces to destabilize a viscous jet, where the electrostatic force is used to disrupt the liquid surface instead of a mechanical disturbance. The electrostatic method can produce beads in the 0.05-5mm range. Another method uses piezoelectric technique for droplet formation combined with electrostatic charging of the droplets as the droplets fall towards the gelling solution. This technique is also combined with the use of surfactants, which help the very small droplets enter the gelling solution. A tesla coil, as shown in Figure 2.16, can be utilized to impart the

necessary charge on the droplets before they enter the gelling solution. The beads are shown as being coated with a poly-L-lysine solution.[66]

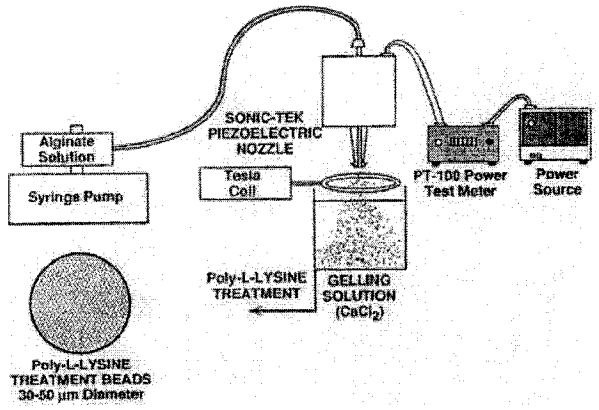

Figure 2.16. Electrostatic bead generator coupled with a tesla coil.[66]

Still smaller beads that are less than 0.2mm in diameter can be produced using the emulsification (including external and internal gelation, membrane emulsification, and microchannel emulsification) technique, which will be discussed in the following section.[94-100]

2.10 Emulsions

Emulsions are dispersed systems of two (or more) insoluble liquids. Almost all emulsions contain water as one phase and an organic liquid as the other phase. The organic phase is normally referred to as 'oil,' but it does not have to be an oil. There are examples of non-aqueous emulsions (such as emulsions of fluorocarbons in hydrocarbons) as well as emulsions of two aqueous phases (such as dextran and polyethylene glycol). The droplets in an emulsion are referred to as the dispersed phase, while the surrounding liquid makes up the continuous phase. Depending on which is the dispersed phase and which is the continuous phase, there are two types of emulsions: oil-

in-water (o/w) and water-in-oil (w/o) emulsions. Water-in-oil emulsions are also known as "reverse micelles." They provide a well suited medium for solubilizing proteins, amino acids, and other biological molecules in a non-polar environment. Systems with an emulsion as the dispersed phase are called multiple emulsions, i.e., water-in-oil-in-water (w/o/w) emulsions. Such systems are of interest in drug delivery.

Emulsification starts with a premix of the fluid phases containing the emulsifier. The emulsification includes two mechanical steps: first, deformation and disruption of droplets, which increases the specific surface area of the emulsion; and secondly, the stabilization of these newly formed interfaces by surfactants.[101] The energy transferred by mechanical homogenization is usually not sufficient to produce small and homogenous droplets. A much higher energy is required, significantly higher than the difference in surface energy $\Delta A\gamma$ (where γ is the surface or interfacial tension and ΔA is the area of the newly formed interface), since the viscous resistance during agitation absorbs most of the energy and creates heat. The entropy of dispersion of the droplets is equal to $T\Delta S$, and, therefore, the free energy of formation of the system is given by the expression, [102]

$$\Delta G = \Delta A\gamma - T\Delta S \qquad 2.4.$$

With macroemulsions, the interfacial energy term is much larger than the entropy term so the process of emulsification is non-spontaneous. Therefore, energy is needed to produce the emulsion by the use of high speed mixers. Present day high-force dispersion uses ultrasonication, especially for the homogenization of small quantities, although rotor-stator dispersers or high pressure homogenizers are equally preferred. Using a high pressure homogenizer with an orifice valve, it is possible for the droplets to spend enough time in the laminar flow for a large number of disruption steps to occur, but hardly any

surfactant molecules adsorb at the newly forming interface, because the adsorption time is longer than the disruption step. For this reason, a special design has to be conceived that will make the droplets stay longer in an elongational flow to allow time for the surfactant molecules to adsorb at the interface.

The process of homogenization can be monitored by different methods, e.g., turbidity and surface tension measurements.[101] With increasing sonication time the droplet size decreases and therefore the entire oil/water interface increases. Since a constant amount of surfactant has now to be distributed at a larger interface, the interfacial tension as well as the surface tension at the air/dispersion interfaces increases, which can then be measured. Also, since the free energy of formation of the system is positive, the emulsion tends to break down by flocculation and coalescence, which reduces the interfacial energy.

To reduce flocculation and coalescence, an energy barrier is created between the droplets, thus preventing close approach. This energy barrier is mainly achieved by using emulsifiers as already discussed. A cosurfactant can also be used in the system. The co-surfactant is usually a medium chain fatty alcohol, acid, or amine. It is usually chosen to be widely different in hydrocarbon moiety size compared to the surfactant. The role of the surfactant along with the cosurfactant is to lower the interfacial energy to a very small, even negative value, thus stabilizing the emulsion. A second emulsifier can also be employed to assist in obtaining and maintaining the homogeneity of the particles. As the concentration of the emulsifier increases, the size of the particles formed decreases because the emulsifier stabilizes the individual microspheres and inhibits their agglomeration. Similarly, as the degree of agitation increases, the size of the particles

formed decreases.[79] The emulsions of the water-in-oil type are readily formed using nonpolar alkanes that are liquid at room temperature and possess an alcohol-water partition coefficient, or log *P* value, in the range 3.5-8. In general, hydrocarbons such as toluene, *o*-xylene, or isooctane are used as the oil phase. The point of concern, however, is that the crosslinking agent should not be soluble in the oil phase. Neither should the aqueous solution be miscible with the hydrocarbon used as the oil phase. The hydrocarbon used should be pure, substantially non-volatile, and non-polar. All of the above factors will be discussed in detail as the relevant literature is reviewed.

Wan et al., were the earliest researchers to use the emulsification technique for the preparation of alginate microspheres.[94] They observed that the size, shape, and surface characteristics of the microspheres formed were markedly affected by the stirring speed, rate of addition of the calcium chloride, and concentration and composition of the encapsulating material. In a further attempt to improve drug encapsulation, the technique of preparation of the alginate microspheres was modified. Instead of adding the aqueous phase to the organic phase, the latter was slowly added to the aqueous phase while stirring to form an oil-in-water dispersion, which gradually inverted to a water-in-oil dispersion. The researchers observed that the microspheres formed had smoother surfaces when compared to those prepared without phase inversion. It was also noted that the efficiency of drug encapsulation was 65%, up from 2%. The low drug encapsulation efficiency observed in the previous method was due to the use of dehydrating solvents (isopropyl alcohol, acetone), in which the drug was found to be soluble.

Wan et al., also reported on the influence of hydrophile-lipophile balance (HLB) on alginate microspheres.[96] Microscopic examination of the samples withdrawn from the

dispersions before the addition of calcium chloride showed the aqueous phase dispersed as fine globules in the organic phase at all concentrations of surfactants used. However, upon the addition of calcium chloride, marked clumping was observed at 0.5% w/w surfactants. Less clumping was observed at 1.0% and 1.5% w/w, while at 2.0% w/w, the extent of clumping was insignificant. The surfactants were apparently required to prevent the immature (not completely gelled) microspheres from being distorted and/or fused together. Sorbitan trioleate (SPAN 85) and poly-oxy sorbitan trioleate (TWEEN 85) were used in different mass ratios to achieve different HLB's. Clumps of microspheres were formed at HLB 3.5. It was also observed that smaller microspheres were formed at HLB 4.5-5.0 as reflected by higher proportions of microspheres measuring 0-9.9μm and the absence of microspheres larger than 50μm.

A study of the effect of HLB on the mean size of the microspheres showed a curve with a minimum at HLB 5.0. The effect of HLB was attributed to the packing of the surfactant molecules at the interface of the aqueous globules, forming a barrier to the calcium ions that were required to form a semi rigid microsphere with the sodium alginate. Surfactant mixtures with a higher HLB had a higher proportion of hydrophilic surfactant, and hence a greater affinity for the aqueous calcium chloride solution. The rate of drug release was also increased on increasing HLB. A reason for this was attributed to the higher proportion of lipophilic surfactant in the surfactant mixture with a lower HLB. The surfactant was not easily removed from the microspheres on washing due to their hydrophobic nature and would therefore adsorb on the surface of the microspheres, in turn impeding the diffusion of water in the microspheres during the drug dissolution study and slowing the release of drug out of the microspheres.

Chan et al., further showed that the rate of drug release from alginate microspheres can be reduced if co-polymers in the form of cellulose derivatives were added to the alginate solution before the spheres were made.[103] To accomplish this reduction, different cellulose derivatives like hydroxypropylmethyl cellulose (HPMC), hydroxypropyl cellulose (HPC), methyl cellulose (MC), and sodium carboxymethylcellulose (NaCMC) were mixed with the alginate solution. The microspheres prepared from these cellulose derivatives showed a higher degree of indentation on the surface, probably because these microspheres contained ~30% less sodium alginate, and thus less sodium alginate was available to form the calcium alginate matrix, leading to a softer matrix. It was noted that the drug encapsulation efficiency increased with increasing viscosity of HPMC. A higher degree of agglomeration of microspheres was observed when cellulose derivatives were incorporated with sodium alginate. Only HPC was found to retard the release of drug from the microspheres.

Similarly, the effects of poly(vinlypyrrolidone) and ethyl cellulose on alginate microspheres has also been researched.[104] Ethyl cellulose was found to produce marked aggregation of the microspheres, which also showed a lower drug content, but a slower drug release. The retardation in drug release was attributed to the formation of aggregated microspheres with a less permeable matrix. The microspheres containing poly(vinylpyrrolidone) exhibited a better flow property, but lower drug content and higher drug release rates were also observed.

In addition, the effects of aldehydes and methods of crosslinking on properties of alginate microspheres have been demonstrated to further sustain the release of drug from the microspheres.[97] Methanal was used to crosslink starch, gelatin, and albumin. Since the

crosslinkage in starch was due to the formation of bonds between the hydroxyl groups of the neighboring starch polymer chains, alginate, having many hydroxyl groups could also be crosslinked with methanal. The addition of methanal in solution or dispersion form to the continuous phase resulted in stronger microspheres, which had a lower tendency of aggregation during drying. On the other hand, marked aggregation of microspheres was observed when the pre-formed microspheres were harvested and soaked directly in a smaller volume of methanal solution. The effect of other types of aldehydes such as pentanedial, octanal, and octadecanal was also reported, and it was found that the microspheres treated with octanal and octadecanal showed marked aggregation compared to those treated with methanal and pentanedial. Also, the aldehydes were found to impart acidity to the aqueous solutions to varying extents, resulting in varying drug loss from the microspheres.

The preparation and characterization of alginate microspheres under different conditions, including various alginate concentrations, different surfactants, different alginate viscosity, and sonication was also reported.[105] Decreasing the alginate concentration decreased the microsphere size. However, a high degree of clumping of the small microspheres was observed. The influence of the type of surfactants was also evaluated by using four different surfactants, namely sodium desoxycholate, PVA, Pluronic F68, and TWEEN 85. TWEEN 85 produced less heterogeneous and smaller microspheres compared to the other three surfactants used. The effect of alginate viscosity was also studied, and it was found that the low viscosity grade sodium alginate produced much smaller microspheres as compared to medium viscosity grade alginate.

Increasing the alginate molecular weight could extend the total number of crosslinking between the guluronic acid units and the calcium, and, therefore, the microsphere size.

Since the particle size cannot be easily controlled and the microspheres tend to coagulate into large masses before hardening properly, an internal gelation using the emulsification technique was proposed, whereby the calcium ions are rapidly liberated within the ionic polysaccharide from an insoluble citrate complex. Calcium ion release was initiated by gentle acidification with an oil-soluble acid, which partitions to the aqueous alginate phase.[106,107] Since dispersions could be produced industrially in large equipment, the scale up potential of this process is unlimited. Also, since no toxic reagents or solvents were used, biological and food applications were possible. Another report discussed the production of alginate microspheres by internal gelation using the emulsification technique.[108] It was pointed out that the process of internal gelation using the emulsification technique may provide an alternative method to produce discrete microspheres with less calcium salt. Glutaraldehyde and isopropyl alcohol were used to further harden the microspheres after fabrication but were found to be unsuitable since the microspheres produced exhibited marked clumping and distorted shaping. It was hypothesized that the carbon dioxide liberated from the calcium carbonate in the presence of acid led to a porous microsphere matrix, which was weaker and succumbed to the pressure of filtration.

Thus, the preparation and characterization of alginate microspheres by a new emulsification method was proposed. This method discussed treating the alginate solution with an excess of sodium hydroxide and, subsequently, with a very concentrated solution of calcium chloride.[109] It was pointed out that the microspheres made using the droplet

generation technique and the emulsification technique use relatively low alginate concentrations and diluted calcium chloride solutions. This composition resulted in microspheres with a loose internal structure, which were good for encapsulating cells but unsatisfactory for low molecular weight compounds like drugs, which could be rapidly released from the matrix. Thus, a high alginate concentration was used to produce microparticles having a dense and homogenous internal structure with small pores and a mean size of 350μm. The produced beads showed a microreticular structure, presenting a high degree of crosslinking, a high dry-matter content, and a low specific solvent uptake compared to macroreticular gels.

Membrane emulsification has received increasing attention over the past 10 years.[110] In this method, the dispersed phase is forced under applied pressure to permeate through a membrane into a continuous phase. Surfactant molecules in the continuous phase stabilize the newly formed interface to prevent droplet coalescence immediately after formation. The resultant droplet size is controlled primarily by the choice of the membrane and not by the generation of turbulent droplet breakup. Thus, emulsions with narrow droplet size distribution can be produced.

You et al., worked on the preparation of regular sized alginate microspheres using the membrane emulsification technique.[111] It was found that the microspheres prepared using 1 wt% sodium alginate solutions were easily crushed due to their poor solidity. On the other hand, 4 wt% sodium alginate solutions were too viscous to pass through the membrane, unless high pressure was applied to the dispersed phase. The high pressure, in turn, gave the microspheres a broad size distribution. When the sodium alginate concentration was 2 wt% with an applied pressure of 0.4×10^5 Pa, it was found that there

was minimum wetting of the glass membrane, and monodisperse microspheres were obtained with a mean size of 4μm. Three different types of drugs (cationic, anionic, and non-ionic) were also incorporated in the microspheres, and their release was studied over time. The cationic drug released most slowly from the alginate matrix, probably due the ionic interaction between the drug and the negatively charged matrix. The negatively charged matrix repelled the anionic drug (fastest release), and so the release profile of the non-ionic drug was somewhere in between the other two drugs.

Sugiura et al., used a microchannel emulsification technique[112-116] to prepare monodispered lipid microspheres using the setup shown in Figure 2.17. The emulsification mechanism is almost the same as that in a membrane emulsification, thus, a hydrophobic microchannel is necessary to produce a w/o emulsion. The figure shows the glass plate firmly attached to the microchannel plate to cover the top of the slits fabricated on the microchannel plate and to form the microchannels between them. Regular size emulsion droplets can be created by forcing the dispersed water phase in the continuous oil phase through the microchannels. In a recent paper the preparation of 50-200μm calcium alginate beads has been discussed that uses a novel microfluidics device utilizing a micro-nozzle array.[117] Alginate solution was extruded through a micronozzle and was sheared by the viscous drag flow of oil flow to form calcium alginate droplets after reacting with calcium chloride downstream.

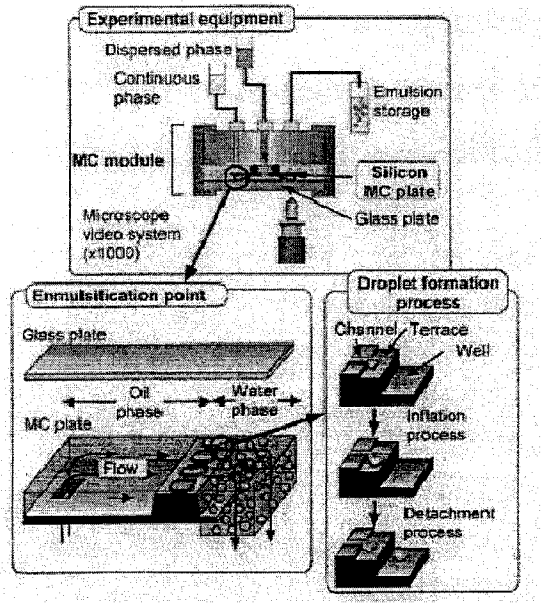

Figure 2.17. Channel emulsification technique for making uniform alginate microspheres.[112]

In the above section, various methods of preparation of alginate gel beads were reviewed, each with its own advantages and disadvantages. Large diameter beads (>1mm) are typically produced using the syringe extrusion method with a low production rates (mL/hour). However, small microspheres are often preferred for many applications in order to reduce problems of mass transfer limitations and to assure optimal rates of conversion because a reduction in size leads to an increase in the surface area available for reactions. Coaxial air-jet devices, electrostatic bead generators, and vibrating needles can be used to produce smaller beads (down to 100μm). However, as the bead number produced per unit of time is somewhat independent of size, techniques for small droplet generation are not well suited to industrial scale-up.[107] The emulsification technique (external gelation), on the other hand, can be used to make much smaller beads (<10μm) with disadvantages of harsh chemical use, and broad size distribution, although it is most

suited for industrial scale-up. The internal gelation method using the emulsification technique leads to beads that are not strong and are easily broken. The membrane emulsification technique provides good control over the bead size, and it is possible to obtain a pretty narrow size distribution, but there are many factors to be controlled in a complicated setup to get the desired bead size. Thus, considering all of the methods for preparation, the emulsification technique (external gelation) was chosen for use in the project, as it is well-established and allows tight control over all parameters. The use of these alginate gel beads as protein/enzyme encapsulation devices will be discussed in the following section.

2.11 Enzyme and Protein Encapsulation in Alginate Microspheres

The main principle behind enzyme immobilization is to entrap the protein in a semi-permeable support material. [118] This entrapment prevents the enzyme from leaching out, while allowing the substrates to pass through.[119] Some essential features of the immobilization matrix are non-reactivity and compatibility with the enzymes. Because of the three-dimensional structure of enzymes that determines their specific function, it is critical that the encapsulation matrix has a minimal effect upon the structure and function of the proteins. The immobilization process should also be mild enough that the enzymes are not denatured. Generally speaking, physical immobilization of enzymes in polymeric vehicles is one of the most advantageous methods because it is rapid and simple, the retained enzyme activity is usually quite high, and there are no chemicals involved that may deactivate the enzyme. The major limitation of physical entrapment is, however, that unlike chemical immobilization where substrates can reach the immobilized enzymes for

interaction, the physically immobilized enzyme cannot interact with larger substrates that are not able to diffuse into the matrix.

In search of suitable matrices for enzyme and protein immobilization, ionically crosslinked alginate hydrogels have been thoroughly investigated.[120,121] Various proteins that have been microencapsulated in alginate microspheres include albumin, bovine serum albumin (BSA), fibrinogen, gamma globulin, horseradish peroxidase (HRP), IgG, insulin, myoglobin, nerve growth factor, ovalbumin, TGF-alpha, TGF-beta, interleukin-2 (IL-2), and many others.[69] Among enzymes, glucose oxidase (GOx), lactase, and urease have been successfully encapsulated in large size calcium alginate microspheres, primarily because the syringe extrusion technique was used to make the microspheres.[122-126] For the glucose oxidase encapsulation study, some of the capsule characteristics such as the thickness and the stability and diffusional properties of the gel membrane were examined.[122] The enzyme encapsulation efficiency was calculated by dissolving the microcapsules, and was found to be in the range of 70-95% for different calcium chloride concentrations. The diffusion of the enzyme from the alginate microcapsules was also studied over time and was found to be dependent on the starting alginate and calcium chloride concentrations as well as the gelation time. The maximum reaction rate (V_{max}) and the Michaelis constant (K_m) of the free and encapsulated GOx were also calculated. It was shown that V_{max} for the encapsulated GOx was considerably lower than for the free GOx, implying that the membrane for the microcapsules offered a significant resistance to the transport of substrates. Therefore, the immobilization procedure was found to limit the accessibility of the glucose molecules to the active sites of the enzyme and cause a decrease in the maximum reaction rate.

Blandino et al., also discussed that the glucose oxidase may be deactivated by the hydrogen peroxide formed during the transformation of glucose to gluconic acid.[127] Thus, GOx deactivation could be limited by means of co-immobilization with the enzyme catalase (CAT), which catalyzes the decomposition of hydrogen peroxide to molecular oxygen and water, which was demonstrated in their work.

Alginate-chitosan has also been used by several groups to immobilize different enzymes. In a particular case, novel alginate-chitosan core-shell microcapsules were used by Amiji et al., to immobilize β-galactosidase.[119] Alginate-chitosan microcapsules were prepared such that the enzyme was entrapped in a biocompatible core, while the permeability control over the substrates and products was maintained by the shell structure. The calcium alginate core was initially formed and coated with chitosan, which was then crosslinked using sodium tripolyphosphate (Na-TPP). In this condition, the phosphate ions of the Na-TPP were able to extract the calcium ions of the calcium alginate and liquefy the core. Chitosan was chosen as the shell polymer since the researchers could modify its surface by complexation-interpenetration of anionic polymers to improve biocompatibility and also have the ability to create controlled porosity in chitosan membranes. Barium was also employed to make barium alginate microcapsules. The researchers achieved more than 60% loading efficiency for the calcium alginate microcapsules, while 100% loading efficiency was obtained with the barium alginate microcapsules.

A similar experiment was conducted by Coppi et al., in which a spray drying technique was used to prepare microcapsules of alginate-chitosan to encapsulate BSA. [128] A three-phase release behavior of the BSA release was observed with an initial slow

phase releasing ~5% of the protein at the end of two hours in a gastric environment, a second burst phase in which more than 40% of the loading was delivered in 15 minutes, and a third sustained phase achieving the release of ~60% in eight hours in an intestinal environment. It was concluded that the three phase release was attributable to the pH-dependent behavior of the microparticle polymer material. The first phase could be related to the calcium alginate network and the alginate-BSA complex resistance to the acidic medium, the second to their disruption in intestinal fluid, and the third to the alginate-chitosan network, which delayed the release of the remaining BSA.

In a separate experiment, urease was encapsulated in alginate beads and chitosan membranes were used to protect it from α-chymotrypsin.[126] Urease is sufficiently large (MW 544,800Da) that it does not diffuse out of the alginate beads, however, small proteases such as chymotrypsin may be able to diffuse into the beads, potentially deactivating the encapsulated urease. Thus, the alginate beads (prepared using the droplet generation method) were coated with chitosan, poly-L-lysine, or poly(methylene co-guanidine) membranes. The researchers observed a 98% loss in urease activity for uncoated beads. The intermediate molecular weight chitosan provided the highest level of chymotrypsin exclusion, with an average of 48% activity retention. Lyophilization of the beads was also discussed as a means to retain activity. Lyophilization dehydrates the beads, causing them to shrink, thus reducing their pore size. As the beads are rehydrated, they do not regain their initial diameter, thus the pores are effectively smaller than that of the original beads. The rehydrated uncoated and chitosan coated beads retained 71% and 89% of the encapsulated urease activity, respectively.

Similarly, carboxymethylated (CM) chitosan-alginate microspheres were used for encapsulating BSA.[129] Cationic and anionic derivatives of chitosan have been used because of the low solubility of chitosan at physiological pH. Also, the derivatives of chitosan have many of the same properties as chitosan, such as biodegradability, biocompatibility, and antibacterial and antifungal bioactivity. The microspheres were prepared from CM-chitosan and alginate using an emulsion phase separation technique. Their structure and morphology were characterized using infrared spectroscopy and scanning electron microscopy. The microspheres formed had dense structures on a smooth surface. The BSA encapsulated in the microspheres was quickly released in Tris-HCl buffer (pH 7.2), whereas there was a very small amount of BSA released under acidic conditions (pH 1.0), probably due to the electrostatic interaction between the NH_4^+ groups of CM-chitosan and the COO^- groups of alginic acid as well as the dense structure caused by the calcium crosslinked bridge.

Skjak-Braek et al., studied microcapsules of alginate-chitosan and reported on the capsule stability and permeability.[84] They used the one-stage procedure for making the capsules which included dropping the alginate solution in a chitosan solution and then adding a gelling agent to make the capsules. This process yielded capsules that do not have much stability in environments with low concentration of calcium ions. The two-stage process, on the other hand, led to capsules having much higher stability. This was in part due to the chitosan layer, which acted as an effective barrier to material encapsulated inside. They also showed that the use of high-G alginate instead of the poly-M being used, led to a decrease in the permeability of the capsules. It was noted that the release of

trapped materials from inside of the capsules was dependent on the ionic strength of the diffusing medium rather than the molecular weight.

Similarly, protein loss by microencapsulation of lactase in alginate beads was studied by Dashevsky.[125] The protein adsorption was shown to be affected by pH, and that maximum adsorption was found at a pH slightly below the isoelectric point of the protein. A commercial droplet generator was used to produce the beads. A 44% water leakage from the beads was observed when 1% (w/v) alginate was used to make the beads. Since enzymes are water soluble, they can be lost along with the liquid. To reduce water leakage during the formation of the beads, bentonite was added to the alginate solution. Bentonite is known to be insoluble in water, but swells into a homogenous mass occupying about 12 times the volume of the dry powder. Water loss was reduced to 28%. The protein loss was thus reduced from 36% to 3%.

Various proteins/enzymes have been immobilized in alginate microspheres, but the use of small beads for the encapsulation of glucose oxidase enzyme has not been demonstrated. Available techniques for making the alginate beads can be modified to successfully entrap the enzyme inside alginate microspheres, and the beads can be coated with suitable materials to achieve long term stability of the enzyme. It is worth noting at this point that the diffusion/leaching of the encapsulated material from small-size alginate microspheres have not been well researched to date. The next section discusses some of the work that has been done, building up to a description of the impact this dissertation will have on future studies in this area.

2.12 Diffusion of Macromolecules from Alginate Microspheres

As the sphere size is reduced into the micro- and nano-scale, the diffusion properties cannot be assumed to follow observations at the macroscale due to the large surface area to volume ratio. For diffusion through alginate microspheres, Tanaka et al., found that larger solutes like albumin, γ-globulins, and fibrinogen had no trouble diffusing out of these gel beads, when in fact they could not diffuse into them.[130] It was therefore suggested that the structure of the calcium alginate microspheres formed in the presence of large protein molecules was very different from that of the gels formed in their absence. To slow diffusion of these macromolecules from alginate beads, it was suggested that in addition to increasing the alginate concentration, the beads could also be coated with a suitable material. While some reports on diffusion of macromolecules into and out of alginate matrices are available,[69,81,131,132] these reports have not considered the effect of specialized coatings to control release from alginate microspheres.

Kikuchi et al., studied pulsed dextran release from calcium alginate gel beads.[81] Pulsatile or pulsed drug release has been defined as rapid release of a certain amount of drug within a short period after a lag time. In this paper, the release of dextran with a molecular weight of 145kDa was investigated. The release of dextran from the calcium alginate gel beads was performed using a dissolution test apparatus. The calcium alginate gel disintegrated through the ion exchange of calcium ions chelated with the carboxylate anions in the alginate and sodium ions in the PBS. A two-phase release profile of calcium ion was observed from alginate gel beads. In the first phase, released calcium levels increased monotonically for up to 60%, and then calcium ion release became discontinuous. The second phase of calcium release (45-120 minutes) was accompanied

by alginate disintegration which occurred when the calcium ion in the egg-box structure released in the medium leading to electrostatic repulsion between carboxylate anion which enhanced the swelling of alginate gels and eventually facilitated their erosion.

Another experiment was performed involving release of FITC-dextrans (FD) with molecular weight ranging from 9.4kDa-145kDa.[133] Dextran release was observed to be molecular weight dependent, with the release pattern changing from pseudo first-order for dextran with 9.4kDa molecular weight to sigmoidal for dextran with molecular weight of 145kDa. A rapid dextran release was observed in simulated intestinal fluid at pH 6.8, while minimal release was observed at pH 1.2. On the other hand, time programmed pulsatile release of FD was achieved by utilization of alginate gel beads coated with poly(carboxy-n-propylacrylamide-co-dimethylacrylamide) of varying coating thickness from 25 to 125μm.[134] For lower molecular weight FD, the release followed a Fickian diffusion according to $t^{1/2}$ dependence, indicating that the drug diffusion was the main driving force for release of lower molecular weight dextran. On the other hand, the release of higher molecular weight FD exhibited a burst-effect preceded by a preset lag time. As already discussed, their release rates were governed by the disintegration of the alginate gel. The lag time could be regulated by the copolymer coat thickness.

Similarly, multilayer coatings involving chitosan/alginate,[84] poly-L-lysine /alginate,[135-137] and other polyelectrolyte coatings have been proven for use as barrier membranes on alginate microspheres to slow release of encapsulated macromolecules.[119,138-142] Pommersheim et al., observed less than 30% enzyme retention using poly(ethyleneimine) and poly(acrylic acid) multilayers on large size (>200μm) alginate microspheres, while Amiji et al., observed 60% enzyme encapsulation efficiency

using novel alginate-chitosan core shell microcapsules. However, none of these previous reports involved glucose oxidase, which is the object of the study here.

Even though the application of multilayer film coatings can reduce leaching of macromolecules from alginate microspheres, because of Coulombic interaction, the joint force between layers is not strong enough to prevent complete leaching. This problem can be solved by causing the coatings to crosslink. The different strategies for crosslinking make use of glutaraldehyde,[143] incorporation of diazoresins,[144] and coating materials containing sulfonate groups, carboxylic acid groups, or phenol groups,[145,146] that are subsequently exposed to UV-light, and crosslinking using a photocross-linkable polyelectrolyte.[147] Crosslinked films have been shown to be more stable at higher pH values, and have increased resistance to solvent etching. [148,149] This strategy resembles that used by other groups when forming layered polymer films with covalent linkages.[150,151] However, postdeposition cross-linking preserves the advantages inherent in synthesis by simple electrostatic adsorption, with minimal deposition times and no need for organic solvents.[144] Thus, the work reported with the release of macromolecules from alginate microspheres suggest that a suitable coating can reduce the leaching of the macromolecule by a significant amount. In addition it can provide a biocompatible interface to the sensors which is important to discuss in the project's context.

2.13 Biocompatible Nanofilm Coatings on Alginate Microspheres

While alginate gel beads have been investigated as vehicles for enzyme encapsulation, another interesting possibility is the encapsulation of glucose oxidase and an oxygen-sensitive metal-ligand fluorophore complex within micron-sized hydrogel

microspheres to make implantable glucose sensors.[152,153] One of the most significant problems when using such implantable biosensors in the real world is surface fouling, that is, the rapid accumulation of adsorbed material on the working surface of sensors. Such foreign material can lead to drift and eventually sensor failure as a result of disruption of the sensitive material or prevention of analyte transport into the sensitive reagent layer. A major cause of concern, particularly in environmental, clinical, or bioreactor monitoring, is the formation of protein layers or the adhesion of microorganisms and cells.[154,155] Sensor biofouling makes long-term monitoring difficult and requires frequent maintenance operations and probe replacement.[156] Sensor biofouling is common to every monitoring technique that operates *in situ* (electrochemical, optical, electrical, thermal, etc.). Thus, the ability to engineer the interactions of cells with surfaces to reduce sensor biofouling is of primary importance for biomedical applications.

As already mentioned, among the different strategies used to modify surfaces, the deposition of polyelectrolyte multilayers has emerged as a versatile tool. Various materials can be used for creating biomimetic architectures including polysaccharides (e.g., chitosan (CH), alginate, hyaluron, chondroitin sulfate (CS), and heparan sulfate)[135-137,157,158] polypeptides (e.g., poly(L-lysine), poly(L-glutamic acid), poly(L-aspartic acid), and poly(L-ornithine)),[159-163] proteins such as collagen, gelatin, and human serum albumin (HSA),[164,165] and other natural materials like poly(hydroxyethyl methacrylate), poly(acrylamide), poly(*N*,*N*-dimethyl acrylamide), dextran, humic acid and poly(ethylene glycol) (PEG).[166,167]

Because the layer-by-layer self assembly process creates nanofilms whose properties can be controlled by the deposition conditions, several groups have begun to realize the potential of multilayers for various biomedical applications. Mendelsohn et al., showed that poly(acrylic acid)/poly(allylamine hydrochloride) multilayers can in fact be either adhesive or non-adhesive to cells, depending on the pH of preparation of the films.[168] Similarly, it has been shown that cells can be deposited on poly(L-lysine) /poly(L-glutamic acid) multilayers, and on poly(styrene sulfonate)/poly(allylamine hydrochloride) films for several days while maintaining their phenotype.[169] Also, the improvement in stability and cell adhesion properties of polyelectrolyte films involving poly(L-lysine)/hyaluronan, which were crosslinked using the carbodiimide reaction, has been reported.[170] There have also been reports involving these materials in the monolayer form to render a surface either adhesive, as for poly(L-lysine), or non-adhesive, as for poly(acrylic acid) coupled to poly(ethylene glycol).[171]

On the other hand, polysaccharides differ from most of these other synthetic polyelectrolytes and polypeptides, by their multifunctional monomers. Serizawa et al., prepared dextran sulfate/chitosan films at high ionic strengths (>0.5M NaCl) that possessed alternating anti- and procoagulation activity for the dextran sulfate and chitosan ending films, respectively. Richert et al., investigated chitosan/hyaluronan multilayer films as antimicrobial coatings.[160]

Also, surface modification by poly(ethylene glycol) is a well known strategy for rendering surfaces protein resistant. The nonfouling properties of such surfaces have been attributed to steric repulsion and excluded volume effects between proteins in solutions and the PEG modified surface.[172] Microencapsulation of islets in PEG-amine modified

alginate-PLL-alginate microcapsules has been investigated,[173] in which two different positively charged derivatives of PEG (methoxypolyoxyethylene amine, and polyoxyethylene bis[amine]) were coated onto alginate-PLL-alginate microcapsules to improve their biocompatibility. In a separate experiment, the biocompatibility of microcapsules made by the co-acervation of alginate and PLL was enhanced by coating the surface of these microcapsules with PEG.[174] The hydrogel was formed by an interfacial photopolymerization technique using visible light from an argon ion laser. In this report, a light absorbing chromophore, eosin Y, was immobilized on the microcapsule surface. This configuration led to the formation of the PEG hydrogel only on the surface of the microcapsule. The PEG-coated microcapsules were found to be less inflammatory and were seen to not elicit a fibrotic response as was the case for alginate-PLL microcapsules. Another study discussed poly(ethylene oxide)-graft-PLL copolymers to enhance the biocompatibility of PLL-alginate microcapsules.[175]

The microcapsules formed of PLL-graft-MPEG and alginate demonstrated reduced protein adsorption, complement binding and cell adhesion *in vitro* compared to those made with unmodified PLL.[176] When these microcapsules were implanted, the tissue response against them in the first week was composed of monocytes/macrophages, granulocytes, fibroblasts, erythrocytes, multinucleated giant cells, and basophiles. These cells reacted against the microcapsules in a time dependent manner. The reaction was most probably regulated by the cytokines secreted by the macrophages, which were present in the vicinity of the graft. The response was associated with the release of bioactive proteins such as trombin and fibronectin, which adhered to the capsule surface and provided binding sites for the cells.

The tissue reaction can be blocked if it were possible to apply immunomodulating agents, which act on macrophages, and thus block the release of the bioactive proteins. In a recent paper, the co-encapsulation and temporal release of immunomodulating factors such as dexamethasone was discussed.[177] It was found that a stable release of 0.2μg dexamethasone per capsule per day was found to be sufficient to completely avoid the tissue response and overgrowth of cells on the microcapsules until 28 days after transplantation, thus demonstrating the effectiveness of coencapsulants. The next section discusses the effect of the multilayer coatings on the diffusion coefficient of the entrapped enzyme from alginate microspheres. These results will be useful in determining a combination of coatings to achieve stable encapsulation of the enzyme inside alginate microspheres.

2.14 Modeling Diffusion of Macromolecules from Alginate Microspheres

Alginate gels have a wide pore size distribution due to the open lattice structure of the matrix.[126] Larger pores result in enzyme leakage or release, or access to undesired reactants. As already discussed, Tanaka et al., investigated the diffusion of macromolecules from and into alginate gels. It is interesting to establish a suitable mathematical model to quantitatively describe the diffusion of the enzyme from alginate microspheres into the solution in which the spheres are stored. Though there have been studies concerning diffusion into and out of the beads,[178,179] there has been no report discussing the diffusion coefficient calculation for coated alginate microspheres.

The effective diffusion coefficient can be calculated using assumptions that the spherical beads are all of the same size (diameter *a*), with homogenous properties

throughout. The volume of the free liquid, excluding the space occupied by the spheres, is V_L, while the volume of the spheres is V_S, and the radius of the beads is R. If the gel beads initially contain solute at a concentration of C_S^0, and are put in a liquid bath that has no solute, there will be diffusion out in the bath and an increase in solute concentration with time. After an extended contact time, the final "equilibrium" liquid concentration is C_L^∞. Under conditions of adequate stirring, there is no resistance to mass transfer at the liquid-bead interface, thus a modification of Cranks's derivations results in mathematical expressions that will allow the determination of the effective diffusion coefficient, D_E, of the solute. The substrate concentration in the bulk solution for diffusion out of the beads can then be expressed as follows:

$$C_L = \frac{C_s^o}{1+\alpha}[1 - 6\alpha\sum_{n=1}^{\infty}\frac{e^{-D_E q_n^2 t/R^2}}{9(1+\alpha)+\alpha^2 q_n{}^2}] \qquad 2.5$$

$$\text{or } \frac{C_L}{C_L^\infty} = 1 - \sum_{n=1}^{\infty}\frac{6\alpha(1+\alpha)e^{-D_E q_n^2 t/R^2}}{9(1+\alpha)+\alpha^2 q_n{}^2} \qquad 2.6$$

where the values of q_n are the non zero roots of

$$\tan q_n = \frac{3q_n}{3+\alpha q_n^2} \qquad 2.7$$

$$\text{and } \alpha = V_L/V_S \qquad 2.8.$$

These equations can be fitted with curve fitting tool to model the diffusion of glucose oxidase from alginate microspheres, and diffusion coefficients computed for various cases. In conclusion, this chapter discussed relevant literature pertaining to glucose sensors, techniques for enzyme immobilization, alginate structure and techniques of microsphere preparation, with an argument for using the emulsification technique for the preparation of alginate microspheres and encapsulating the enzyme in them. In

addition, prior work describing alginate immobilization of enzymes has been reviewed, and it was noted that there were no reports for enzyme immobilization in small size alginate microspheres, making this work novel. Also, there were no reports that discussed the application of multilayer thin films on small size alginate microspheres. This work is therefore expected to have a significant impact on future studies in the area of enzyme immobilization and stabilization.

The work described in this dissertation is thus the integration of LbL self assembly technique with the alginate immobilization of macromolecules using an emulsification technique adapted from previous reports,[94] to form microspheres in the size range of 2-50μm diameter, due to their intended application as implantable glucose sensors for diabetic monitoring.[153] To gain insight into the relationship between macromolecule loading and release with variable number of self-assembled layers on top of the gel beads, the loss of encapsulated material was monitored spectroscopically via FITC-labeled dextran (different MW) and FITC-labeled glucose oxidase, which was loaded into the calcium-alginate gel beads during the emulsion process. In addition, the enzyme activity was monitored over time and compared over different polyelectrolyte coatings. Biocompatible coatings were also tested and *in vitro* cytotoxicity tests conducted to determine the coating with the "optimum" response. This work thus describes the fabrication method used to produce the microspheres, their characterization, the effect of ultrathin film coatings on the leaching of the enzyme, and their stabilization inside alginate microspheres towards the fabrication of a glucose sensor.

CHAPTER 3

MATERIALS AND METHODS

This chapter describes the materials and preparation protocol for fabrication of the alginate microspheres. The emulsification technique used for the fabrication of the alginate microspheres has also been described in detail. After fabrication, the microspheres were coated with different polyelectrolytes and then used for the leaching and activity experiments. The Lowry assay used to calculate the amount of enzyme inside the alginate microspheres has also been described in this chapter. This chapter also covers the *in vitro* cytotoxicity tests completed on the different polyelectrolyte materials and with the microspheres coated with them. Finally, all the instrumentation used for carrying out the measurements has been described.

3.1 Materials

Sodium alginate (low viscosity; 250cps, 3 wt.-%), glucose oxidase from *Aspergillus niger*, (cat. No. G2133, Type VII lyophilized powder 100,000-200,000 units/g solid), lipophilic surfactant sorbitan trioleate (SPAN 85), and hydrophilic surfactant polyoxyethylene sorbitan trioleate (TWEEN 85), were purchased from Sigma. Polyelectrolytes, poly(allylamine hydrochloride) (PAH, MW 15kDa), poly(sodium 4-styrenesulfonate) (PSS, MW 1MDa), poly(diallydimethylammonium chloride) (PDDA, MW 150kDa), poly(acrylic acid) (PAA, MW 450kDa), poly(ethyleneimine) (PEI, MW

750kDa), chitosan (MW 200kDa), diethyl amino ethyl (DEAE) dextran (MW 500kDa), and two different positively charged derivatives of PEG (methoxypolyoxyethylene amine (PEG amine) (MW 10kDa), and polyoxyethylene bis(amine) (PEG bis-amine) (MW 3350Da) were purchased from Sigma. Also, alginate (MW 200kDa), dextran sulfate (MW 500kDa), chondroitin sulfate (MW 10kDa), humic acid (MW 10kDa), phosphate buffered saline (PBS) tablets, the microsphere gelling agent, calcium chloride (96% purity), 1-ethyl-3-(3-dimethylaminopropyl) carbodiimide (EDC), N-hydroxysuccinimide (NHS), peroxidase, *o*-dianisidine, and β-D(+)-glucose were purchased from Sigma. Diazoresin (diazo-10, 4-diazodiphenylamine/formaldehyde condensate hydrogen sulfate-zinc salt) (MW 3000Da) was purchased from PC Associates. The Lowry reagent comprised sodium hydroxide, copper sulphate, sodium potassium tartarate, sodium carbonate, and the Folin-Ciocalteau reagent, all of which were purchased from Sigma. OmniSolv® 2,2,4-Trimethylpentane (Iso-Octane) was purchased from EMD Chemicals Inc. Fluorescein isothiocyanate (FITC, MW 389.4) and FITC-dextran (MW 2MDa, 77kDa, 152kDa, 282kDa, 464kDa, and 2000kDa) were purchased from Sigma. For confocal fluorescence microscopy and fluorescence spectroscopy, glucose oxidase was covalently labeled with FITC using an amine reaction procedure,[180] in pH 9.0 sodium bicarbonate buffer and purified through a Sephadex G-25M column (Amersham Pharmacia Biotech AB). The procedure for labeling the enzyme is initiated by preparing a solution of $NaHCO_3$ in DI water to final concentration of 0.1M. To 1mL of 0.1M $NaHCO_3$ solution, 40mg of GOx was added and pH of the solution adjusted to 9.0. After this, 4mg of FITC dye was mixed with 200μL of dimethyl formamide (DMF) solution and 100μL of the DMF solution was then added to the 1mL GOx solution and pH

readjusted to 9.0. The mixture was then stirred and incubated at room temperature for four hours. At the end of the incubation period, the mixture was eluted through a desalting column to separate the dye labeled enzyme. The following section describes the instrumentation used to perform the measurements for this project.

3.2 Instrumentation

An ultrasonicator (Cole Palmer, CPX-750, 750W total power), or an overhead stirrer (VWR International) was used to disperse water droplets in the oil. A centrifuge (Eppendorf, 5804R) was used to separate the microspheres from the emulsion. A laser scanning confocal microscope (Leica, TCS SP2) was used to image the microspheres. Sizes and particle counts of alginate microspheres were obtained with a Beckman Coulter Counter model Z2 using a 100μm aperture. A ζ-potential analyzer (Brookhaven Instruments Corporation, ZetaPlus) was used to measure the surface charge of the microspheres. A 100W longwave UV lamp (Blak-ray Model B 100P, Entela) was used to irradiate the microspheres to crosslink the {DAR/PSS} nanofilms. A fluorescence spectrometer (Photon Technologies Inc, QM-4) was used in the leaching experiments to measure the fluorescence intensities of suspensions of microspheres and their supernatants. Enzyme activity assays were performed on a Perkin Elmer Lambda 45 UV-Vis spectrometer while the sample temperature was kept constant using a Peltier-controlled cell holder (Quantum Northwest). A 96 well plate reader (Tecan, Inc) was used to measure absorbance for the Lowry assay using a 750nm filter and absorbance for the cell culture activity tests using a 570nm filter. A fluorescence plate reader (Tecan, Phenix Research Products, GENios) was used to measure fluorescence emissions for cell

viability experiments. The preparation of alginate microspheres using the emulsification technique is described in the next section.

3.3 Preparation of Alginate Microspheres

Alginate gel microspheres were prepared by a method modified from Wan et al., for encapsulation of macromolecules,[94] illustrated in Figure 3.1. The preparation of the alginate microspheres using an ultrasonicator is for the purpose of obtaining smaller microspheres (typically <10μm). An overhead stirrer is used to obtain larger (>20μm) microspheres. This is possible due to the formation of a water-in-oil type emulsion, where droplets are stabilized by the use of surfactants, in contrast to the preparation of alginate microspheres using an aqueous solution of alginate slowly dropped into calcium chloride, which will yield large size microspheres (typically >200μm). For the process, 50g of aqueous solution containing 3 wt.-% sodium alginate and 5mL of FITC-conjugated to glucose oxidase (FITC-GOx) were dispersed in 75g of iso-octane containing 1.696g of SPAN 85 using the ultrasonicator at 60% power (smaller spheres), or an overhead stirrer at 1500rpm (larger spheres) for 10 minutes. A solution containing 0.904g of TWEEN 85 in 5g of iso-octane was then added to the emulsion and stirred at the same speed for five minutes to achieve stable water-in-oil emulsion droplets. After this, 20g of aqueous solution containing 10 wt.-% of calcium chloride was added at 250rpm using a pipette to allow calcium chloride slowly to crosslink the alginate. The emulsion was then stirred for another 20 minutes to allow ionotropic gelation of the particles.

The spheres were then separated from the emulsion using a separatory funnel and put in centrifuge tubes. After this, the microspheres were rinsed three times with DI water

by successive centrifugation cycles, then pipetted onto microscope cover slides for imaging. Using a 63X oil-immersion objective or a 10X air objective, several images of each batch were collected with the 488nm Ar-Kr excitation and emission collection of photons in the 520-600nm range. These spheres with the encapsulated macromolecules were also used for all the leaching studies. After preparation, the microspheres were sized and counted using the Coulter counter (100μm aperture), and the total amount of encapsulated enzyme per sample was determined using Lowry assay,[181] enabling determination of effective enzyme concentration inside the microspheres. The Lowry assay consists of the Lowry reagent I comprising, solution A, which was 1% w/v $CuSO_4.5H_2O$, solution B, which was 2% w/v Na/K tartarate solution, solution C, which was 0.2M NaOH, and solution D, which was 4% NaCarbonate solution. The Lowry reagent I was prepared by adding 24.5mL of solution D to 24.5mL of solution C. Then, 0.5mL of solution A, and 1mL of solution B were added to the mixture to get the final Lowry reagent I. For the Lowry reagent II, the Folin Ciocalteu reagent was diluted with DI water in the ratio 1:2 to make 3mL total solution.

For performing the procedure, to a sample volume of 0.25mL, 1.25mL of Lowry reagent I was added, thoroughly mixed, and let sit for 10 minutes at room temperature. At the end of the time period, 125μL of Lowry reagent II was added, and immediately vortexed and incubated for another 30 minutes. A 96-well opaque side assay plate was then taken, and 100μL of the assay was added to each well. Initially, the absorbance of the plate was recorded using an absorbance plate reader with a filter of 750nm to account for the background absorbance. After the incubation, the sample absorbance was recorded using the same conditions. The results were then fit for known glucose oxidase

concentration to estimate the unknown enzyme amount in the microspheres. For this experiment, the interference of all materials (plain alginate solution, the EDTA solution used, and the crosslinking agent) was tested and found to be negligible. The alginate microspheres were completely dissolved in 0.025M EDTA solution before performing the Lowry assay. This process ensures that the enzyme is free from the alginate microspheres and is available to bind to the Biuret reagent used in the Lowry assay. Also, a separate experiment was done with empty alginate microspheres, as well as alginate in solution, to assess the effect on Lowry assay. No difference in absorbance from the control (water) was observed for the different dilutions used.

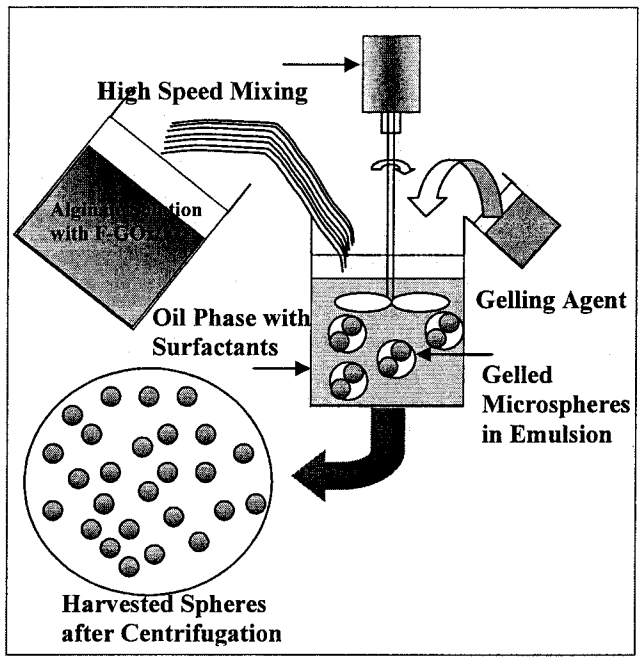

Figure 3.1. Emulsification technique for the production of alginate microspheres

3.4 Layer-by-Layer Self Assembly of Ultrathin Films on Alginate Microspheres

Several different cationic and anionic polyelectrolytes were used for the layer-by-layer self assembly application of the ultrathin film coatings. For deposition of each coating, 1.5mL of cationic polyelectrolyte (2mg/mL in DI water with 0.25M $CaCl_2$) was added to a microcentrifuge tube containing 200μL of microsphere suspension (approx 10^6 spheres). Adsorption was allowed to proceed for twenty minutes, after which time the suspension was centrifuged to separate the spheres from remaining unadsorbed polyelectrolyte. The microspheres were then triple rinsed with DI water by successive centrifugation cycles. A solution of the anionic polyelectrolyte (1.5mL of 2mg/mL in DI water with 0.25M $CaCl_2$) was then added; the spheres were centrifuged to remove the supernatant, and then rinsed three times to complete one bilayer. The surface charge of the microspheres was measured using the zeta potential analyzer after rinsing and prior to addition of each polyelectrolyte. This process was repeated until a total of three bilayer polyelectrolyte films were realized. These microspheres with the encapsulated FITC-dextran or FITC-glucose oxidase were used in the experiments described in the next section. Specific details have been covered in the following chapters discussing dextran studies and enzyme studies.

3.5 Leaching of Macromolecules From Alginate Microspheres

For wet storage loss experiments, microspheres (containing FITC-dextran or FITC-glucose oxidase) with zero (uncoated alginate), one, two, and three bilayer coatings were suspended in individual cuvettes containing 1.5 mL of PBS buffer at pH 7.4. The

fluorescence of each suspension was first measured to establish the baseline concentrations, using 488nm excitation, and emission collected between 500-600nm. The samples were initially scanned immediately after putting the spheres in the cuvette, and thereafter at regular intervals to track the amount of FITC being released into the solution. This scanning was accomplished by first scanning the full suspension of the spheres, then removing the supernatant by centrifugation and recording the fluorescence from the supernatant to determine the contribution of the supernatant to the full suspension intensity at each point. A standard solution (FITC-dextran, 7μM in 2mL PBS) was also scanned at each point in time to allow correction for instrumental variations. All samples were covered and stored at room temperature under dark conditions. The relative fluorescence comparing the different coatings was then used to determine the contribution of each coating towards final leaching of the macromolecules (dextran or glucose oxidase) from the microspheres.

3.6 Activity of Encapsulated Glucose Oxidase in Alginate Microspheres

Glucose oxidase activity was monitored through a colorimetric assay based on the oxidation of *o*-dianisidine through a peroxidase coupled system on a UV-Vis spectrometer from Perkin Elmer. The GOx activity assay comprised 2.4 mL of *o*-dianisidine solution, 0.5 mL of β-D-glucose solution, and 0.1 mL of peroxidase solution. During continuous stirring with a magnetic bar, and keeping the temperature constant at 25°C, 100μL of GOx-loaded alginate microspheres suspended in DI water (approximately 10^6 spheres) was added to the assay, and the absorbance at 500nm was monitored as a function of time, resulting in a catalytic profile of the encapsulated GOx. The experiment

was repeated for the polyelectrolyte-coated microspheres over a period of three to six months (described in subsequent chapters), and the results were compared by calculating the initial slope of the curves. In each case, the results were normalized to the mass of glucose oxidase present in the spheres as determined using the Lowry assay. Both the leaching and the activity results were analyzed using the two-tailed student's t-test.

3.7 Cell Culture

Unless stated otherwise, all cell culture reagents were purchased from Atlanta Biologicals (Norcross, GA). Standard cell culture techniques were used for all cell experiments. NIH-3T3 fibroblasts were purchased from American Type Culture Collection [ATCC], (Manassas, VA). 3T3 cells were cultured in a humid 37°C/5%CO_2 incubator in pH 7.4 growth media consisting of Dulbecco's Modified Eagle Medium (DMEM) high glucose supplemented with 10% calf serum, 100 units/mL penicillin, 100μg/mL streptomycin, and 10μg/mL gentamycin. Cells were grown near confluence in Fisher cultureware, washed twice with warm Hank's balanced salt solution (HBSS), detached with trypsin (1X) (Sigma), and passaged once a week. For attachment and proliferation assays, the cells were resuspended in normal serum containing media (calf serum) after the trypsinization (1:1), and then spun down in a centrifuge at 1000 rpm for five minutes. The cells were then resuspended in fresh media (3-5 mL), and 100μL of cell suspension was added to a microcentrifuge tube containing 100μL of HBSS and 80μL of trypan blue (Sigma) for counting with a hemocytometer to determine cell viability prior to seeding. For all the experiments, the cells were seeded at ~10,000 cells/cm^2 density onto sterilized 96-well assay plates for conducting the cell behavior, proliferation, and activity assays.

3.7.1 Materials

The experiments were conducted in two parts. For the first part, all cell experiments were conducted with opaque sided 96-well assay plates (BD Biosciences, Falcon Optilux). The cationic and anionic polyelectrolytes (PAH, PSS, chitosan, DEAE dextran, PEG amine, PEG bis-amine, alginate, dextran sulfate, chondroitin sulfate, and humic acid) (1nM concentration) were prepared in 0.25M $CalCl_2$ solution, made using DI water filtered through a 0.2μm cellulose acetate syringe filter. The 96-well assay plates were initially coated with 200μL of 2mg/mL solution of PEI per well to render the substrates positive. Some wells were not coated as they were used as the control in the experiment (termed TCPS–tissue culture polystyrene). After 20 minutes, the PEI solution was removed from the wells, and the wells were washed twice with filtered water. The anionic polyelectrolytes were then applied to the wells for 20 minutes. PSS was applied to those wells that had to be coated with the cationic polyelectrolytes. There were two washes between each coating. Finally, the assay plate was left under UV light for 30 minutes to sterilize it before it was stored in the incubator. For the second part, alginate microspheres were coated with a monolayer of the polyelectrolyte materials as described in section 3.4, and used in all the experiments for live-dead and activity assays.

3.7.2 Methods: Cell Behavior

For the first part, fibroblasts were seeded in culture media (DMEM) in the 96-well plates to a final density of 2000 cells per well and incubated for 24 hours and 72 hours for the cell viability and activity assays at 37°C in an atmosphere of 5% CO_2. Following incubation, the cells were imaged using a brightfield microscope. For cells attached to the substrate (coated well plates) the normal fibroblast morphology is expected to be spindle

shaped cells, and in some cases cells will appear elongated and trianguloid. Filopodia or pseudopods will appear leading to cell movement in a certain direction. For cells not attached to the substrate, there will be a more rounded morphology. The cellular activity will be dependent on the attachment of the cells to the substrate. The cell morphology was compared for the different polyelectrolyte materials used. TCPS was used as the control and cell behavior was compared against the control. For the second part, the alginate microspheres coated with a monolayer of the different polyelectrolyte materials were brought in contact with the cells already attached to the uncoated 96-well plates, and cell morphology compared to the control.

3.7.3 Methods: Live/Dead Viability Assay

For the viability assay of the cells in coated substrates, the cells were incubated for 72 hours before conducting the assay. The reagents in the Live/Dead assay kit (Molecular Probes L3224, Eugene, OR) provide two color discriminations of live and dead cell populations. The membrane-permeant calcein acetoxymethyl (AM) is cleaved by intracellular esterases in live cells to yield cytoplasmic green fluorescence. Dead cells with compromised membranes are stained with the membrane impermeant nucleic acid dye, ethidium homodimer-1. Using excitation at ~495nm, fluorescence emission from calcein AM and from ethidium homodimer-1 (EthD-1) are distinct at ~515nm and ~635nm, respectively. For the reagent, 4μL of EthD-1 was mixed with 1μL of calcein AM in 2mL of HBSS solution, 40μL of the mixture was added to each well of the 96-well plate, and then incubated for 20 minutes. The fluorescence emission was then recorded using a Tecan fluorescence plate reader. Background fluorescence was accounted for by using the results from wells with no cells in them. The results from

three separate wells were expressed as a percentage of fluorescence intensity from live cells in coated wells compared to the fluorescence intensity of live cells in the TCPS control. Similar experiments were performed for cells in contact with microspheres coated with the different polyelectrolyte materials at the end of 24 hours.

3.7.4 Methods: Cell Activity Assay

For both parts, cellular activity was determined by MTT assay, (Cell Growth Determination Kit, MTT based, CGD-1, Sigma) which is based on the mitochondrial conversion of the tetrazolium salt of 3-(4,5-dimethylthiazol-2-yl)-2,5-diphenyl-2H-tetrazolium bromide (MTT). Solutions of MTT solubilized in tissue culture media or HBSS, without phenol red, are yellowish in color. Mitochondrial dehydrogenases of viable cells cleave the tetrazolium ring, yielding purple MTT formazan crystals, which are insoluble in aqueous solutions. The crystals are dissolved in acidified isopropanol. The resulting purple solution is spectrophotometrically measured and results expressed as an absorbance value. For the first part, after the fibroblasts were incubated in the coated wells for 24 hours and 72 hours, 20μL MTT solution (5mg/mL in RPMI-1640 [Sigma]) was added to each well and incubated at 37°C for four hours. The medium and the MTT were replaced after the incubation time by the MTT solvent (0.1N HCl in anhydrous isopropanol) in a volume equal to the original cell culture volume, and stirred gently for 10 minutes to dissolve the crystals. The absorbance values were measured using an absorbance microplate reader at a wavelength of 570nm, blanked by subtracting background absorbance at 690nm. The background absorbance from wells containing no cells was subtracted from the readings. Cell activity was then expressed as a proportion of the absorbancy values of TCPS in same cell culture media. On thing to keep in mind

here is that the cellular activity depends on cellular adhesion, therefore, unattached cells are expected to be less active than attached cells. In another experiment, seven known cell numbers counted using a hemocytometer (1000, 2000, 3000, 5000, 10000, 20000, and 25000 cells) were incubated in uncoated 96-well plates for 24 hours and the MTT assay was performed on them. The absorbance values were used to construct a curve for cell number versus absorbance. This standard curve was then used to predict the cell numbers at the end of 24 hours and 72 hours for the experiments performed with cells in contact with microspheres coated with the different polyelectrolyte materials. The results were expressed as number of active cells at 24 hours and 72 hours for cells in contact with microspheres. All the cell viability and cell activity results for the experiments conducted with microspheres were then normalized to the control to calculate a biocompatibility index (B.I), which can be used to compare the polyelectrolyte materials.

The following chapters in this dissertation describe the experiments performed with alginate immobilization of macromolecules (dextran and glucose oxidase) and their stabilization by using self-assembled ultrathin film coatings. The enzyme activity was also monitored over time to ensure that the enzyme activity was preserved for long term use.

CHAPTER 4

RELEASE OF DEXTRAN FROM ALGINATE MICROSPHERES

The work described here is the integration of the LbL self assembly technique with the alginate immobilization of macromolecules using emulsification technique to form microspheres in the size range of 2-10μm diameter. To gain insight into the relationship between macromolecule loading and releasing with molecular size and the number of self-assembled layers coating the gel microbeads, the loss of encapsulated material was monitored using a model macromolecule, FITC-labeled dextran (FD), with molecular weights (MW) ranging from 77kDa to 2000kDa, which was pre-loaded into the calcium-alginate gel beads. FITC labeled dextran has typically been used as a marker for translational diffusion of macromolecules in cells and especially for kinetic studies on drug release from delivery systems. In addition, it is available in different MW and has the same charge as GOx at physiological pH; therefore, it can be used in this project to characterize the retention and release from alginate matrix.[136,137,182] This work describes the fabrication method used to produce the microspheres, their characterization, and the effect of ultrathin film coatings on the leaching of the dextran of different sizes from inside the alginate microspheres. For this experiment, three different commonly used polyelectrolyte combinations were compared. {PDDA/PSS} was chosen as a strong-

strong polyelectrolyte pair, while {PAH/PSS} was the weak-strong pair, and PEI was chosen because it has received attention in retention of enzymes in Pommersheim's work, and it will be interesting to compare the results from their study.[140,141] In all cases, comparisons were performed to test the hypothesis that multilayer films decrease loss rate in a manner that shows the leaching rate is inversely proportional to film thickness and macromolecular size.

4.1 Layer-by-Layer Self Assembly of Ultrathin Films on Alginate Microspheres

Three cationic polyelectrolytes (PAH, PDDA, and PEI) were used for the layer-by-layer self assembly application of the ultrathin film coatings, while PSS was the anionic polyion in all cases. For each coating step, 1.5mL of cationic polyelectrolyte (2mg/mL in DI water with 0.25M $CaCl_2$) was added to a microcentrifuge tube containing 200μL of microsphere suspension (approx $2x10^6$ spheres). The $CaCl_2$ to the polyion solution provides the bivalent ions necessary for stabilization of the calcium alginate matrix. Adsorption was allowed to proceed for 20 minutes, after which time the suspension was centrifuged to separate the spheres from remaining unadsorbed polyelectrolyte. The microspheres were then triple-rinsed with DI water by successive centrifugation cycles. A solution of PSS (1.5mL of 2mg/mL PSS in DI water with 0.25M $CaCl_2$) was added; the spheres were centrifuged to remove the supernatant and then rinsed three times to complete one bilayer. The surface charge of the microspheres was measured using the zeta potential analyzer after rinsing and prior to addition of each polyelectrolyte. This process was repeated until a total of three bilayer polyelectrolyte films were obtained.

4.2 Determination of Dextran Leaching from Alginate Microspheres

For wet storage loss experiments, microspheres with zero (uncoated alginate), one, two, and three bilayer coatings were suspended in individual cuvettes containing 1.5 mL of PBS buffer at pH 7.4. Using 488nm excitation, the fluorescence emission of each suspension was first measured to establish the baseline concentrations. For the leaching studies, the samples were initially scanned immediately after putting the spheres in the cuvette, and thereafter at regular intervals to track the amount of FD being released into the solution. This process was accomplished by removing the supernatant by centrifugation and recording the fluorescence from the supernatant to determine the contribution of the supernatant to the full suspension intensity at each point. The supernatant was then put back in the sphere suspension. A standard solution (FD, 7μM in 2ml PBS) was also scanned at each point to account for instrumental variations. All samples were covered and stored at room temperature under dark conditions. In total, the leaching experimental data covered a wide range of variables, such that all possible combinations of molecular weight (77, 152, 282, 464, and 2000 kDa) were encapsulated with alginate spheres coated with zero, one, two, and three bilayers of each polyion combination (PSS/PAH, PSS/PDDA, PSS/PEI). These data were then compared to assess the effect of different variables on the leaching through the microspheres.

4.3 Results and Discussion

Microspheres formed from the crosslinking of alginate and FITC-dextran emulsion droplets are presented in Figure 4.1. The spheres appear bright green with uniform intensity distribution when imaged with the confocal microscope. The average size was

found to be 2.38 ± 0.72μm for a sample size of 3350 spheres (Figure 4.2). These results show that the alginate microspheres produced in the process are small (<10μm, surface area to volume ratio ~ 6) compared to other cases where polyelectrolyte multilayer coating have been applied, and are relatively spherical and uniform.

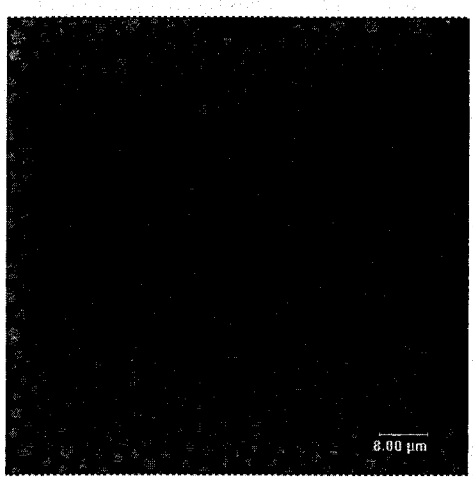

Figure 4.1. Confocal image of alginate microspheres with encapsulated FITC-dextran with a scale bar of 8μm.

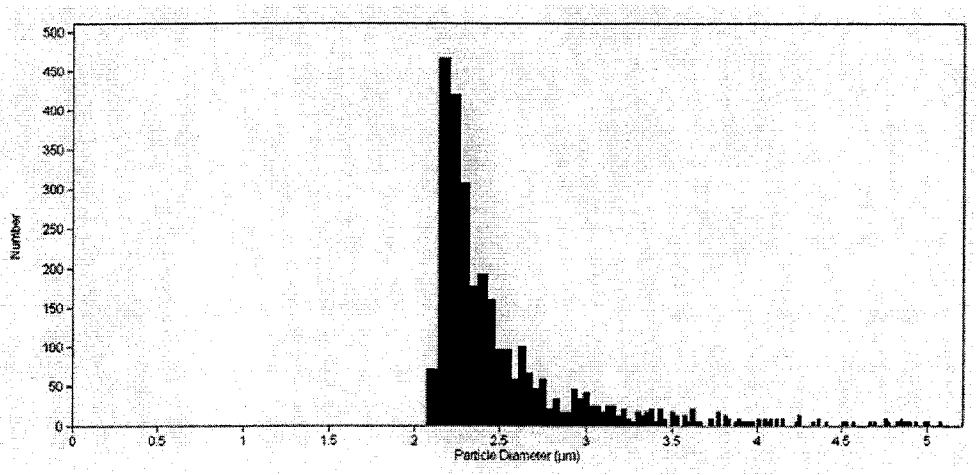

Figure 4.2. Coulter counter results for sphere size.

Following fabrication and size characterization of the alginate microspheres, deposition of multilayer nanofilms on the microspheres was investigated. The surface charge of the polyelectrolyte-coated microspheres was measured using the zeta potential analyzer, the results of which verify reversal of the surface charge of the microspheres at each step due to polyelectrolyte adsorption (Figure 4.3).

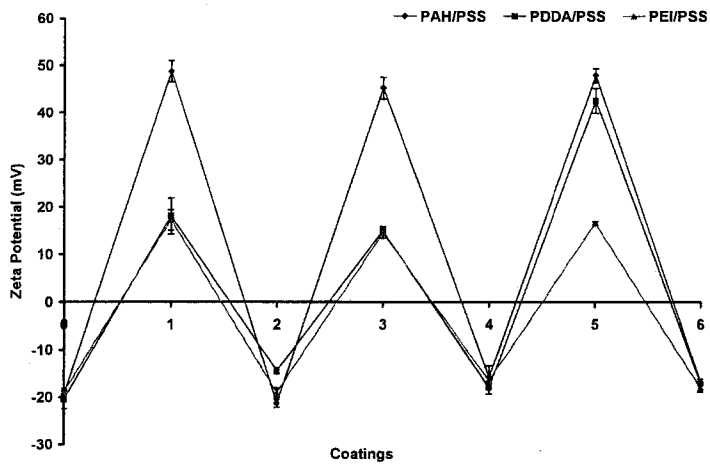

Figure 4.3. Surface charge reversal demonstrated using zeta potential measurements for different coatings on alginate microspheres.

4.3.1 Leaching of FITC-Dextran from Alginate Microspheres

Leaching of FD from the alginate microspheres was studied using fluorescence spectroscopy, where release of the encapsulated FD from the microspheres resulted in an increase in the fluorescence intensity of the supernatant as shown in Figure 4.4. Identical experiments were performed to determine the time-dependent loss of FD from microspheres for each of the different structures.

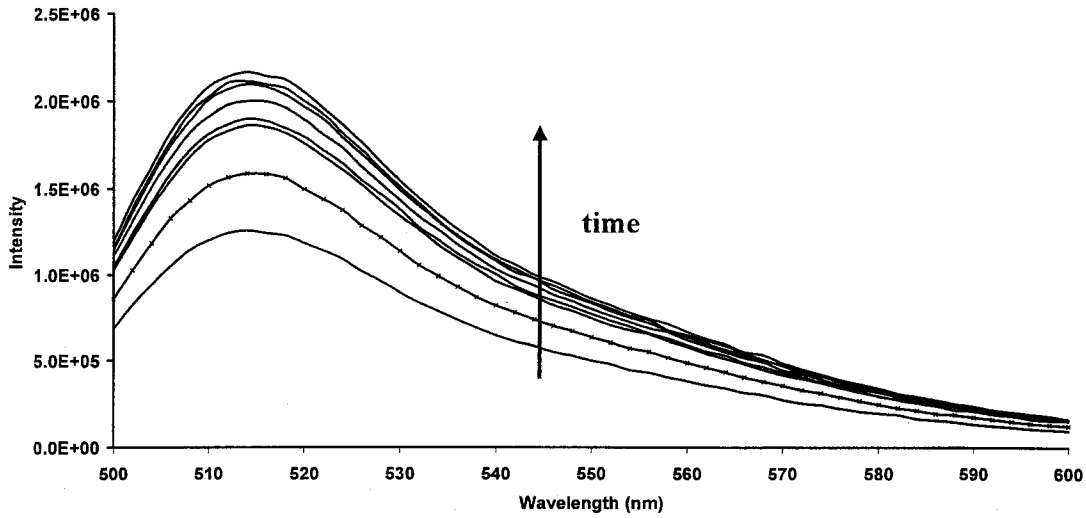

Figure 4.4. Fluorescence spectra for release of FITC-dextran from alginate microspheres.

Results from a typical experiment are given in Figure 4.5, where the leached amount for a single molecular weight FD (2MDa) is plotted versus time for microspheres coated with $\{PAH/PSS\}_n$ (n = 0-3). The released amount of dextran is plotted as the ratio of supernatant intensity to the full suspension intensity. This means that there is equal amount of FD inside the spheres and out in the supernatant when the ratio reaches 1.0. The results thus show that approximately 30% of the encapsulated material comes out of bare microspheres within four days. Given the high molecular weight of the dextran used for these experiments, these results suggest that bare alginate microspheres have relatively large pores that allow large and small molecules to pass through.

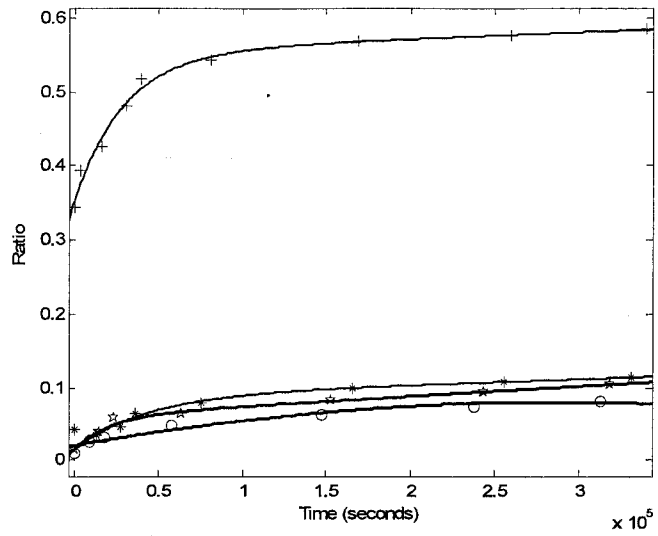

Figure 4.5. Leaching versus time for $\{PAH/PSS\}_n$ (n = 0-3) multilayers (from top to bottom) for FD 2MDa. Solid lines indicate the fitted results obtained using Crank's mathematical model.

In contrast, the release profiles for microspheres coated with PSS/PAH multilayer nanofilms show that the application of these coatings significantly reduces the loss of encapsulated material. The total leaching of the 2MDa dextran drops to less than 7% over the same time span. Furthermore, if the initial release rates are directly compared, it can be seen that the encapsulated FD is lost from bare microspheres at 1%/hr, whereas the loss is slowed by an order of magnitude (0.1%/hr) for microspheres coated with a three-bilayer system. Confocal images of the coated microspheres taken after two months verify that the FD does not simply get trapped in the walls of the polyelectrolyte coatings but is homogenously distributed inside the microspheres. No further leaching of entrapped macromolecule was observed even when the supernatant was replaced with a fresh PBS buffer solution, indicating that the entrapment is stable over time.

These results suggest that the ultrathin film coatings, applied in a simple and mild manner to microscale templates, are effective in reducing loss of the large encapsulated macromolecules from small microspheres. However, the relative effect of the common polyelectrolyte combination (PAH/PSS) compared to other materials is also important to assess. Similar time-dependent release profiles for microspheres containing FD 2MDa MW coated with $\{PDDA/PSS\}_n$ (n = 0-3) multilayers are shown in Figure 4.6. By comparison to the PAH/PSS films, it is clear that PDDA/PSS films are not as effective in stopping loss of encapsulated material, as about 20% of the FD 2MDa MW is still lost from the microspheres coated with a single bilayer over the same time period. However, in the case of PDDA/PSS, the application of additional polyelectrolyte layers does further reduce leaching. This might be attributed to the higher molecular weight (ten times) of PDDA compared to PAH, and the known thicker layer formation that likely provides a longer diffusion distance and therefore decreases the chemical gradient driving force. In contrast, the lack of significant effect for additional layers of PAH/PSS suggests either much thinner films or a different mechanism of interaction with the macromolecules that slows diffusion. For $\{PDDA/PSS\}_n$ multilayers, the rate of release of the encapsulated FD decreases from 0.7%/hr in bare microspheres to 0.35%/hr in three-bilayer-coated microspheres, again confirming that these coatings are not as effective in reducing loss of the encapsulated macromolecule compared to $\{PAH/PSS\}_n$ multilayers.

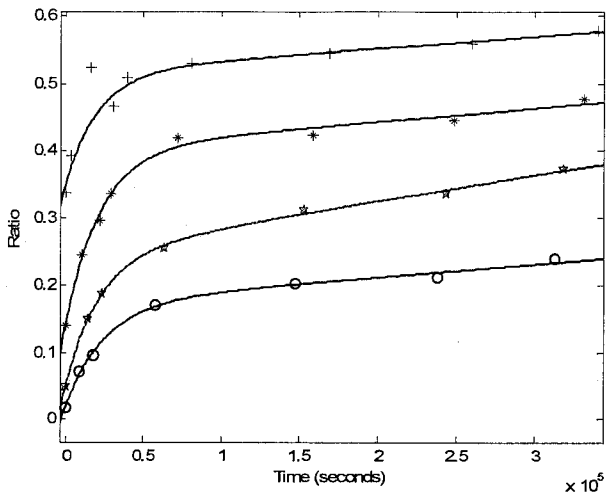

Figure 4.6. Leaching versus time for {PDDA/PSS}$_n$ (n = 0-3) multilayers (from top to bottom) for FD 2MDa. Solid lines indicate the fitted results obtained using Crank's mathematical model.

Similar to the data described above, time dependent release profiles for microspheres containing 2MDa FD coated with {PEI/PSS}$_n$ (n = 0-3) multilayers are shown in Figure 4.7. These data also exhibit features similar to those from {PDDA/PSS}: the polyelectrolyte was not very effective in reducing loss of the encapsulated material, as nearly 20% of the encapsulated material was released from the microspheres over four days, even with three bilayers of adsorbed molecules. The rate of release of the encapsulated FD decreased from 0.95%/hr in bare microspheres to 0.55%/hr in microspheres with {PEI/PSS}$_3$. It has been shown that the polycation/polyanion bilayer thickness depends on the charge density of the polyions.[77] It has also been demonstrated that more than 10% of polyion side groups have to be ionized for a stable reproducible multilayer assembly via alternate electrostatic adsorption. High ionization of polyions results in smaller film growth (1-2nm), and lower ionization gives a larger growth step

(3-6nm), probably explaining why PEI forms thinner layers than the other polyelectrolytes used.

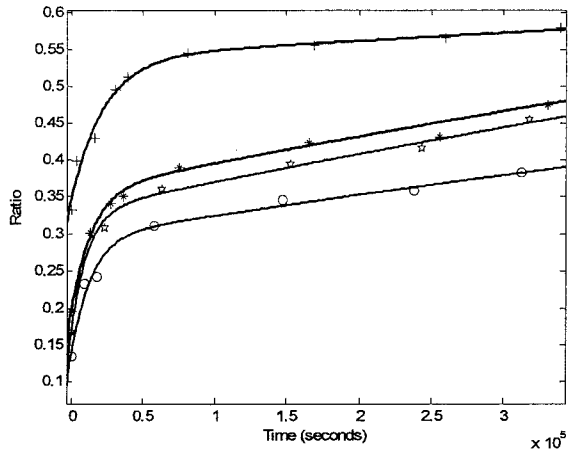

Figure 4.7. Leaching versus time for $\{PEI/PSS\}_n$ (n = 0-3) multilayers (from top to bottom) for FD 2MDa. Solid lines indicate the fitted results obtained using Crank's mathematical model.

The results presented in the time-dependent release measurements were reorganized into a bar graph for direct comparison as seen in Figure 4.8a. The results shown are for the final ratio of supernatant intensity to the full suspension intensity at the end of four days with the standard deviation calculated using three separate readings in the spectrofluorometer. The first obvious point of note is the clear reduction in total leaching of the encapsulated material due to application of multilayer coatings for all three coatings used. In terms of best retaining the encapsulated molecules, it can be interpreted from this chart that the $\{PAH/PSS\}_n$ multilayers are most effective in reducing leaching of the 2MDa FD from the alginate microspheres compared to $\{PDDA/PSS\}_n$ or $\{PEI/PSS\}_n$ multilayers. A reason for this effectiveness might be that the $\{PAH/PSS\}_n$ multilayers are more tightly packed than the $\{PDDA/PSS\}_n$ or the $\{PEI/PSS\}_n$

multilayers, which helps in keeping the material inside the microspheres. $\{PEI/PSS\}_n$ multilayers form thinner layers, thus exhibiting worse leaching results.[162,183] The leaching rate for the release of FD 2MDa from alginate microspheres coated with the three different polyelectrolytes has been plotted as a bar graph in Figure 4.8b. This plot once again confirms that the FD is released from PEI/PSS coated microspheres at a much faster rate than the PDDA/PSS and PAH/PSS-coated microspheres. The release rate is also affected by the number of coating layers on the alginate microspheres.

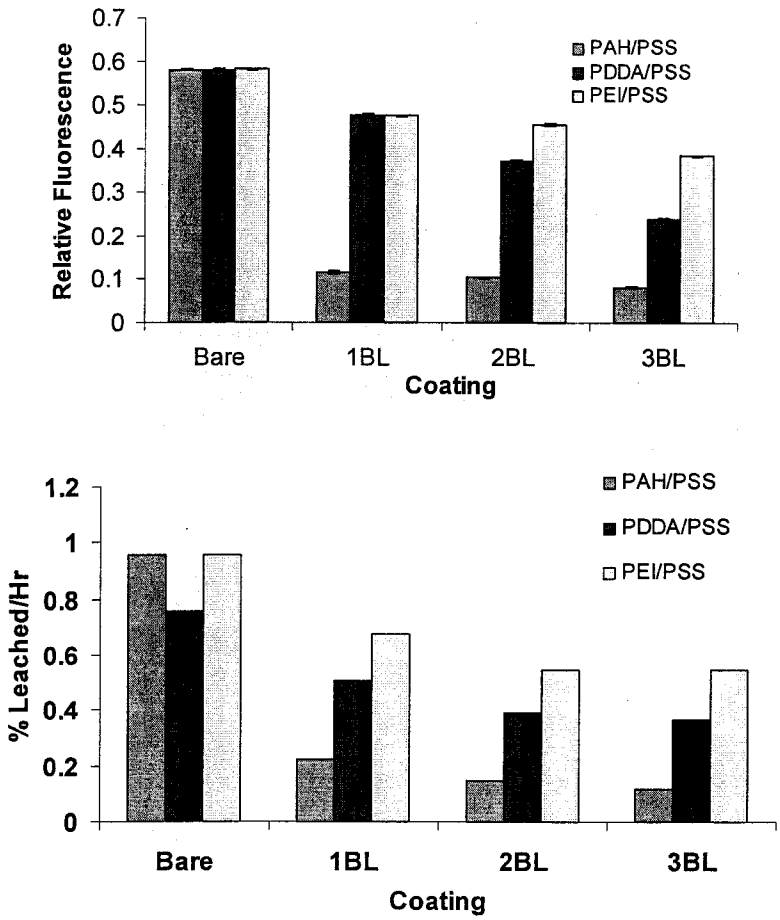

Figure 4.8. (a) Comparison of coating on leaching of 2MDa FD from alginate microspheres. Error bars are calculated using three separate readings in the spectrofluorometer (b) Comparison of rate of leaching of 2MDa FD from alginate microspheres.

4.3.2 Size-Dependent Release of FITC-Dextran

The experiments described in detail above were repeated for each of the coating configurations and thicknesses to study the release of dextran molecules of different molecular weights. The total fractional loss after four days of wet storage, were calculated as averages of three successive readings in the spectrofluorometer. The results were compiled in bar graphs for each polyelectrolyte combination to better understand the effect of molecular weight and coating thickness on leaching of the macromolecules through alginate microspheres. Figures 4.9-4.11 contain these measurements for each case, plotted in semilog-y graphs grouped by molecular weight. By comparing the data between graphs, the influence of the specific coatings can be directly compared.

The losses measured for different molecular weight FD from $\{PAH/PSS\}_n$-coated alginate microspheres are presented in Figure 4.9. It is clear from these results that the leaching of the encapsulated material from the alginate microspheres is dependent on the molecular weight of the encapsulated material, though the size dependence is not as strong for bare alginate spheres as those with polyelectrolyte coatings. There was no significant difference between losses observed for any of the molecular weights considered below 2MDa when encapsulated in alginate; however, when the PAH/PSS overlayers were applied, the total loss of FD was observed to decrease. Thus, in general, the larger molecular weight FD had lower losses compared to the lower molecular weight FD.

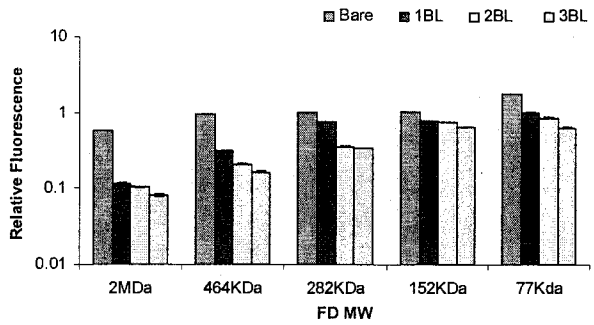

Figure 4.9. Comparison of leaching through $\{PAH/PSS\}_n$ (n = 0-3) multilayers for different MW FD. Error bars are calculated using three separate readings in the spectrofluorometer.

Furthermore, when plotting the data together on a log scale, the general trend of decreasing permeability of the particles to FD can be observed for increasing layers of polyelectrolyte coating. Interestingly, for the smallest molecules (77kDa) encapsulated within the microspheres coated with $\{PAH/PSS\}_n$ (n = 0-3), total release of FD was found to be less than some of the higher molecular weight molecules. This result might be attributed to self quenching; when high loading concentrations or high labeling ratios are used, quenching of one fluorophore by another tends to occur.

To confirm this hypothesis, scans were taken of the supernatants after diluting them with PBS buffer. The diluted supernatant showed a higher fluorescence emission signal than the undiluted supernatant, thus proving that quenching is the cause for lowered FITC fluorescence seen from 77kDa FD samples. The graphs were thus modified to reflect the actual fluorescence intensity after correcting for self quenching.

The leaching results obtained with different MW FD was then fitted according to Crank's mathematical model to calculate the diffusion coefficient of different MW FD

from the microspheres coated with {PAH/PSS} multilayers. These results have been presented in Table 4.1. What is immediately evident is that, starting with the uncoated microspheres, there is a decreasing trend in the values for the diffusion coefficients for the different molecular weights with each additional bilayer. The higher molecular weight FD leaches much slower than the lower molecular weight FD and in all cases there is a reduction in the diffusion coefficient values with each additional bilayer. These results follow the same trend described in Figure 4.9. The model was applied by modifying Crank's equation to reflect the difference in molar concentration of the FD used for the separate experiments with different MW of the FD.

Table 4.1. Diffusion coefficients for dextran in alginate microspheres coated with PAH/PSS nanofilms ($D_e \times 10^{-12}$ cm^2/sec). FD stands for FITC-Dextran. Zero bilayer is uncoated microsphere. Variability in D_e is less than 1% for n = 3 measurements.

Molecular weight of FD	Bilayers			
	0	1	2	3
2MDa	2.90×10^{-1}	5.25×10^{-2}	4.29×10^{-2}	4.10×10^{-2}
464kDa	2.79	4.28×10^{-1}	2.90×10^{-1}	9.66×10^{-2}
282kDa	4.99	4.34×10^{-1}	3.43×10^{-1}	2.83×10^{-1}
152kDa	7.32	4.85×10^{-1}	4.60×10^{-1}	3.04×10^{-1}
77kDa	18.2	4.4	6.6×10^{-1}	2.8×10^{-1}

Similarly, Figure 4.10 contains the bar graph for release of FD from alginate microspheres coated with $\{PDDA/PSS\}_n$ multilayers. These results show that $\{PDDA/PSS\}_n$ multilayers are not as effective in reducing the total leaching of the encapsulated material compared to $\{PAH/PSS\}_n$ multilayers. The amount of FD leached from the alginate microspheres for lower molecular weight FD is not significantly different from the uncoated microspheres, and in all cases nearly 40% of the encapsulated material has been lost, even after coating the microspheres with up to three bilayers of

PDDA/PSS. In fact, for all dextrans smaller than 2MDa, there is no apparent difference in total loss.

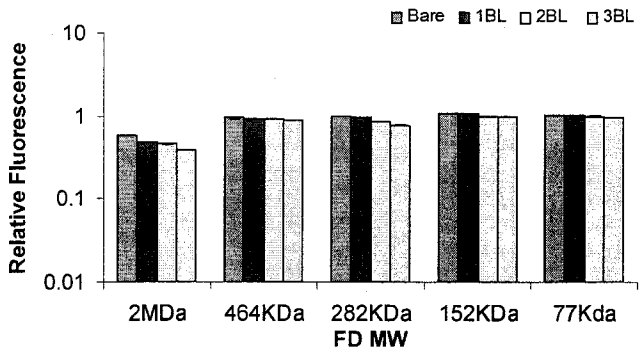

Figure 4.10. Comparison of leaching through $\{PDDA/PSS\}_n$ (n = 0-3) multilayers for different MW FD. Error bars are calculated using three separate readings in the spectrofluorometer.

Similarly, the diffusion coefficients comparing the different molecular weight FD through alginate microspheres coated with PDDA/PSS multilayers is presented in Table 4.2. The higher molecular weight FD exhibit a reduced diffusion coefficient with each additional bilayer, but there is no significant change in the diffusion coefficients for lower molecular weight FD's. These results confirm the observations made earlier regarding the poor stability provided by {PDDA/PSS} nanofilms to the encapsulated FD.

Table 4.2. Diffusion coefficients for dextran in alginate microspheres coated with PDDA/PSS nanofilms ($D_e \times 10^{-12}$ cm^2/sec). FD stands for FITC-Dextran. Zero bilayer is uncoated microsphere. Variability in D_e is less than 1% for n = 3 measurements.

Molecular weight of FD	Bilayers			
	0	1	2	3
2MDa	4.15×10^{-1}	3.19×10^{-1}	3.05×10^{-1}	2.92×10^{-1}
464kDa	2.36	3.61×10^{-1}	3.37×10^{-1}	3.18×10^{-1}
282kDa	5.31	3.18	1.48	1.36
152kDa	7.08	6.66	2.70	2.60
77kDa	18.2	15.3	14.4	15.1

Finally, the results for release of FD from alginate microspheres coated with $\{PEI/PSS\}_n$ multilayers are presented in Figure 4.11. By comparison with Figure 4.10, it is clear that the total loss figures for $\{PEI/PSS\}_n$ multilayers are nearly identical to what was observed for $\{PDDA/PSS\}_n$ multilayers. For all dextrans less than 2MDa, the results for the coated microspheres are essentially the same as what was observed for bare microspheres. It is possible that the films formed from PDDA/PSS and PEI/PSS are porous, because polyelectrolytes are adsorbing not as extended chains but either as coils or as aggregates, presumably having formed such structure in solution. Adsorption of such large structures will give rise to a rough surface consisting of domains with characteristic length scale related to the size of the adsorbing entities[88,183] Aggregation was observed for PEI/PSS and PDDA/PSS coated microspheres, which might be another reason for insufficient coverage of the microspheres compared to PAH/PSS multilayers, thus leading to greater leaching through these coatings.

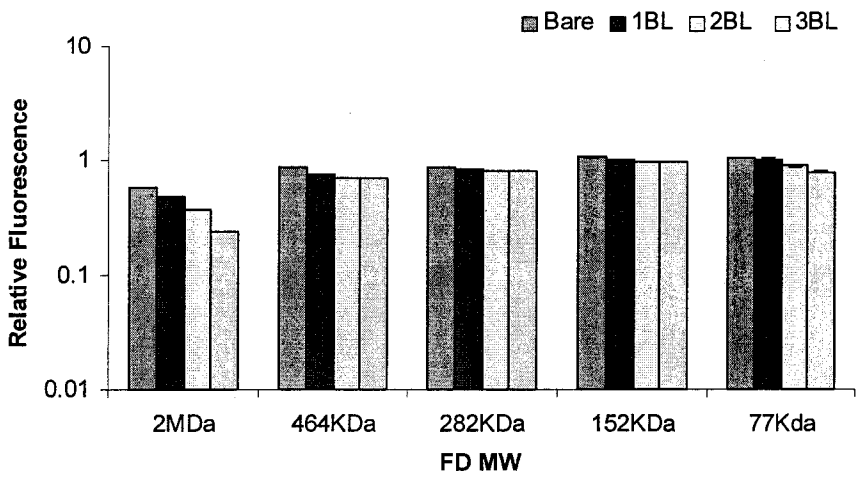

Figure 4.11. Comparison of leaching through $\{PEI/PSS\}_n$ (n = 0-3) multilayers for different MW FD. Error bars are calculated using three separate readings in the spectrofluorometer.

Similarly, the diffusion coefficients comparing the different molecular weight FD through alginate microspheres coated with PEI/PSS multilayers is presented in Table 4.3. There is no significant change in the diffusion coefficients for the FD through alginate microspheres for all cases except the 2MDa FD. These results confirm the observations made earlier regarding the poor stability provided by {PEI/PSS} nanofilms to the encapsulated FD.

Table 4.3. Diffusion coefficients for dextran in alginate microspheres coated with PEI/PSS nanofilms ($D_e \times 10^{-12}$ cm^2/sec). FD stands for FITC-Dextran. Zero bilayer is uncoated microsphere. Variability in D_e is less than 1% for n = 3 measurements.

Molecular weight of FD	Bilayers			
	0	1	2	3
2MDa	3.67×10^{-1}	2.90×10^{-1}	2.28×10^{-1}	2.12×10^{-1}
464kDa	2.48	7.5×10^{-1}	7.46×10^{-1}	7.33×10^{-1}
282kDa	6.79	4.38	3.48	3.05
152kDa	7.95	6.11	5.54	5.18
77kDa	18.2	12.4	13.2	12.2

These results are in agreement with the findings of Okano et al, who investigated the effect of calcium alginate gel dissolution on release of different molecular weight dextran[81,133] They reported that the dextran was released in a molecular weight dependent manner: a diffusion controlled release for lower molecular weight dextran, and alginate gel disintegration governed release for a higher molecular weight dextran. Their study, however, did not involve the release of dextran with multilayer coatings on calcium alginate gels. Osmotic pressure was suggested as a major factor in facilitating gel disintegration, which can be reduced with multilayer coatings.[134]

In summary of these findings, the experimental results show that the application of multilayer thin films to the alginate microspheres was effective in reducing the loss of the

encapsulated material from the microspheres, with $\{PAH/PSS\}_n$ multilayers being more effective than the $\{PDDA/PSS\}_n$ and $\{PEI/PSS\}_n$ multilayers. There are various other materials that can similarly be used as coatings to decrease leaching of the encapsulated macromolecule, and the results presented here suggest that different materials will behave differently in terms of reducing loss through the macromolecule carrier.

Since the loss of a model macromolecule, FITC-dextran, from micron-sized alginate spheres coated with different polyelectrolytes was studied in this experiment, it is appropriate to further discuss the relation of these studies to potential encapsulation of other molecules. For example, the biosensor applications discussed in the introduction require immobilization of functional enzymes to drive reactions as part of the transduction scheme. On one hand, the matrix should ensure efficient, stable entrapment of the enzyme, which can be aided by the application of additional coatings as demonstrated here. However, while diffusion from the gel matrix depends upon porosity of the gel and concentration gradients, the influence of electrostatic forces between the negatively-charged alginate and the charged encapsulant cannot be neglected. Recent work has shown that positively charged macromolecules spontaneously load into alginate-templated polyelectrolyte capsules, and can be expected to be more stable than the methods of loading currently in use.[184] The glucose oxidase is anionic at pH 7.4 and is expected to be repelled by the alginate matrix. The molecular weight of the glucose oxidase enzyme used in the next part of this study is 160kDa, and it remains to be seen if the application of similar coating combinations will be successful in retaining the enzyme inside the alginate microspheres.

CHAPTER 5

ENZYME STABILIZATION - PAH/PSS, PDDA/PSS AND PAH/PAA COATINGS

Work presented in the previous chapters has shown that the application of self-assembled ultrathin film coatings can reduce leaching of different molecular weight dextran from alginate microspheres, but because of Coulombic interaction, the joint force between layers may not be strong enough to prevent complete leaching. This problem can be solved by causing the layers to crosslink. The different strategies make use of glutaraldehyde[185] and incorporate diazoresins[144] that are subsequently exposed to UV-light.[147] Crosslinked films have been shown to be more stable at higher pH values and have increased resistance to solvent etching.[148,149] This strategy resembles that used by other groups when forming layered polymer films with covalent linkages.[151,186] However, postdeposition cross-linking preserves the advantages inherent in synthesis by simple electrostatic adsorption with minimal deposition times and no need for organic solvents. The work described here is the integration of the LbL self assembly technique with the immobilization of glucose oxidase enzyme (GOx) in alginate microspheres, both using commonly used polyelectrolyte material combinations and crosslinked films to reduce leaching. In this work, alginate microspheres of diameter <10μm were used. To gain insight into the relationship between GOx loading and release with variable number of self-assembled layers of poly(allylamine hydrochloride), poly (diallyldimethyl

ammonium chloride), and poly(sodium 4-styrenesulfonate) on the gel beads, the loss of encapsulated material was monitored spectroscopically via the FITC-labeled glucose oxidase which was loaded into the calcium-alginate gel beads during the emulsion process. As an alternative method, we also investigated the cross-linking of poly(allylamine hydrochloride) and poly(acrylic acid) with water soluble 1-ethyl-3-(3-dimethylaminopropyl) carbodiimide (EDC), a reaction that is favored by the presence of N-hydroxysuccinimide (NHS). The enzyme activity was monitored over time and compared over different polyelectrolyte coatings. This work describes the fabrication method used to produce the microspheres, their characterization, and the effect of ultrathin film coatings on the leaching of the enzyme and their stabilization inside alginate microspheres towards the fabrication of a glucose sensor. The modeling for calculating the diffusion coefficient of the encapsulated glucose oxidase through uncoated and coated alginate microspheres was also accomplished and diffusion coefficient values compared over different coating combinations used.

5.1 Layer-by-Layer Self Assembly of Ultrathin Films on Alginate Microspheres

Two cationic polyelectrolytes (PAH, PDDA) were used for the layer-by-layer self assembly application of the ultrathin film coatings, while PSS, and PAA were the anionic polyions used. For deposition of each coating, 1.5mL of cationic polyelectrolyte (2mg/mL in DI water with 0.25M $CaCl_2$) was added to a microcentrifuge tube containing 200μL of microsphere suspension (approx 10^6 spheres). Adsorption was allowed to proceed for twenty minutes, after which time the suspension was centrifuged to separate the spheres from remaining unadsorbed polyelectrolyte. The microspheres were then

triple rinsed with DI water by successive centrifugation cycles. A solution of the anionic polyelectrolyte (1.5mL of 2mg/mL PSS or PAA in DI water with 0.25M $CaCl_2$) was then added; the spheres were centrifuged to remove the supernatant, and then rinsed three times to complete one bilayer. The surface charge of the microspheres was measured using the zeta potential analyzer after rinsing and prior to addition of each polyelectrolyte. This process was repeated until a total of three bilayer polyelectrolyte films were realized.

5.2 Crosslinking of PAH and PAA Multilayers

EDC was used to conjugate the PAH/PAA multilayers using NHS as a catalyst. The coupling chemistry is based upon the reaction of activated carboxylic sites with primary amine groups.[187] Briefly, 10 mL of a 0.05M phosphate buffered saline solution (pH 5.0) was prepared and 200 μL of one to three bilayers PAH/PAA coated alginate microspheres were transferred to the solution. To the same solution, 20 mg of EDC and 12 mg of NHS were then dissolved and stirred for three hours. The spheres were then centrifuged to separate the unreacted EDC-NHS and rinsed three times before using them for the leaching and activity studies.

5.3 Determination of Glucose Oxidase Leaching from Alginate Microspheres

The leaching of glucose oxidase from alginate microspheres (both uncoated and coated) was accomplished using the protocol described in section 3.5. The leaching results were then fitted in MATLAB using Crank's equations as described in section 2.14,

to calculate the diffusion coefficient of glucose oxidase through the uncoated and coated alginate microspheres.

5.4 Activity of Glucose Oxidase in Alginate Microspheres

The activity assay of the encapsulated glucose oxidase enzyme was performed according to the protocol described in section 3.6. The experiment was repeated for the polyelectrolyte-coated microspheres over a period of three months and the results compared by calculating the slope of the curves. In each case, the results were normalized to the mass of glucose oxidase present in the spheres as determined using the Lowry assay. Both the leaching and the activity results were analyzed using the two-tailed student's t-test.

5.5 Results and Discussion

5.5.1 Fabrication Results

A confocal micrograph of microspheres with encapsulated FITC-GOx formed with the emulsification technique is presented in Figure 5.1. The spheres appear bright green with uniform intensity distribution when imaged with the confocal microscope. The average size was found to be $2.68 \pm 0.63\mu m$ for a sample size of ~3000 spheres.

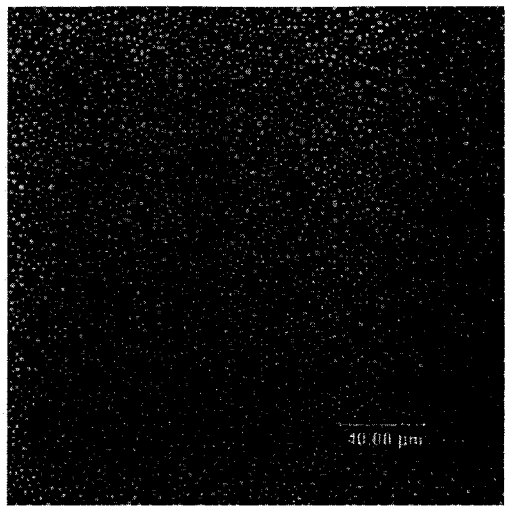

Figure 5.1. Confocal image of FITC-glucose oxidase loaded microspheres with a scale bar of 40μm.

The graph for the size distribution obtained using the Coulter counter is shown in Figure 5.2, which proves that the majority of spheres obtained are in the 2-3μm range. Because of the high sonication power used to disperse the emulsion, the final droplet size was typically less than 5μm diameter. Following fabrication and size characterization of the alginate microspheres, deposition of multilayer nanofilms on the negatively charged microspheres was investigated.

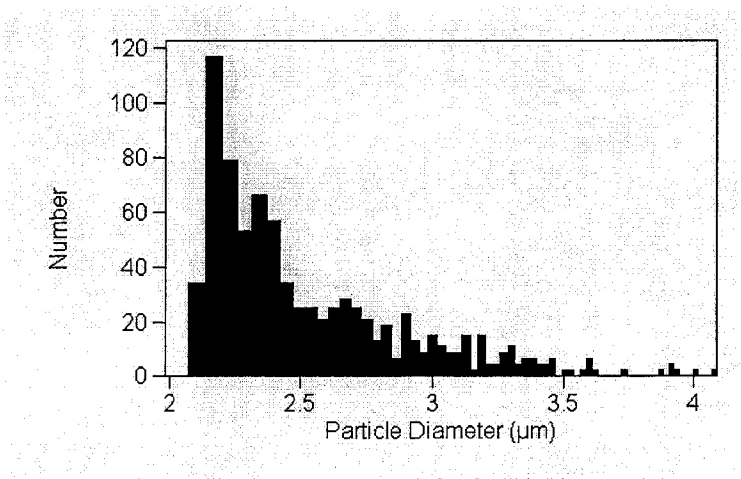

Figure 5.2. Sizing histogram obtained using the Coulter counter.

The surface charge of the polyelectrolyte-coated microspheres was measured using the zeta potential analyzer; measured values which are average of three readings are presented in Figure 5.3. These results verify reversal of the surface charge of the microspheres at each step due to polyelectrolyte adsorption. The assembly of nanofilm coatings was also confirmed using CLSM as shown in Figure 5.4. As mentioned, multilayer coatings on top of alginate microspheres has been demonstrated by Pommersheim et al., but there has no report demonstrating surface charge reversal by means of the zeta potential for the commonly used polyelectrolytes on top of alginate microspheres.[138,140]

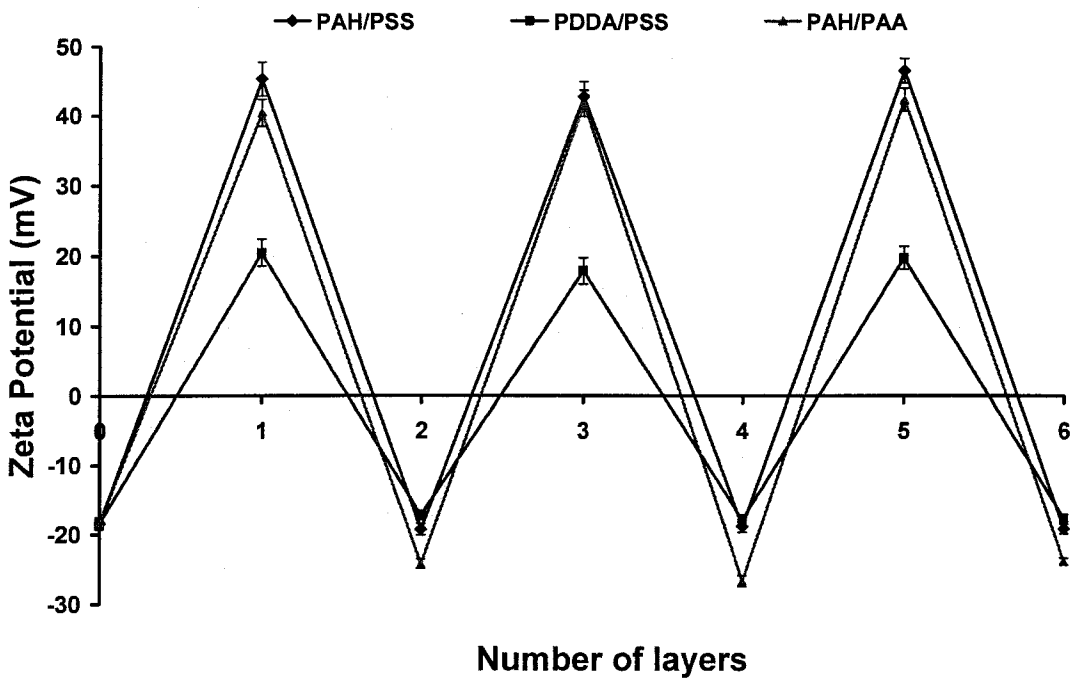

Figure 5.3. Charge reversal at each coating step demonstrated by the ζ-potential.

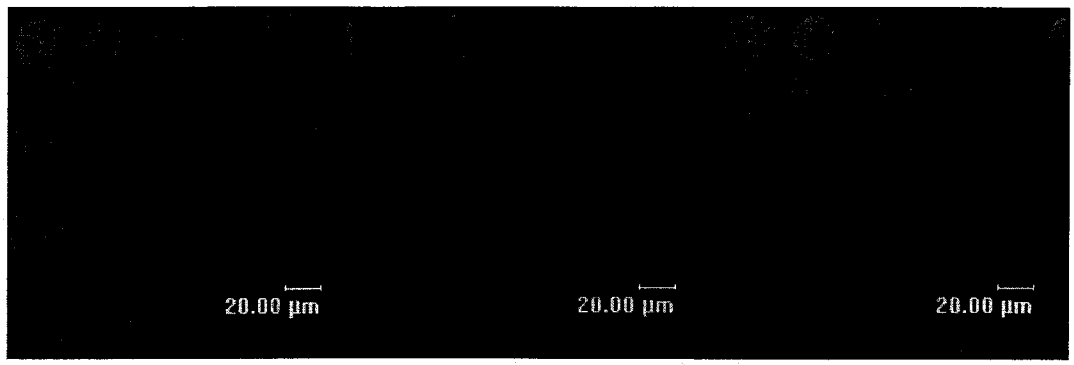

(a) (b) (c)

Figure 5.4. Confocal micrographs of alginate microspheres containing glucose oxidase enzyme. (a) Alginate microspheres with encapsulated enzyme (green dye labeled), (b) microspheres coated with polyelectrolytes (red dye labeled), (c) micrograph depicting the overlaid image

5.5.2 Leaching of FITC-Glucose Oxidase from Alginate Microspheres

Loss of FITC-GOx from the alginate microspheres was studied using fluorescence spectroscopy, where release of the encapsulated FITC-GOx from the microspheres resulted in an increase in the fluorescence intensity of the supernatant. The leaching results for the alginate microspheres containing the enzyme were compared between the different polyelectrolyte materials used for the coating process and the number of coating layers. Results from a typical experiment are given in Figure 5.5, where the leached amount for FITC-GOx is plotted versus time for microspheres coated with $\{PAH/PSS\}_n$ (n = 0-3). Some interesting observations may be made from this graph. The results show that approximately 50% of the encapsulated material comes out of bare microspheres within four days. This result suggests that bare alginate microspheres have relatively large pores that allow large and small molecules to pass through. Since diffusion-driven leaching would result in equilibrium between the compartments, it is believed that eventually all of the encapsulated material is lost.

Swelling of the alginate matrix could also be attributed for the fast release of the encapsulant.[188,189] The "swelling–dissolution–erosion" process is highly complex. In systems based on sodium alginate cross-linked with calcium chloride, the osmotic pressure gradient that exists between the alginate gel and the environment comprises an important factor in the swelling process. Also, release behavior of drugs from alginate beads have been reported to be influenced by the ionic nature of the drug, i.e., cationic, anionic, and non-ionic.[111] Glucose oxidase being anionic at pH 7.4, will repel the negatively charged alginate matrix, leading to faster release.

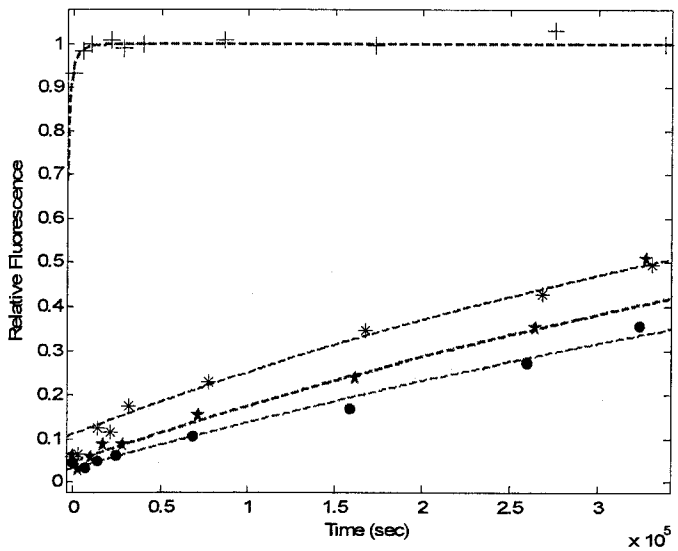

Figure 5.5. Leaching versus time for $\{PAH/PSS\}_n$ (n = 0-3) multilayers for FITC-GOx. Captions include bare microspheres (+); spheres coated with one bilayer (•); spheres coated with two bilayers (⋆) and spheres coated with three bilayers (•). Dashed lines indicate the fitted results.

In contrast, the release profiles for microspheres coated with PAH/PSS multilayer nanofilms demonstrate that the application of these coatings significantly reduces the loss of encapsulated material. The total leaching of the FITC-GOx drops to less than 30%

over the same time span. These results suggest that the nanofilm coatings, applied in a simple, fast, and mild manner to microscale templates, are effective in reducing loss of the large encapsulated macromolecule from small microspheres. However, the relative effect of the different nanofilm combination is also interesting to study. Thus three polyelectrolyte combinations were compared. {PDDA/PSS} was chosen as a strong-strong polyelectrolyte pair, while {PAH/PSS} was the weak-strong pair, and {PAH/PAA} was chosen as the crosslinked pair to allow direct comparison of the effect of these commonly used polyelectrolytes. Time-dependent release profiles for FITC-GOx loaded microspheres coated with $\{PDDA/PSS\}_n$ (n = 0-3) multilayers are shown in Figure 5.6.

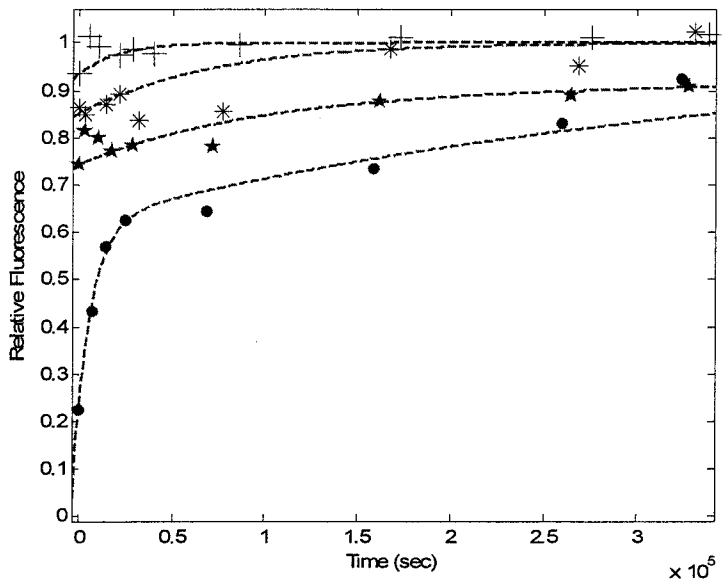

Figure 5.6. Leaching versus time for $\{PDDA/PSS\}_n$ (n = 0-3) multilayers for FITC-GOx. Captions include bare microspheres (+); spheres coated with one bilayer (·); spheres coated with two bilayers (⋆) and spheres coated with three bilayers (•). Dashed lines indicate the fitted results.

The total leaching for the bare microspheres is still seen to be around 50% over the time span. However, by comparison to the {PAH/PSS} films, it is clear that {PDDA/PSS} films are not as effective in stopping loss of encapsulated material, as about 45% of the encapsulated GOx is still lost from the microspheres coated with a single bilayer over the same time period. One reason for this is that the $\{PAH/PSS\}_n$ multilayers are thicker and more tightly packed than the $\{PDDA/PSS\}_n$ multilayers, which helps in keeping the material inside the microspheres.[162,183] It is also possible that the films formed from {PDDA/PSS} are more porous, because polyelectrolytes are adsorbing not as extended chains but either as coils or as aggregates.[183]

Similarly, the time dependent release profiles for microspheres coated with PAH/PAA multilayer nanofilms show that the application of these coatings does not significantly reduce the loss of encapsulated material, and the total leaching of the GOx still remains around 50% over the same time span (Figure 5.7[a]). Furthermore, an increase in leaching with more bilayers is observed. This increase might be attributed to the adsorption/dissolution process reported by Kovacevic et al.[190] They showed that in solutions containing both weak polyelectrolytes and appropriate salt, the buildup of multilayers is modified and becomes an adsorption/dissolution process. In contrast, the release profiles for microspheres coated with crosslinked PAH/PAA multilayer nanofilms show that the application of these coatings does in fact, significantly reduce the loss of encapsulated material (Figure 5.7[b]). The total leaching of the GOx drops to less than 10% for crosslinked $\{PAH/PAA\}_1$ over the same time span. These results suggest that the crosslinking of the coatings somehow reduces the pore sizes in the applied multilayers, enabling better retention of the enzyme. As a consequence of crosslinking,

the rigidity and density of the films may also be increased,[170] which might explain the reduced leaching through crosslinked multilayers.

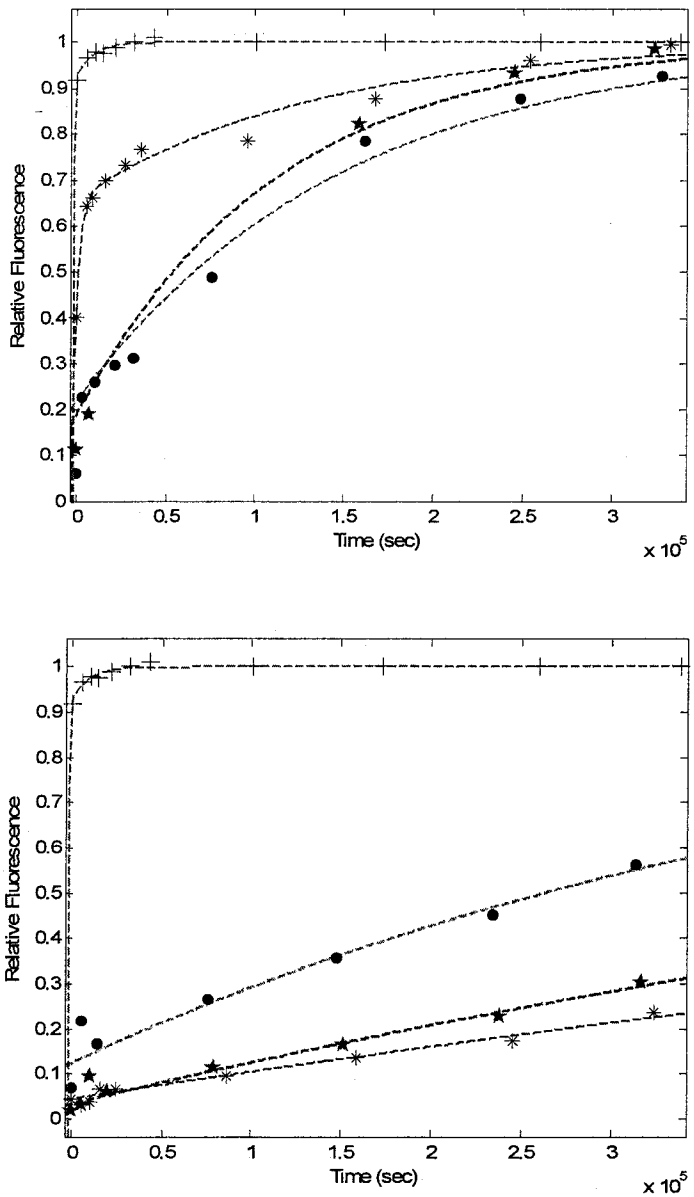

Figure 5.7. (a) Leaching versus time for $\{PAH/PAA\}_n$ (n = 0-3) multilayers for FITC-GOx. (b) Leaching versus time for crosslinked $\{PAH/PAA\}_n$ (n = 0-3) multilayers for FITC-GOx. Captions include bare microspheres (+); spheres coated with one bilayer (•); spheres coated with two bilayers (⋆) and spheres coated with three bilayers (•). Dashed lines indicate the fitted results.

The results presented in the time-dependent release measurements described are reorganized into a bar graph for direct comparison in Figure 5.8(a). The results shown are for total leached amount at the end of four days (n=3 measurements).

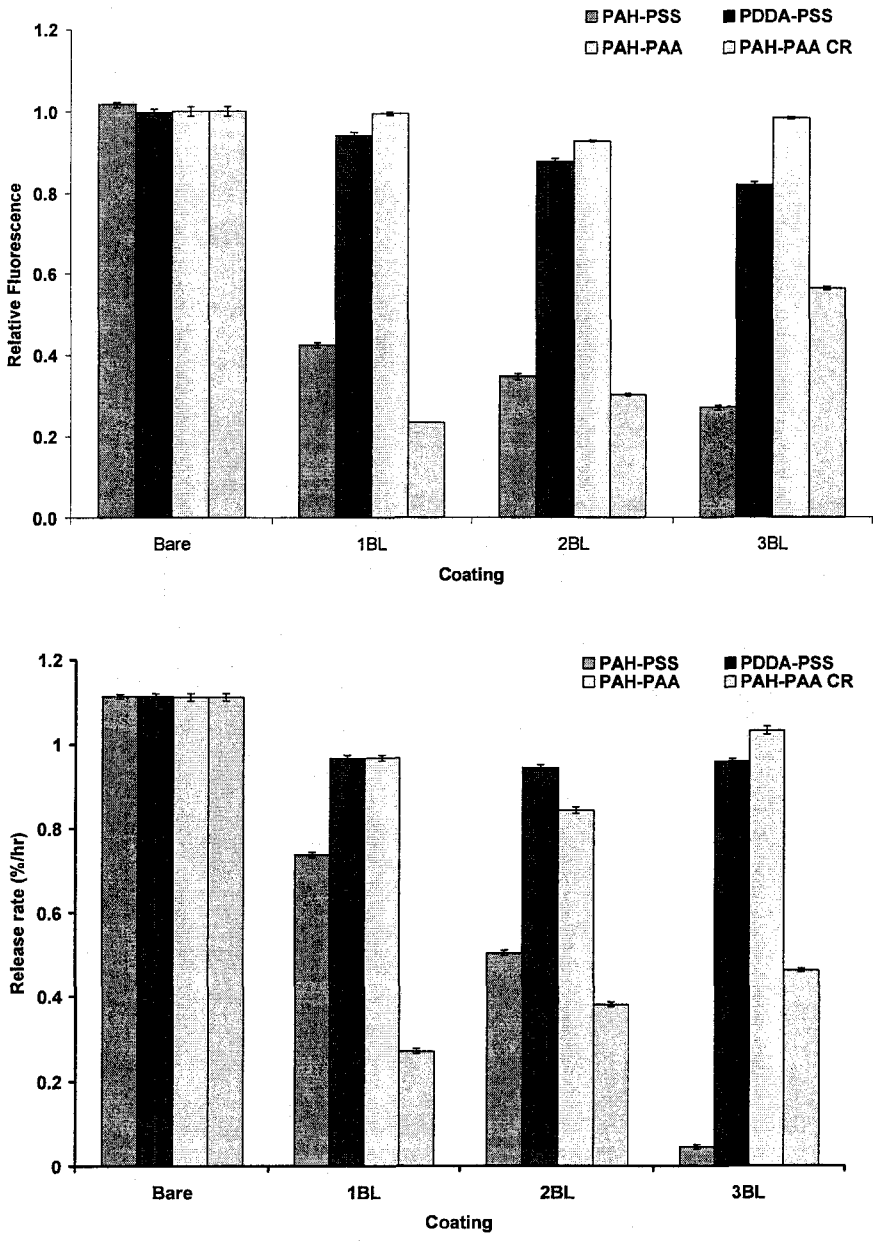

Figure 5.8. (a) Comparison of the effects of the number of coating layers on GOx leaching from alginate microspheres, (b) Leaching rate comparison for different polyelectrolytes from alginate microspheres. The legend CR stands for crosslinked.

In terms of best retaining the encapsulated molecules, it can be interpreted from this chart that the $\{PAH/PAA\}_1$ multilayer is most effective in reducing leaching of the FITC-GOx from the alginate microspheres compared to $\{PDDA/PSS\}_n$ and $\{PAH/PSS\}_n$ multilayers confirming our hypothesis that the crosslinking does in fact lead to stronger attraction between the layers compared to plain electrostatic attraction. Similarly, the leaching rate of the enzyme has been plotted in Figure 5.8(b) for the four different combinations used. It is evident that the additional layers do not make a difference in the leaching rate of the enzyme through the alginate microspheres for PDDA/PSS multilayers. This leaching rate result agrees with the leaching results presented before. On the other hand, the leaching rate of the enzyme through PAH/PSS multilayer coated microspheres decreases with the addition of each layer, reaching a very low value for the 3BL PAH/PSS coated microspheres, implying that there is increasing obstruction to the diffusion of the enzyme from the microsphere with each additional layer. On the other hand, the leaching rate for the crosslinked $\{PAH/PAA\}_1$ is lowest for the {PAH/PAA} multilayers, again confirming that crosslinking has reduced the porosity of the coatings.

5.5.3 Diffusion Coefficient for Glucose Oxidase through Uncoated and Coated Alginate Microspheres

MATLAB curve fitting tool was used to fit the experimental results using Crank's mathematical model for diffusion through a sphere, to enable the calculation of the diffusion coefficients for the enzyme out of alginate microspheres for the different materials used. The results have been presented in Table 5.1. What is immediately evident is that the effective diffusion coefficient of the enzyme through crosslinked $\{PAH/PAA\}_n$ coated alginate microspheres is about 100X to 400X smaller than the

diffusion coefficient through uncoated microspheres. This result confirms the observations that were made earlier regarding the crosslinked films. The {PDDA/PSS} coated microspheres, on the other hand, are much more porous than the {PAH/PAA} coated microspheres with the effective diffusion coefficient of glucose oxidase being less than 2X smaller than that from uncoated microspheres. Finally, the effective diffusion coefficients of the enzyme through {PAH/PSS} coated microspheres are between 150X and 200X smaller than the diffusion coefficient through uncoated microspheres.

Table 5.1. Diffusion coefficients for glucose oxidase in alginate microspheres coated with different polyelectrolyte nanofilms ($D_e \times 10^{-12}$ cm^2/sec). Variability in the estimated values is less than 1%.

Film combination	Bilayers		
	1	2	3
PDDA/PSS	2.1	1.54	1.28
PAH/PSS	1.63×10^{-2}	1.41×10^{-2}	1.31×10^{-2}
PAH/PAA	9.86×10^{-1}	6.24×10^{-2}	8.26×10^{-2}
Crosslinked PAH/PAA	5.87×10^{-3}	9.07×10^{-3}	1.94×10^{-2}

*** Uncoated microspheres have a D_e of 2.47×10^{-12} cm^2/sec**

In summary of these findings, the experimental results show that the application of crosslinked multilayer thin films to the alginate microspheres was effective in reducing the loss of the encapsulated material from the microspheres, with crosslinked $\{PAH/PAA\}_1$ multilayers being more effective than the $\{PAH/PSS\}_n$ or the $\{PDDA/PSS\}_n$ multilayers. These results can be helpful in tailoring the transport properties of the alginate microspheres and will ultimately be used in encapsulating and protecting sensor chemistry for implantable enzymatic systems.

5.5.4 Activity and Stabilization of Encapsulated Glucose Oxidase in Alginate Microspheres

In order to use the GOx-encapsulated alginate microspheres as practical glucose sensors, stable activity of the encapsulated enzyme must be realized. As a baseline for further comparisons, the activity of uncoated, $\{PAH/PSS\}_n$, $\{PDDA/PSS\}_n$, $\{PAH/PAA\}_n$, and $\{PAH/PAA\}_n$-crosslinked (n=1-3) coated microspheres was assessed immediately following microsphere fabrication and following 1, 4, and 12 weeks of storage in phosphate buffer. Figures 5.9(a-d) show the results of this experiment with all activities normalized to total enzyme mass per sample as determined by Lowry assay. The amount of enzyme calculated using the Lowry assay at the start of the experiment is shown in Table 5.2. The molar concentration of GOx at the end of one week, four weeks, and twelve weeks can be calculated from the leaching data.

Table 5.2. Comparison of molar concentration of GOx inside alginate microspheres versus different nanofilm coatings (CR stands for crosslinked).

Film combination	GOx concentration (mM)		
	1BL	2BL	3BL
PDDA/PSS	62	53.2	50.7
PAH/PSS	60.6	54.7	61.5
PAH/PAA	49.4	50.2	49.7
Crosslinked PAH/PAA	55.7	52.4	50.4

*** Uncoated microspheres have 66.7mM GOx, initially.**

Figure 5.9(a-d) contains activities per unit mass of uncoated, $\{PAH/PSS\}_n$, and $\{PDDA/PSS\}_n$ (n=1-3) coated microspheres after 1, 4, and 12 weeks wet storage. It is instructive to begin the analysis by observing the activity of uncoated microspheres over 12 weeks (Figure 5.9[a]). After 1 week, the effective activity of the uncoated microspheres is decreased by approximately 78% from the initial value. Over the next 11 weeks, there is no further significant reduction in effective activity for the uncoated microspheres. Thus, while the activity of the uncoated microspheres is remarkably stable after the first week of wet storage, the process is far from efficient due to the large loss in effective activity over the first week. This initial loss in effective activity warrants a closer look. Since the effective activity is the activity normalized to enzyme mass, it is counter-intuitive to expect a difference in effective activity over time due to enzyme leaching.

However, if one considers the existence of two populations of encapsulated enzyme, one which is weakly immobilized, and one which is strongly immobilized. This difference may be easily explained. The weakly immobilized enzyme is expected to have a relatively high effective activity, since it is highly mobile and presumably more accessible to enzyme substrates than the strongly immobilized enzyme, which is expected to have lower effective activity. Thus, the initial loss of activity was attributed to leaching of a mobile fraction of enzyme not physically attached to the alginate matrix after encapsulation; this "free" enzyme was assumed to have a greater effective activity per unit mass than the immobilized enzyme, which is responsible for the activity of the microspheres after the mobile GOx has leached from the spheres. To test this theory, the activity of glucose oxidase in solution was measured and normalized by unit mass, then

compared to the activity per unit mass of alginate microspheres freshly prepared (which presumably contain both "free" and alginate-immobilized GOx), and after 4 weeks of storage (which presumably contains only alginate-immobilized GOx due to their excellent stability after this point). It was discovered that the activity of GOx stably immobilized within the alginate microspheres, when compared on a per unit mass basis, was only 5% of free GOx activity, while the activity of freshly prepared alginate microspheres was 24% of free GOx activity. If all of the encapsulated enzyme were either immobilized on the alginate matrix or free to diffuse about the microsphere interior, one would expect the effective activity to be the same regardless of the amount of enzyme leached, since the activity is normalized to unit mass. Thus, the discrepancy in effective activity for freshly prepared alginate microspheres and microspheres from which a significant mass of enzyme has leached lends credence to the assumption that initially, the enzyme encapsulated within the microsphere is a mixture of free and immobilized enzyme, whereas after one week, the free enzyme has leached out leaving only the immobilized enzyme. Thus, the goal of multilayer nanofilm coatings is to retain as much as possible of the initially encapsulated mobile GOx within the microspheres, resulting in higher catalytic activity.

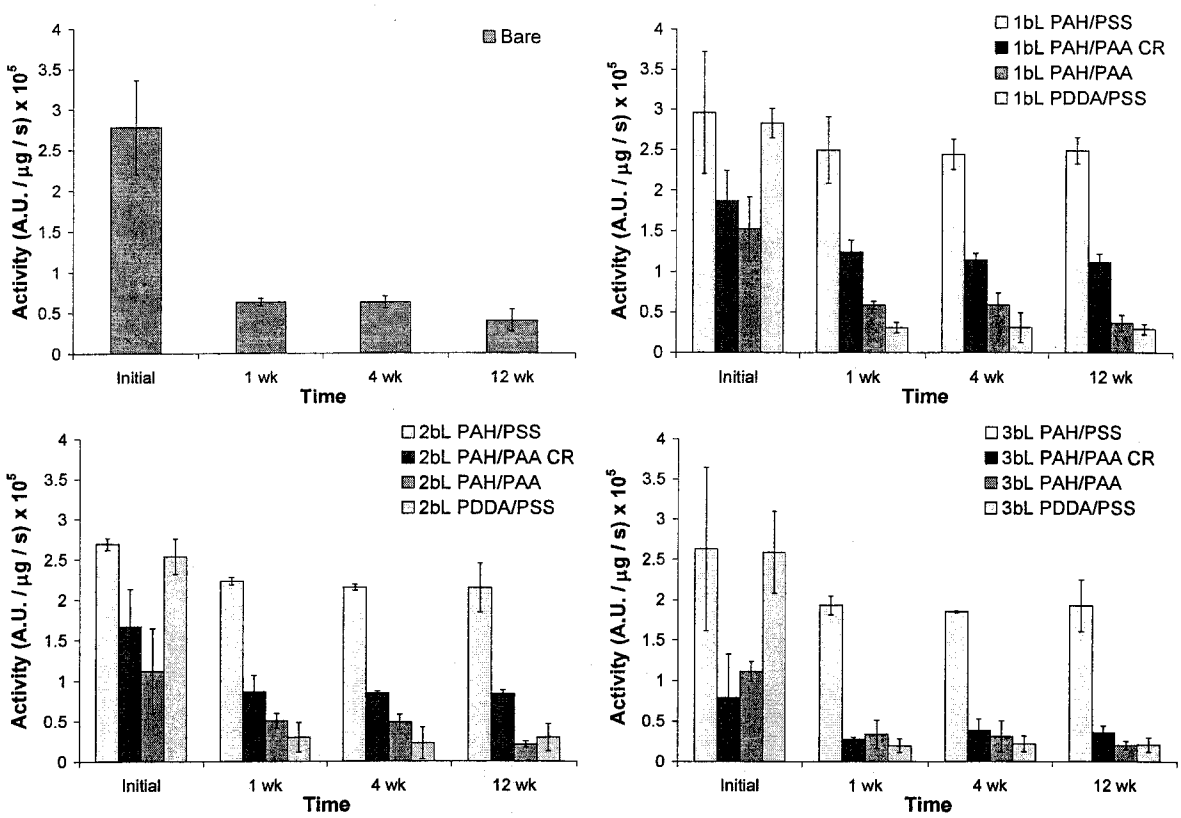

Figure 5.9. Comparison of coating on effective activity over time of glucose oxidase inside alginate microspheres. (a) Effective activity of bare microspheres over time. Effective activity of microspheres coated with (b) one bilayer of polyectrolyte films, (c) two bilayers of polyelectrolyte films, and (d) three bilayers of polyelectrolyte films. (Error bars ± one standard deviation, n =3.)

Further inspection of Figure 5.9 reveals the effect of the {PAH/PSS} nanofilm coatings on retention of the mobile GOx fraction. From the figure, it is clear that $\{PAH/PSS\}_1$ coated microspheres were advantageous for enzyme stabilization over bare microspheres, with only a 16% loss in activity for $\{PAH/PSS\}_1$ microspheres over 12 weeks (Figure 5.9(b)). After one week, the catalytic activity was essentially stable in all cases, with no significant change in effective activity. However, it is also apparent from the figure that {PDDA/PSS} coated microspheres were not suitable for stabilization of

enzyme activity, with no significant difference between uncoated alginate and {PDDA/PSS}-coated alginate at any time point. This result is expected from the leaching results, in which it was shown that the effective diffusivity of GOx through {PDDA/PSS} films is two orders of magnitude faster than through {PAH/PSS} films (Table 5.1).

The effective catalytic activity values of bare, $\{PAH/PAA\}_n$, and $\{PAH/PAA\}_n$-crosslinked (n = 1 – 3) coated alginate microspheres at the time of preparation and after 1, 4, and 12 weeks of wet storage are also presented in Figure 5.9(a-d). As expected from the previous results, the low effective activity over time of bare alginate is evident from Figure 5.9(a), with a 78% loss of catalytic activity (compared to the initial value) over one week. However, further examination of Figure 5.9(b-d) reveals the effect of addition of uncrosslinked and crosslinked {PAH/PAA} multilayers on temporal catalytic stability. In all cases, the addition of polyelectrolyte coatings resulted in higher effective activity (compared to their respective initial values) after 12 weeks, with a 82% loss in activity in the worst case (for uncrosslinked $\{PAH/PAA\}_3$, Figure 5.9[d]), and 40% loss in activity in the best case (for crosslinked $\{PAH/PAA\}_1$, Figure 5.9[b]). Thus, in the case of crosslinked $\{PAH/PAA\}_1$-coated microspheres, catalytic activity is doubled after 12 weeks compared with bare microspheres alone. Furthermore, the results also show the utility of crosslinking the {PAH/PAA} multilayers: catalytic activity tripled after 12 weeks for crosslinked $\{PAH/PAA\}_1$ compared with uncrosslinked $\{PAH/PAA\}_1$ (Figure 5.9[b]). As before, these data follow the data for leaching, with the crosslinked films exhibiting lower diffusivities for GOx than the uncrosslinked films (Table 5.1). These results are promising, as they suggest that as little as one bilayer of crosslinked

polyelectrolyte material is sufficient to significantly retain more of the high-activity, "free" GOx within the spheres as well as the less active, alginate-immobilized GOx. Overall, what is apparent from these findings is that the use of {PAH/PSS} multilayers significantly retained more "free" enzyme (most active) within the spheres over time as compared to {PDDA/PSS}, {PAH/PAA}, or {PAH/PAA}-crosslinked coated microspheres. These results are confirmed by the leaching results; {PAH/PSS} films resulted in overall effective diffusivities for GOx that were much lower than the values for any other film combination. While {PAH/PSS} films were the most preferable for retention of highly active mobile GOx within the microspheres, both uncrosslinked and crosslinked {PAH/PAA} films were acceptable for enzyme stabilization, with the crosslinked films being the slight better of the two. Finally, {PDDA/PSS} films were not useful for stabilization of enzyme activity, and their use would not be encouraged in applications in which long-term stabilization of glucose oxidase activity is required.

In conclusion, work with the macromolecule (dextran and glucose oxidase) encapsulation and stabilization has shown that multilayer coatings are effective in reducing leaching through the alginate matrix. The encouraging results obtained with the use of chemical conjugation techniques for enzyme retention provides the basis for using a photocrosslinkable diazoresin to improve the retention of the enzyme within the alginate matrix. This work is described in the next chapter and follows similar experimental procedures described in this chapter.

CHAPTER 6

ENZYME STABILIZATION - DAR/PSS COATINGS

The application of self-assembled ultrathin film coatings can reduce leaching of dextran and glucose oxidase from alginate microspheres. Work in the previous chapter demonstrated that the chemical conjugation of the nanofilm coatings was beneficial in improved retention of enzymes inside the alginate microspheres. The diffusion of enzymes from the gel matrix was dependent upon the porosity of the gel and concentration gradients, as well as the permeability of the thin-film coatings to the enzyme. In an effort to identify thin-film coating with increased resistance to enzyme leaching, photocrosslinkable coatings were investigated. It has been shown that polyelectrolyte complexes formed using diazoresins as the cationic polyelectrolyte can be made to convert their linkage from a weak ionic interaction to a covalent bond upon irradiation with UV light.[144] This conversion can be accomplished with a variety of materials alternated with the diazoresins, including those coatings containing sulfonate groups, carboxylic acid groups, or phenol groups.[145] Crosslinked diazo-resin films have been shown to be more stable at higher pH values; to exhibit increased resistance to solvent etching;[148,149] and to result in denser, more rigid films.[170]

The work described here is the integration of the LbL self assembly technique with the immobilization of glucose oxidase enzyme (GOx) in alginate microspheres, specifically using photocrosslinkable materials for nanofilm coatings. To compare the

immobilization properties of crosslinked and uncrosslinked coatings of different thickness with uncoated spheres, the relationship between enzyme loading, release, and effective activity was studied over a period of six months. The simple modifications to the layer-by-layer self-assembly technique described here may enable development of approaches to entrap and stabilize biomolecules for a wide range of applications.

6.1 Layer-by-Layer Self Assembly of Ultrathin Films on Alginate Microspheres

The diazoresin (DAR) was used as the cationic polyelectrolyte in the ultrathin film coatings, while PSS was the anionic polyion. For deposition of each coating, 1.5mL of polyelectrolyte (2mg/mL of DAR in 0.25M $CaCl_2$ or 2mg/mL PSS in 0.25M $CaCl_2$ aqueous solution) was added to a microcentrifuge tube containing 200μL of calcium alginate microsphere suspension (approximately 10^6 spheres). Adsorption was allowed to proceed for twenty minutes, after which time the suspension was centrifuged to separate the spheres from remaining unadsorbed polyelectrolyte. The microspheres were then triple-rinsed with DI water by successive centrifugation cycles. The process was repeated for the oppositely charged polyelectrolyte and alternated until a total of three bilayer polyelectrolyte films were realized. The microsphere samples with one, two, and three bilayers of {DAR/PSS} were then irradiated under UV lamp for five minutes to crosslink the multilayer walls, followed by a final rinse in DI water.

6.2 Determination of Glucose Oxidase Leaching from Alginate Microspheres

The leaching of glucose oxidase from alginate microspheres (both uncoated and coated with uncrosslinked and crosslinked films) was accomplished using the protocol

described in section 3.5. The only difference in the experimental protocol was that the supernatant scan intensity at each time period was compared to the fluorescence intensity of a standard FITC-dextran solution, since the DAR nanofilms were quenching FITC fluorescence from the FITC labeled GOx.

6.3 Activity of Glucose Oxidase in Alginate Microspheres

The activity assay of the encapsulated glucose oxidase enzyme was performed according to the protocol described in section 3.6. The experiment was repeated for the polyelectrolyte coated microspheres over a period of six months, and the results were compared by calculating the slope of the curves. In each case, the results were normalized to the mass of glucose oxidase present in the spheres as determined using the Lowry assay. Both the leaching and the activity results were analyzed using the two-tailed student's t-test.

6.4 Results and Discussion

6.4.1 Fabrication Results

A confocal micrograph of microspheres with encapsulated FITC-GOx formed with the emulsification technique is presented in Figure 6.1. The spheres appeared bright green, with uniform intensity distribution. The average size from three measurements was found to be $3.2 \pm 0.8\mu m$ for a sample size of ~12000 spheres.

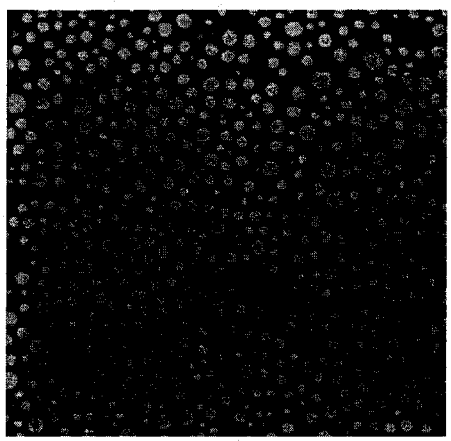

Figure 6.1. Confocal image of FITC-glucose oxidase loaded microspheres.

Following fabrication and size characterization of the alginate microspheres, deposition of multilayer nanofilms on the microspheres was performed. The surface charge of the polyelectrolyte-coated microspheres was measured using the ζ-potential analyzer, which verified reversal of the surface charge of the microspheres at each step due to polyelectrolyte adsorption as shown in Figure 6.2. The zeta potential values are averages of three readings. Thus, formation of DAR/PSS multilayers was verified.

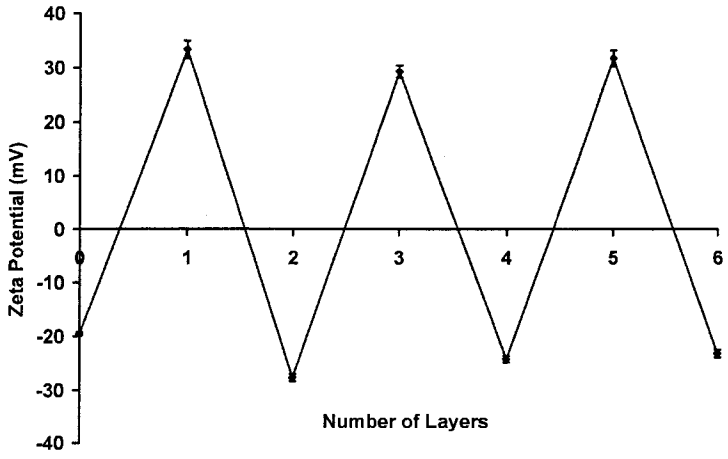

Figure 6.2. Zeta potential measurements on microspheres during DAR/PSS assembly depicting charge reversal at each step. (Error bars ± one standard deviation; n=3.)

UV-Vis absorbance spectroscopy was also used to observe the deposition of one to three bilayers of {DAR/PSS} on alginate microspheres. The absorbance at 380nm attributed to the π-π^* transition of the diazonium group, and exhibited a linear increase with the number of {DAR/PSS} bilayers on alginate microspheres. The diazonium group is very active and may be decomposed easily under UV-irradiation or heat.[191] Alginate microspheres coated with $\{DAR/PSS\}_3$ multilayers were irradiated with a UV lamp for different times to identify the conditions necessary for complete conversion. As shown in Figure 6.3(a), the diazonium groups gradually decompose under UV irradiation, with a decrease in absorbance at 380nm and the appearance of an isosbestic point at 340nm, which is in accordance with previous reports.[145] From this study, it was determined that irradiation for 30 seconds would be sufficient to completely crosslink the DAR/PSS in the nanofilms. The procedure for coating the microspheres with DAR/PSS and subsequently crosslinking them under UV irradiation has been illustrated in Figure 6.3(b).

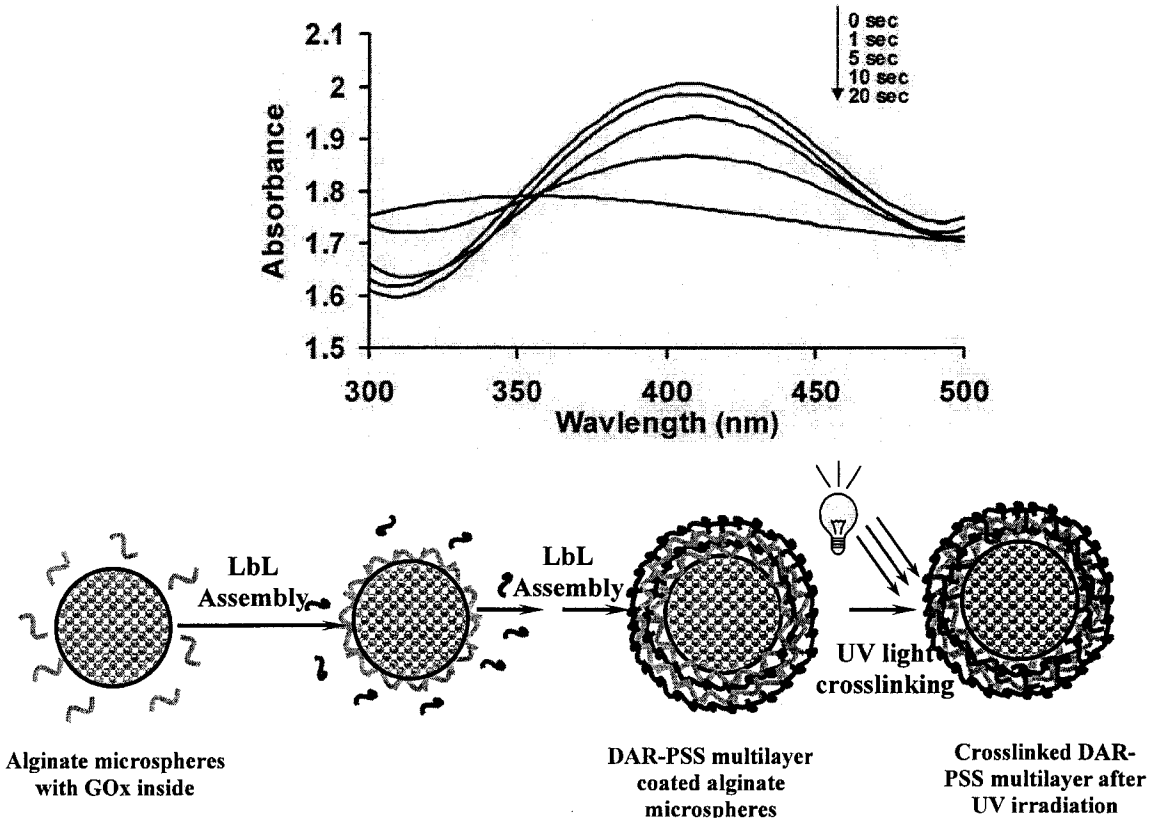

Figure 6.3 (a) UV-Vis absorption spectra of $\{DAR/PSS\}_3$ multilayer coated alginate microspheres after irradiation with UV light for 0 second, one second, five seconds, 10 seconds and 20 seconds (b) Schematic diagram of enzyme encapsulation in crosslinked DAR-PSS coated alginate microspheres.

6.4.2 Leaching of FITC-Glucose Oxidase from Alginate Microspheres

Loss of FITC-GOx from the alginate microspheres was studied using fluorescence spectroscopy, where release of the encapsulated FITC-GOx from the microspheres was observed as an increase in the fluorescence intensity of the supernatant. The leaching results for the alginate microspheres containing the enzyme were compared for the uncrosslinked {DAR/PSS} versus the crosslinked {DAR/PSS} multilayers. Results from the experiment are given in Figure 6.4(a), where the leached amount for FITC-GOx is

plotted versus number of coatings of $\{DAR/PSS\}_n$ (n = 0-3) (uncrosslinked case) and compared to the crosslinked $\{DAR/PSS\}_n$ (n = 1-3) multilayers. The results show that bare microspheres leach approximately 50% of the standard concentration in four days, suggesting that bare alginate microspheres have relatively large pores that allow large and small molecules to pass through. Since diffusion-driven leaching would result in equilibrium between the compartments, it is believed that eventually all of the encapsulated material is lost. Swelling of the alginate matrix could also be attributed for the fast release of the encapsulant. Release behavior of encapsulants from alginate beads have also been reported to be influenced by the ionic nature of the encapsulant, i.e., cationic, anionic, and non-ionic.[111] Glucose oxidase, being anionic at pH 7.4, will repel the negatively charged alginate matrix, leading to faster release. Conversely, the release profiles for microspheres coated with DAR/PSS multilayer nanofilms show that the application of these coatings does significantly reduce the loss of encapsulated material, which reduces to less than 20% of standard concentration over the same time span. However, there are negligible differences in the total leaching of the enzyme from alginate microspheres coated with more than one bilayer of polyelectrolytes. Crosslinking of the nanofilm coatings using UV irradiation also resulted in reduced leaching from alginate microspheres, although no significant differences were observed for each additional coating. When the leaching rate was compared for the different coatings, as shown in Figure 6.4(b), a dramatic difference was seen for the comparison between the uncrosslinked films and the crosslinked films.

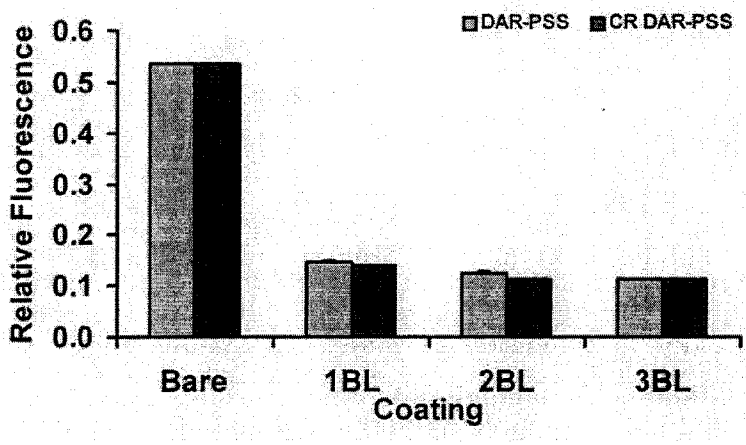

(a)

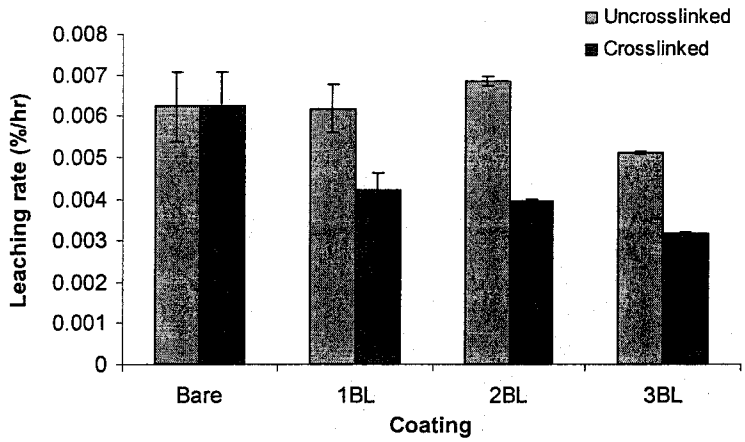

(b)

Figure 6.4. (a) Comparison of coating on leaching of glucose oxidase from alginate microspheres. (b) Comparison of coating on leaching rate of glucose oxidase from alginate microspheres (error bars ± one standard deviation, n=3).

The leaching rate for uncrosslinked films was observed to be higher than the leaching rate for the crosslinked films, with the results of the t-tests being significantly different between the uncrosslinked and crosslinked films in all cases. The same cannot be said for the comparison between bare and coated microspheres (uncrosslinked), in which case, the results were insignificant. These results suggest that the crosslinking of the coatings substantially reduces the pore sizes in the applied multilayers, as expected,

enabling better retention of the enzyme. As a consequence of crosslinking, the rigidity and density of the films are increased,[173] which explains the reduced leaching rate through crosslinked multilayers. In addition, it has been shown that multilayers of crosslinked DAR/PSS result in a bilayer thickness of 14nm,[192] which is substantially thicker than the bilayer thickness of 2-5nm reported for standard PAH/PSS films.[193] In summary of these findings, the experimental results show that the application of {DAR/PSS} multilayer thin films to the alginate microspheres was effective in reducing the loss of the encapsulated material from the microspheres. The leaching rate was also seen to decrease with nanofilm crosslinking.

6.4.3 Activity of Encapsulated Glucose Oxidase in Alginate Microspheres

To determine the effect, if any, of thin-film assembly on activity of encapsulated enzyme, the activity of the coated microspheres was studied over six months of wet storage (0.01M PBS, room temperature). Figure 6.5(a-d) summarizes the results of the experiments to determine the effect of uncrosslinked and crosslinked {DAR/PSS} films on the effective catalytic activity per unit mass of encapsulated GOx (determined for each sample using Lowry assay). The GOx concentration was calculated for all coatings at each time period (Table 6.1) to aid in the understanding of the results. What is apparent is that the bare microspheres lose ~40% of the initially encapsulated enzyme over four weeks. Due to disintegration of the alginate matrix, there were no spheres remaining at the end of 24 weeks and, therefore, it was not possible to calculate the molar concentration of the enzyme present. The DAR/PSS coated microspheres retain more than 70% of the initially encapsulated enzyme for all cases.

Table 6.1. Comparison of molar concentration of GOx inside alginate microspheres versus time and DAR/PSS bilayers (CR stands for crosslinked).

Alginate Microspheres	GOx concentration (mM)			
	0-week	1-week	4-week	24-week
BARE	49.1	29.1	27.8	-
1BL	54.3	41.8	40.4	41
1BL CR	61	46.7	44.3	40.8
2BL	52.6	45.5	42.2	41.2
2BL CR	55.6	46.5	44.8	40.4
3BL	52.3	41.4	40.6	41.2
3BL CR	51.2	43.2	44.1	39.7

The activity results show that uncoated alginate microspheres exhibited an 80% reduction in initial activity after one week, with no further reduction in activity after four weeks (Figure 6.5[a]). However, it is also apparent from the figure that the effective activity of uncoated microspheres dropped dramatically after 24 weeks. Although the activity is normalized to unit mass, the observed differences are likely due to the higher initial activity of weakly-bound or free GOx within the microspheres versus the decreased effective activity of the remaining immobilized GOx in weeks one and four; the decreased effective activity after 24 weeks is due to the destruction of the spheres in the phosphate buffer storage solution, leaving only fragments of the spheres containing immobilized GOx. Thus, the effective activity of the microspheres can be viewed as a superposition of the effective activity of mobile encapsulated GOx and the effective activity of immobilized encapsulated GOx, and differences in overall effective catalytic activity can be attributed to varying contributions of both.

For uncoated microspheres, the process can be described as such: initially, the microspheres contain a large amount of mobile GOx as well as a smaller amount of GOx firmly immobilized to the alginate matrix, resulting in high effective activity. However,

after one week, most of the mobile GOx has leached from the microspheres, leaving only the immobilized GOx, which is expected to have lower effective catalytic activity than free GOx. This immobilized GOx is remarkably stable, and there is no further loss of enzyme (and thus effective activity) after four weeks; however, after 24 weeks, the effective activity of the enzyme is reduced due to deactivation. Thus, the goal of multilayer nanofilm coatings is to retain as much as possible of the initially encapsulated mobile GOx within the microspheres, resulting in higher catalytic activity.

The utility of uncrosslinked and crosslinked DAR/PSS coatings to achieve this goal is shown in Figure 6.5(b-d). The application of uncrosslinked $\{DAR/PSS\}_1$ nanofilms resulted in decreased loss of activity over one week, with only 53% loss in initial activity (Figure 6.5(d)). Crosslinking of the $\{DAR/PSS\}_1$ nanofilms resulted in a significant increase in effective activity over uncrosslinked films ($P = 0.07$), with only 51% reduction in initial activity over one week for crosslinked $\{DAR/PSS\}_1$ nanofilms. Similar results were obtained for $\{DAR/PSS\}_{2\text{-}3}$ nanofilms ($P = 0.01$ and 0.1, respectively). After four weeks, there was no statistically significant difference between uncrosslinked and crosslinked films of one, two, or three bilayers. This suggests that, while the microspheres with uncrosslinked coatings experienced a faster loss of mobile GOx than those with crosslinked coatings, after four weeks the amount of mobile GOx in each is relatively the same.

Thus, for shorter-term applications, it seems that there is no practical improvement in effective catalytic activity gained by crosslinking the DAR/PSS films. However, these microspheres are intended for use as engines in implantable biosensors, and as such, will require much longer-term application. Thus, the activity of the

microspheres was assessed after six months of storage to determine whether there is any long-term effect of crosslinking the sphere coatings. These results are also shown in Figure 6.5(b-d). While the $\{DAR/PSS\}_1$ films resulted in no significant difference between uncrosslinked and crosslinked films, both the $\{DAR/PSS\}_2$ and $\{DAR/PSS\}_3$ crosslinked films exhibited higher effective activity than their uncrosslinked counterparts ($P = 0.1$ and 0.01, respectively). Therefore, after six months, the crosslinked films of 2-3 bilayer thickness are likely to be more effective at retaining effective catalytic activity than uncrosslinked films. Further observation of the figure reveals that regardless of crosslinking, the application of nanofilm coatings resulted in the prevention of the dramatic decrease in effective activity after six months observed for the uncoated microspheres, confirming that they act as structural supports to prevent the spheres from degradation. The better performance of the crosslinked films is due to their ability to retain more of the mobile GOx for longer, as evidenced by their slower leaching rates and higher effective activity.

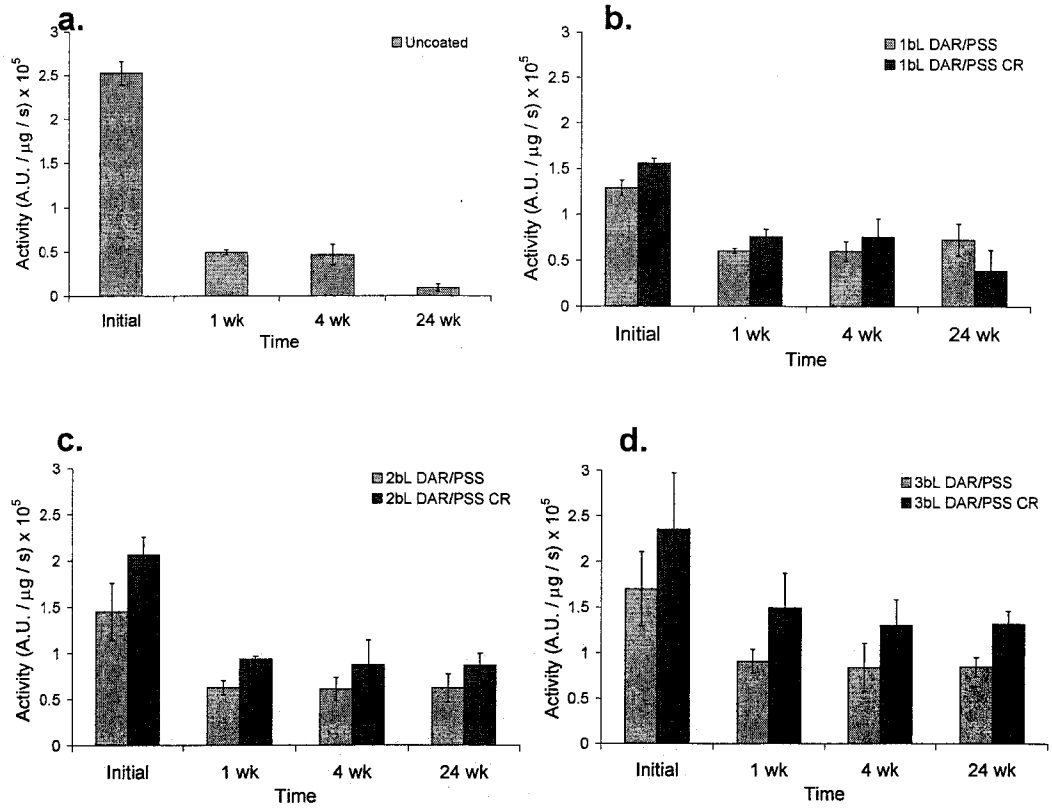

Figure 6.5. Comparison of coating on activity per unit mass over time of glucose oxidase inside alginate microspheres. (a) Activity of bare microspheres over time, (b) Activity of microspheres coated with one bilayer of uncrosslinked (DAR/PSS) and crosslinked (DAR/PSS CR) films, (c) Activity of microspheres coated with two bilayers of uncrosslinked (DAR/PSS) and crosslinked (DAR/PSS CR) films. (d) Activity of microspheres coated with three bilayers of uncrosslinked (DAR/PSS) and crosslinked (DAR/PSS CR) films. (Error bars ± one standard deviation, n=3.)

These results suggest that {DAR/PSS}-crosslinked films are preferable for catalytic stability over uncrosslinked films over a one week period; after four weeks, there is no statistically significant difference between uncrosslinked and crosslinked films of any number of layers investigated. However, after six months, two and three bilayer crosslinked DAR/PSS films exhibit higher effective activity than uncrosslinked films.

Furthermore, both uncrosslinked and crosslinked {DAR/PSS} nanofilms are superior to bare alginate alone, and thicker films result in more higher effective activity over six months regardless of whether or not the films are photocrosslinked. In summary, uncoated spheres exhibited rapid loss of activity, retaining only 20% of initial activity after one week and experiencing a dramatic reduction in effective activity over 24 weeks, whereas the uncrosslinked and crosslinked {DAR/PSS}-coated spheres retained more than 50% of their initial activity after four weeks and remained stable even after 24 weeks for the two and three bilayer films. Thus, nanofilms comprising more polyelectrolyte layers maintained higher overall activity compared to films of same composition but fewer layers, and crosslinking the films increased retention of activity over uncrosslinked films after 24 weeks. These findings demonstrate that enzyme immobilization and stabilization can be achieved by using simple modifications to the layer-by-layer self-assembly technique.

In summary, work in the previous chapters has shown that the total loss of encapsulated material was reduced to less than 25%, and 15% with the application of a single {PAH/PSS} and crosslinked {PAH/PAA} coating, respectively, in comparison to at least 45% loss observed with uncoated and {PDDA/PSS}-coated microspheres. The activity of the encapsulated enzyme was also tested over 12 weeks, and it was found that {PAH/PSS} and crosslinked {PAH/PAA}-coated spheres retained more than 84% and 60% of their initial activity, respectively, whereas uncoated and {PDDA/PSS}-coated microspheres retained less than 20% of initial activity. On the other hand, uncrosslinked and crosslinked {DAR/PSS}-coated spheres retained ~50% of their initial activity after 24 weeks. Therefore, the {DAR/PSS} multilayer films were not found to provide any

improvement over existing techniques for increased retention of the enzyme. Therefore, a combination of the methods used in the previous chapters involving chemical conjugation and {PAH/PSS} multilayers is expected to provide enhanced retention of the enzyme. This work described in the next chapter is aimed at improved retention of the enzyme within alginate microspheres using chemical conjugation techniques.

CHAPTER 7

ENZYME STABILIZATION USING CHEMICAL CONJUGATION TECHNIQUES

Work presented in the previous chapters has shown that the application of self-assembled ultrathin film coatings can reduce leaching of the enzyme glucose oxidase from alginate microspheres, in turn stabilizing the enzyme activity over time, but even with the application of self assembled ultrathin film coatings, a best case ~16% loss in activity was observed over a period of 12 weeks for $\{PAH/PSS\}_1$ multilayer. In addition, it was observed that postdeposition cross-linking of the films deposited using simple electrostatic adsorption did not lead to improvement in activity results compared to {PAH/PSS} multilayers, while {DAR/PSS} multilayers were only able to preserve ~50% activity at the end of 24 weeks.

While the nanofilm coatings were improvements over the use of bare alginate microspheres, the stability of encapsulation and activity were considered to be less than desirable for long term applications in biosensors. Thus, this chapter describes a further exploration into GOx immobilization by conjugation of the enzyme with the alginate matrix using water soluble 1-ethyl-3-(3-dimethylaminopropyl) carbodiimide (EDC), a reaction that is favored by the presence of N-hydroxysuccinimide (NHS). Leaching studies identical to those described in previous chapters were performed and enzyme activity was monitored over time. This work describes the fabrication method used to

produce the microspheres, their characterization, and the effect of crosslinking on the leaching of the enzyme and their stabilization inside alginate microspheres towards the fabrication of a glucose sensor.

7.1 Conjugation of Glucose Oxidase to Alginate Matrix

EDC was used to conjugate the enzyme to the alginate matrix using NHS as a catalyst. The coupling chemistry is based upon the reaction of activated carboxylic sites of the alginate with primary amine groups of the enzyme glucose oxidase.[187] 1-Ethyl-3-(3-dimethylaminopropyl)-carbodiimide (EDC) is a water-soluble derivative of carbodiimide. Carbodiimide catalyzes the formation of amide bonds between carboxylic acids or phosphates and amines by activating carboxyl or phosphate to form an O-urea derivative. This derivative reacts readily with nucleophiles (Figure 7.1). The reagent can be used to make ether links from alcohol groups, ester links from acid and alcohols or phenols, and peptide bonds from acid and amines. Carbodiimide is often used in the synthesis of peptides as the water-soluble derivative EDC or as the organic soluble derivative, *N,N'*-dicyclohexyl-carbodiimide (DCC). *N*-Hydroxysuccinimide (NHS) is often used to assist the carbodiimide coupling in the presence of EDC. The reaction includes formation of the intermediate active ester (the product of condensation of the carboxylic group and *N*-hydroxysuccinimide) that further reacts with the amine function to yield finally the amide bond. In the reaction EDC converts the carboxylic acid into a reactive intermediate that is susceptible to attack by amines. In some cases EDC and NHS are used as the NHS produces a more stable reactive intermediate that has been shown to give a greater reaction yield.

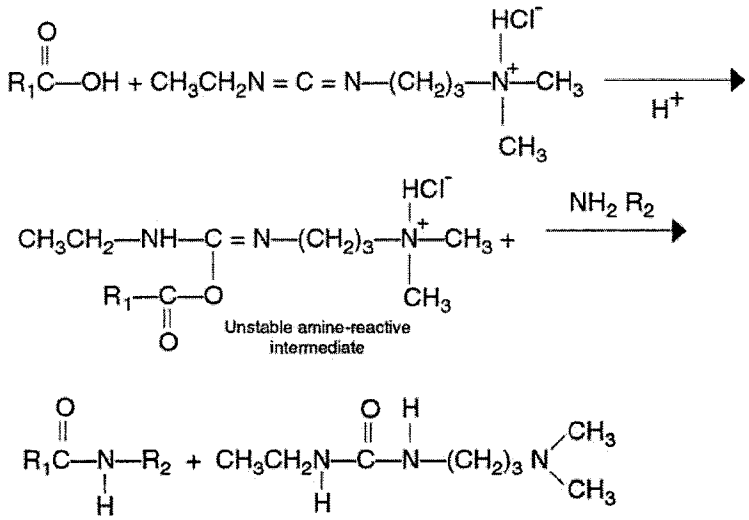

Figure 7.1 Mechanism of activation of carboxylic groups by EDC and further reaction with amines resulting in the amide bond formation. [194]

For the process, 10 mL of a 0.05M phosphate buffered saline solution (pH 5.0) was prepared, and 1 mL of uncoated alginate microspheres was transferred to the buffer solution. In the same solution, 300 mg of EDC and 100 mg of NHS were then dissolved and stirred for four hours. The spheres were then centrifuged to separate the unreacted EDC-NHS and rinsed three times before using them for the leaching and activity studies. To compare results observed with the {PAH/PSS} coating combination that demonstrated improved retention and enzyme stability in alginate microspheres used in chapter 5, {PAH/PSS} multilayers were used in this work using the conjugated microspheres.

7.2 Layer-by-Layer Self Assembly of Ultrathin Films on Alginate Microspheres

A cationic polyelectrolytes (PAH) was used for the layer-by-layer self assembly application of the ultrathin film coatings, while PSS, was the anionic polyion used. For

deposition of each coating, 1.5mL of cationic polyelectrolyte (2mg/mL PAH in DI water with 0.25M $CaCl_2$) was added to a microcentrifuge tube containing 200μL of microsphere suspension (approx 10^6 spheres). Adsorption was allowed to proceed for 20 minutes, after which time the suspension was centrifuged to separate the spheres from the remaining unadsorbed polyelectrolyte. The microspheres were then triple rinsed with DI water by successive centrifugation cycles. A solution of the anionic polyelectrolyte (1.5mL of 2mg/mL PSS in DI water with 0.25M $CaCl_2$) was then added; the spheres were centrifuged to remove the supernatant, and then rinsed three times to complete one bilayer. The surface charge of the microspheres was measured using the zeta potential analyzer after rinsing and prior to addition of each polyelectrolyte. This process was repeated until a total of three bilayer polyelectrolyte films were realized.

7.3 Determination of Glucose Oxidase Leaching from Alginate Microspheres

The leaching of glucose oxidase from alginate microspheres (both uncoated and coated) was accomplished using the protocol described in section 3.5. The leaching results were then fitted in MATLAB using Crank's equations as described in section 2.14 to calculate the diffusion coefficient of glucose oxidase through the uncoated and coated alginate microspheres.

7.4 Activity of Glucose Oxidase in Alginate Microspheres

The activity of the encapsulated glucose oxidase enzyme was performed according to the protocol described in section 3.6. The experiment was repeated for the polyelectrolyte coated microspheres over a period of one month, and the results were

compared by calculating the slope of the curves. In each case, the results were normalized to the mass of glucose oxidase present in the spheres as determined using the Lowry assay. Both the leaching and the activity results were analyzed using the two-tailed student's t-test.

7.5 Results and Discussion

7.5.1 Fabrication Results

A confocal micrograph of microspheres with encapsulated FITC-GOx formed with the emulsification technique is presented in Figure 7.2. The spheres appear bright green with uniform intensity distribution when imaged with the confocal microscope. The average size was found to be 4.25 ±0.49 μm (N >5000 spheres counted).

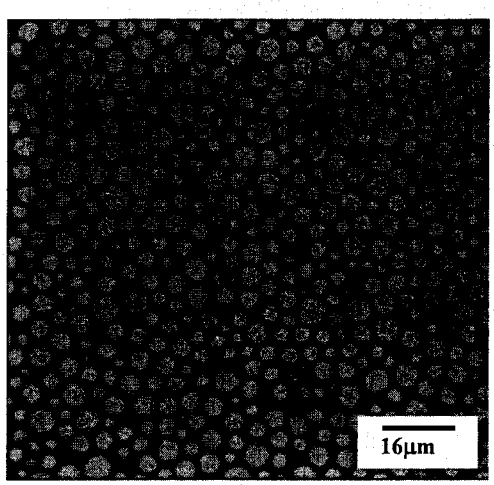

Figure 7.2. Confocal image of FITC-glucose oxidase loaded microspheres with a scale bar of 16μm.

The LbL assembly of polyelectrolyte layers was monitored by electrophoretic mobility measurements. Three bilayers of {PAH/PSS} were deposited on unconjugated microspheres and conjugated GOx-encapsulated alginate microspheres for comparison. It was found that there was no significant difference between alginate cores and conjugated

GOx-encapsulated alginate cores. The surface potential of the microspheres was observed to change regularly from -25 mV for alginate (alginate/GOx) and PSS to +40 mV for PAH (Figure 7.3), indicating the formation of the desired $\{PAH/PSS\}_3$ wall architecture.

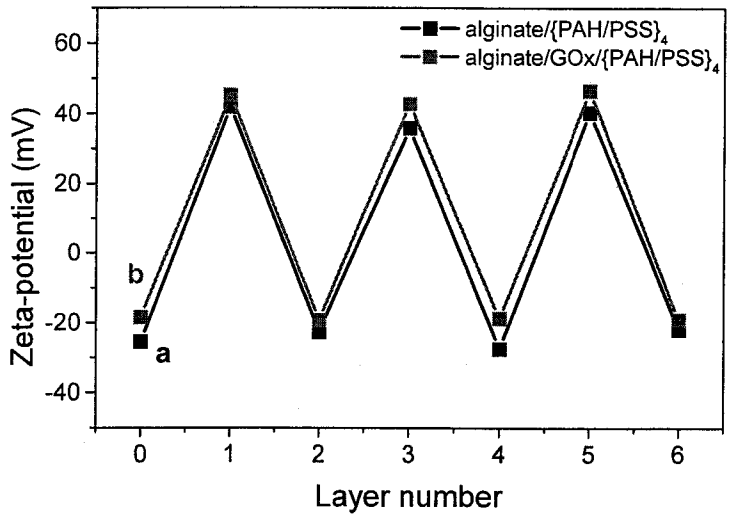

Figure 7.3. ζ-potential measurements for deposition of $\{PAH/PSS\}_4$ on (a) alginate microspheres and (b) conjugated alginate/GOx microspheres. The first measurement (Layer 0) is the surface potential of uncoated alginate microspheres.

7.5.2 Leaching of FITC-Glucose Oxidase from Conjugated Alginate Microspheres

Loss of FITC-GOx from the alginate microspheres was studied using fluorescence spectroscopy, where release of the encapsulated FITC-GOx from the microspheres resulted in an increase in the fluorescence intensity of the supernatant. Results from a typical experiment are given in Figure 7.4, where the leached amount for FITC-GOx is plotted versus time for conjugated microspheres coated with $\{PAH/PSS\}_{n=0-3}$ and compared to uncoated and unconjugated microspheres. Some interesting observations may be made from this graph. The results show that approximately 50% of the

encapsulated material comes out of bare microspheres within four days, suggesting that bare alginate microspheres have relatively large pores which allow large and small molecules to pass through. Since diffusion-driven leaching would result in equilibrium between the compartments, it is believed that eventually all of the encapsulated material is lost. This finding was discussed in the previous chapter and has been included on this graph to compare the leaching results with the conjugated case. In contrast, the leaching results for microspheres conjugated with the enzyme shows that the enzyme is stably encapsulated inside the microspheres. There was ~20% leaching observed for the enzyme over the same time period. These results are encouraging since they prove that the chemical conjugation of the enzyme to the alginate matrix using the carbodiimide chemistry does, in fact, reduce the leaching of the enzyme to a value which is close to the one that was obtained with one bilayer of PAH/PSS on unconjugated microspheres.

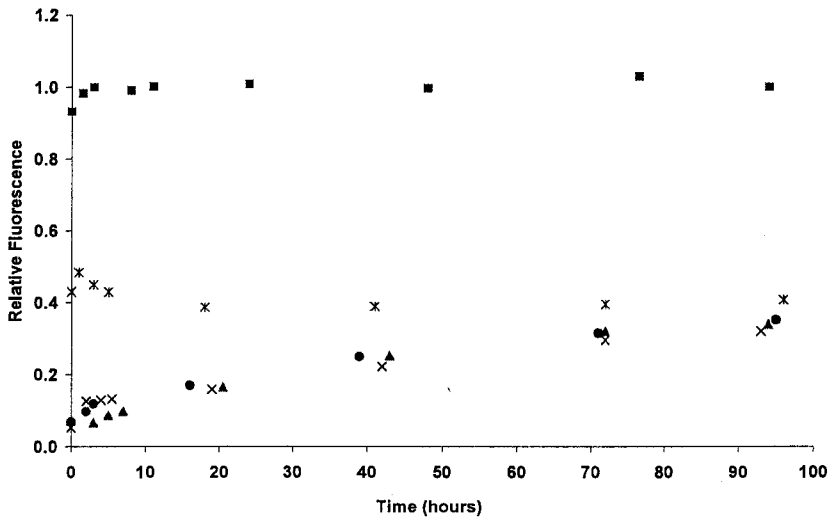

Figure 7.4. Leaching versus time for $\{PAH/PSS\}_n$ (n = 0-3) multilayers for conjugated FITC-GOx-alginate microspheres. Captions include unconjugated bare microspheres (■); bare conjugated spheres (*); spheres coated with one bilayer (•); spheres coated with two bilayers (▲) and spheres coated with three bilayers (x).

The results presented in the time-dependent release measurements described are reorganized into a bar graph for direct comparison in Figure 7.5. The results shown are for total leached amount at the end of four days (n = 3 measurements). An interesting point to note from this graph is that there is insignificant difference between the total leaching for the conjugated uncoated microspheres and the conjugated coated microspheres, again pointing out that now the enzyme is held inside the matrix with chemical crosslinking and is not free to diffuse out; hence, additional layers do not make a difference in the leaching.

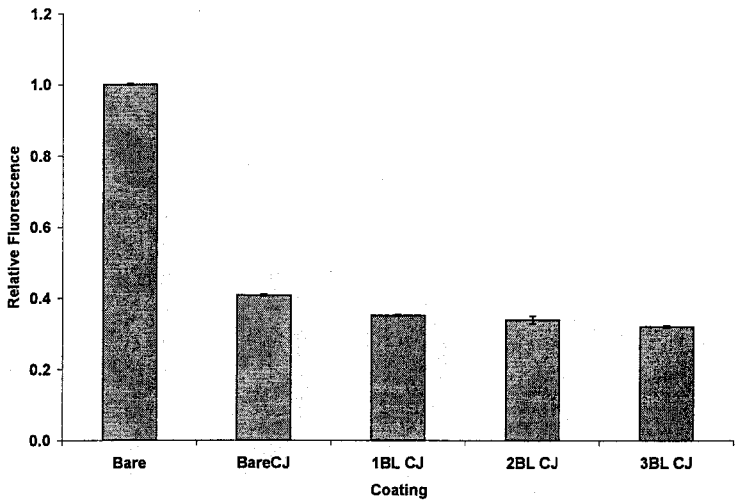

Figure 7.5. Comparison of the effects of the number of coating layers on GOx leaching from alginate microspheres. The legend CJ stands for conjugated.

The leaching results are confirmed by observing the diffusion coefficient values presented in Table 7.1. The uncoated conjugated microspheres have a diffusion coefficient ~2 orders of magnitude smaller than that for the uncoated unconjugated microspheres (data from Chapter 5). The addition of one bilayer of {PAH/PSS} to the uncoated conjugated microspheres leads to a reduction in the diffusion coefficient value

by one order of magnitude, but the addition of further multilayers does not significantly change the diffusion coefficient values for the enzyme through the alginate microspheres.

Table 7.1. Diffusion coefficients for glucose oxidase in conjugated alginate microspheres coated with polyelectrolyte nanofilms ($D_e \times 10^{-12}$ cm^2/sec) compared with unconjugated coated microspheres. Variability in the estimated values is less than 1% (n = 3) (CJ stands for conjugated).

Film combination	Bilayers		
	1	2	3
{PAH/PSS} CJ	1.32×10^{-3}	7.5×10^{-4}	7.1×10^{-4}
PAH/PSS	1.63×10^{-2}	1.41×10^{-2}	1.31×10^{-2}

*** Uncoated unconjugated microspheres have a D_e of 2.47×10^{-12} cm^2/sec, while uncoated conjugated microspheres have a D_e of 1.49×10^{-14} cm^2/sec.**

In conclusion, the leaching results of the enzyme from unconjugated and conjugated alginate microspheres showed that ~20% enzyme still leached out of the conjugated alginate microspheres at the end of five days. A reason for this leaching might be that all of the enzyme was not chemically conjugated to the alginate matrix due to the limited number of reaction sites for the carbodiimide reagent, and therefore, some of the enzyme was free to diffuse out of the alginate matrix.

7.5.3 Activity and Stabilization of Encapsulated Glucose Oxidase in Conjugated Alginate Microspheres

In order to use the GOx-encapsulated alginate microspheres as practical glucose sensors, stable activity of the encapsulated enzyme must be realized. Since chemical conjugation techniques were used for the stable encapsulation of the enzyme, it is expected that there will be some effect on the enzyme activity. As a baseline for further comparisons, the activity of conjugated uncoated microspheres and conjugated coated

microspheres with $\{PAH/PSS\}_{n=0-3}$ multilayers was assessed immediately following microsphere fabrication and following one and four weeks of storage in phosphate buffer. The results of this experiment are shown in Figure 7.6, with all activities normalized to total enzyme mass per sample as determined by Lowry assay. The enzyme amounts calculated as molar concentration of GOx is shown in Table 7.2. This molar concentration of GOx was calculated using the enzyme amount, average size of the microspheres and the concentration of spheres at that time period in 100μL of the sample volume (used for the enzyme activity). It is apparent that the conjugation technique significantly retained more enzyme than the bare unconjugated microspheres at one week and four weeks. These results are in agreement with the leaching results, which showed that the bare unconjugated microspheres leached more than 45% of the enzyme over five days, while the leaching was reduced to less than 20% for the bare conjugated microspheres. This is also reflected in the molar concentration of GOx remaining in the microspheres at the end of four weeks. The coated microspheres lose less than 20% enzyme at the end of four weeks for all cases.

Table 7.2. Comparison of molar concentration of GOx inside alginate microspheres versus time and PAH/PSS bilayers (CJ stands for conjugated).

Alginate Sample	GOx concentration (mM)		
	0-week	1-week	4-week
BARE	66.7	33.4	32.2
BARE CJ	86	68.8	66.7
1BL CJ	70.6	64.4	62.3
2BL CJ	69.8	66.3	61.8
3BL CJ	70.1	58.2	57.7

The effective activity of the enzyme in uncoated conjugated microspheres was reduced by 10% over four weeks. Since the effective activity is the activity normalized to enzyme mass, it is counter-intuitive to expect a difference in effective activity over time due to enzyme leaching. However, if one considers the existence of two populations of encapsulated enzyme, one which is weakly immobilized and one which is strongly immobilized. This result may be easily explained. The weakly immobilized enzyme is expected to have a relatively high effective activity since it is highly mobile and presumably more accessible to enzyme substrates than the strongly immobilized enzyme from the chemical conjugation, which is expected to have lower effective activity. Thus, the initial loss of activity was attributed to leaching of a mobile fraction of enzyme not physically attached to the alginate matrix after the chemical conjugation; this "free" enzyme was assumed to have a greater effective activity per unit mass than the immobilized enzyme, which is responsible for the activity of the microspheres after the mobile GOx has leached from the spheres.

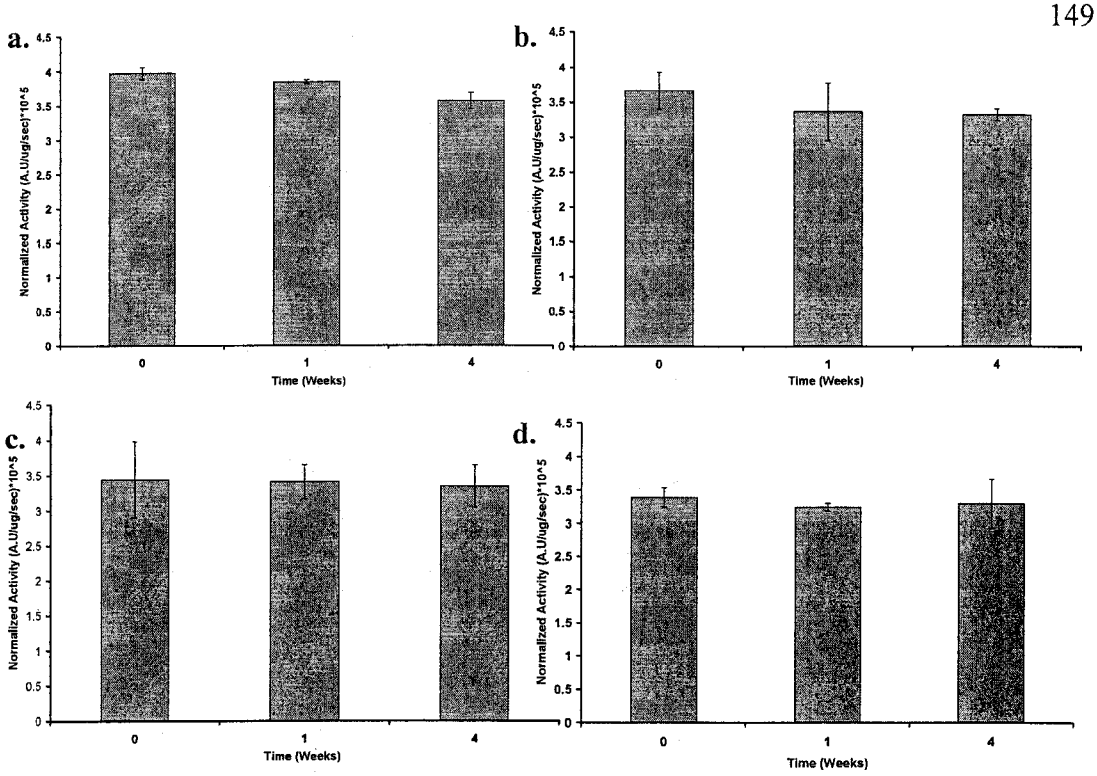

Figure 7.6. Comparison of coating on effective activity over time of glucose oxidase inside alginate microspheres. (a) Effective activity of conjugated uncoated microspheres over time, (b) effective activity of microspheres coated with one bilayer of {PAH/PSS}, (c) effective activity of microspheres coated with two bilayers of {PAH/PSS}, and (d) effective activity of microspheres coated with three bilayers of {PAH/PSS}. (Error bars ± one standard deviation, n=3.)

The activity retention results presented in the section above are a significant improvement over other techniques of immobilization and are expected to play a significant role in building glucose sensors using alginate microspheres. Finally, the effective activity of the encapsulated enzyme inside coated microspheres did not change significantly over time, with a ~2% loss in activity over four weeks. These results demonstrate the utility of nanofilm coatings in enhancing stability of enzyme inside alginate microspheres. Overall, what is apparent from these findings is that the use of conjugation significantly retained more enzymatic activity within the spheres over time

as compared to the previously discussed unconjugated case. These results are also confirmed by the leaching results as explained before, and their use would be encouraged in applications in which long-term stabilization of glucose oxidase activity is required.

In conclusion, the leaching results for microspheres conjugated with the enzyme showed that the enzyme was stably encapsulated inside the microspheres with ~20% of the enzyme being leached over the time period. The chemical conjugation technique provided more stability to the enzyme versus all the other techniques used. The activity results also demonstrated the effectiveness of the chemical conjugation with more than 90% enzyme activity being preserved for all cases over one month of testing. Now that the enzyme has been shown to be stably encapsulated inside alginate microspheres, the next step involves applying a suitable biocompatible coating to the microspheres so that they may be used for *in vivo* testing towards an implantable glucose sensor. The next chapter discusses the leaching and activity results of the enzyme entrapped in alginate microspheres coated with some "biocompatible" coating materials as well as *in vitro* cytotoxicity tests conducted with these materials, both as monolayer and multilayer coatings on alginate microspheres.

CHAPTER 8

ENZYME STABILIZATION - BIOCOMPATIBLE COATINGS

Work in the previous chapters has shown that the enzyme was stably encapsulated inside the alginate microspheres with ~80% retention over four days using the chemical conjugation technique. The activity results also demonstrated the effectiveness of the chemical conjugation with more than 90% of the enzyme activity being preserved for all cases over one month of testing. This chapter aims at providing a "biocompatible" interface to the alginate microspheres towards their final goal of implantable glucose sensors. Various material properties were researched, and the materials chosen for this study included chitosan, alginate, chondroitin sulfate, humic acid, PEG amine, PEG bis(amine), DEAE dextran, and dextran sulfate. The properties of the chosen materials are explained in the following section.

Chitosan, derived from chitin, which is the main structural element of the cuticles of crab and shrimp, has been exploited for numerous biomedical applications such as wound dressing, drug delivery systems, and tissue engineering owing to its biocompatibility.[195,196] Alginate has also been shown to biocompatible and is used for a variety of applications from cell immobilization to tissue engineering to drug delivery.[80,197] On the other hand, poly(ethylene glycol) (PEG), a water-soluble, nontoxic, and nonimmunogenic polymer, has been found to be most effective in terms of repelling proteins compared to other polymers.[166] Several theories have been proposed for the

protein-repelling behavior of PEG, but none of them is adequate to explain its protein-resistant behavior under all the conditions. The biological inertness of the polymer backbone and its solvated configuration give rise to the surface properties for PEG. However, in more than 80% of the cases, steric stabilization force and chain mobility effect, have been sufficient to explain the protein-resistant behavior.[198] The two PEG derivatives used in this project have an amine group terminated structure, either at one end or at both ends.

Chondroitin sulfate glycosaminoglycans are sulfated polysaccharides involved in cell division, neuronal development, and spinal cord injury.[199] While considerable attention has been focused on heparan sulfate glycosaminoglycans, much less is known about the chondroitin sulfate (CS) class. Chondroitin sulfate has a molecular mass of 10-50 kDa, which may contribute to network formation, and it contains a substantial amount of sulfate and carboxylate residues, necessary for interaction and cross-linking.[200] Furthermore, chondroitin sulfate is the only glycosaminoglycan which is predominantly found in cartilage and skin, and it is associated with collagen in connective tissue and tendon *in vivo*.[201] Similarly, dextran sulfate is a polyanion similar to heparin with a branched carbohydrate backbone and negatively charged sulfate groups and can mimic natural mucopolysaccharide (for example chondroitin sulfate, dermatan sulfate).[202] On the other hand, diethylaminoethyl-dextran (DEAE-dextran) is a polycatonic derivative of dextran with wide range of uses including vaccine manufacture, gene therapy, and protein stabilization.[202] Similarly, humic acids (HA) are biopolymers found in soil, sediments, water, and some plants such as tobacco. Humic acids are very heterogeneous in nature and contain species with molecular weight ranging from a few thousand Da to hundreds

of kDa. Their structures are dominated by aromatic moieties containing carboxylic, carbonyl, phenol, catechol, and quinone, along with a few amine groups.[203]

In summary, the properties of the chosen materials will allow tailoring of the surface properties of the alginate microspheres to make them more biocompatible towards long term biosensor use. The alginate microspheres were fabricated using the protocol described in section 3.3. After fabrication, the enzyme was conjugated to the alginate matrix using the protocol described in section 7.1.

8.1 Layer-by-Layer Self Assembly of Ultrathin Films on Alginate Microspheres

Five different cationic polyelectrolytes (PAH, chitosan, DEAE dextran, PEG amine, and PEG bis-amine) were used for the layer-by-layer self assembly application of the ultrathin film coatings, while alginate, dextran sulfate, chondroitin sulfate, and humic acid were the anionic polyions used. The humic acid solution was filtered using a 0.2μm polycarbonate syringe filter before using. For deposition of each coating, 1.5mL of cationic polyelectrolyte (2mg/mL in DI water with 0.25M $CaCl_2$) was added to a microcentrifuge tube containing 200μL of microsphere suspension (approx 10^6 spheres). Adsorption was allowed to proceed for twenty minutes, after which time the suspension was centrifuged to separate the spheres from remaining unadsorbed polyelectrolyte. The microspheres were then triple rinsed with DI water by successive centrifugation cycles. A solution of the anionic polyelectrolyte (1.5mL of 2mg/mL in DI water with 0.25M $CaCl_2$, except alginate) was then added to the PAH-coated microspheres to obtain the negative coating on the microspheres. The spheres were centrifuged to remove the supernatant and then rinsed three times to complete all coatings.

For multilayer coatings, the alginate microspheres were coated with combinations of the cationic and anionic polyelectrolytes. Before assembly on alginate templates, mass-thickness measurements were performed using a Standard Research Systems, Model QCM 100 to confirm alternate deposition of chitosan with chondroitin sulfate, alginate, and humic acid. The alternate deposition of DEAE dextran with chondroitin sulfate and humic acid was also confirmed. The layer-by-layer self assembly of these polyelectrolytes on alginate microspheres was then performed using similar protocol described in section 8.1. Heavy aggregation was noticed for the chitosan-alginate multilayers, limiting the final coating to two bilayers.

8.2 Determination of Glucose Oxidase Leaching from Alginate Microspheres

The leaching of glucose oxidase from alginate microspheres (both uncoated and coated) was accomplished using the protocol described in section 3.5. The leaching results were then fitted using Crank's equations as described in section 2.14 to calculate the diffusion coefficient of glucose oxidase through the uncoated and coated alginate microspheres.

8.3 Activity of Glucose Oxidase in Alginate Microspheres

The activity of the encapsulated glucose oxidase enzyme was performed according to the protocol described in section 3.6. The experiment was repeated for the polyelectrolyte-coated microspheres over a period of one month and the results were compared by calculating the slope of the curves. In each case, the results were normalized to the mass of glucose oxidase present in the spheres as determined using the Lowry

assay. Both the leaching and the activity results were analyzed using the two-tailed student's t-test.

8.4 Results and Discussion

8.4.1 Fabrication Results

A confocal micrograph of microspheres with encapsulated FITC-GOx formed with the emulsification technique is presented in Figure 8.1. The spheres appear bright green with uniform intensity distribution when imaged with the confocal microscope. The confocal line scan proves that a uniform distribution of the enzyme was achieved in the microspheres. The average diameter was found to be 31.89 ± 8.36μm for a sample size of ~800 spheres. The larger size of microspheres obtained in this experiment were a result of the use of the overhead stirrer for creating the emulsion.

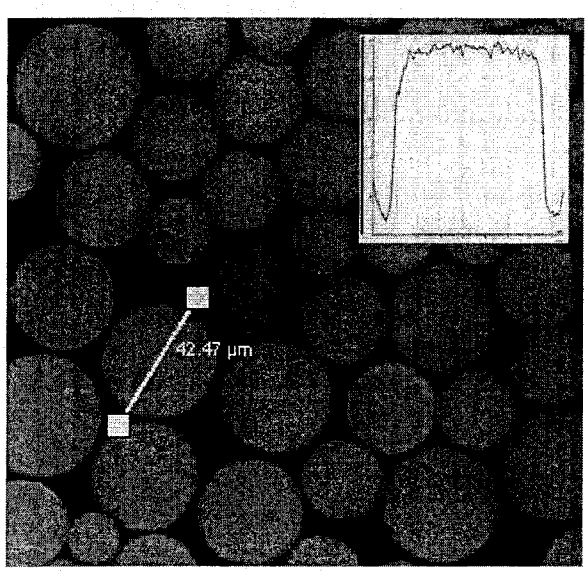

Figure 8.1. Confocal image of FITC-glucose oxidase loaded microspheres. Inset showing a line scan through an alginate microsphere.

Zeta potential measurements were used to confirm deposition of the polyelectrolyte coatings. The results for the different combinations--chitosan-alginate, chitosan-chondroitin sulfate, chitosan-humic acid, DEAE dextran-humic acid, DEAE dextran-chondroitin sulfate, and DEAE dextran-dextran sulfate--are shown in Figure 8.2. It can be seen that chitosan-alginate multilayers were successfully assembled up to the second bilayer; after this point heavy aggregation was observed. What is apparent from the measurements is that the charge reversal is highly uniform for the coatings used, implying that the various materials can be easily deposited in multilayers on these alginate templates using the simple layer-by-layer self-assembly technique.

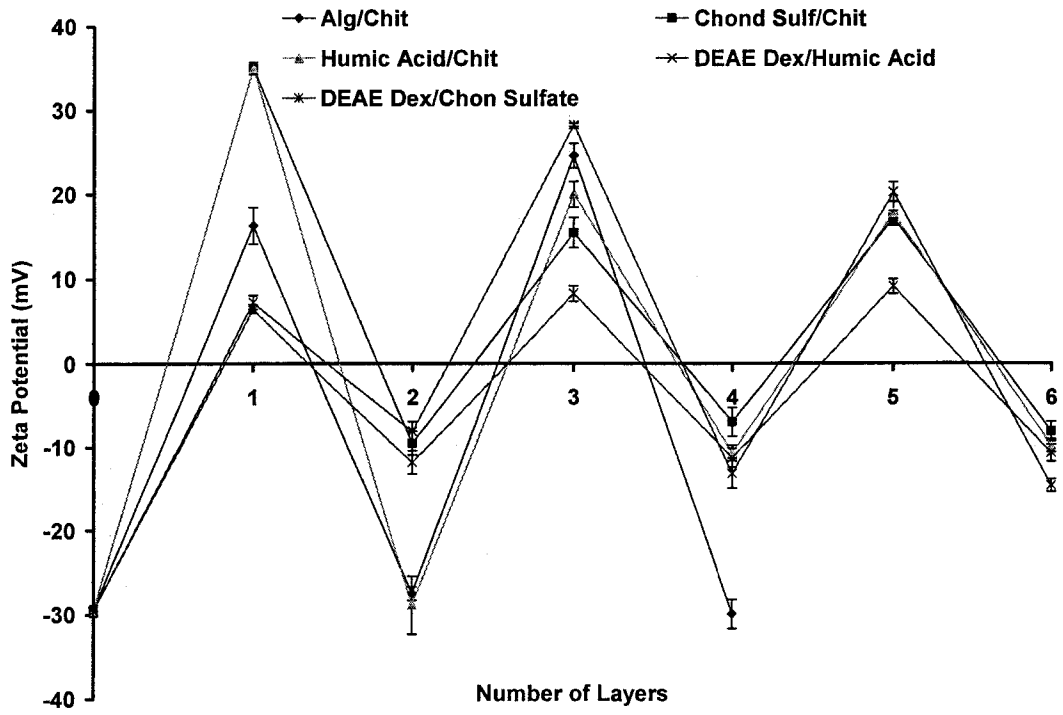

Figure 8.2. Alternate assembly of polyelectrolytes, confirmed using zeta potential.

8.4.2 Leaching of FITC-Glucose Oxidase from Conjugated Alginate Microspheres

Loss of FITC-GOx from the alginate microspheres was studied using fluorescence spectroscopy, where release of the encapsulated FITC-GOx from the microspheres resulted in an increase in the fluorescence intensity of the supernatant. Results from a typical experiment are given in Figure 8.3, where the leached amount for FITC-GOx is plotted versus time for uncoated microspheres and microspheres coated with the cationic and anionic polyelectrolytes. These results are very similar to the leaching results presented in section 7.5 and prove that the chemical conjugation of the enzyme to the alginate matrix using the carbodiimide chemistry does, in fact, reduce the leaching of the enzyme to a value that is close to the one that was obtained with one bilayer of PAH/PSS on unconjugated microspheres.

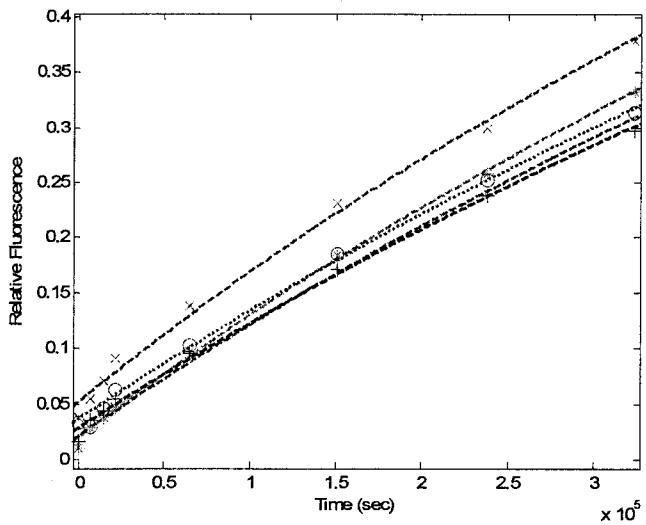

Figure 8.3. (a) Leaching versus time for alginate microspheres. Captions include bare microspheres (×), and spheres coated with one PEG amine layer (◦), one PEG bisamine layer (⋆), one chitosan layer (•), and one DEAE layer (+). Dashed lines indicate the fitted results obtained using Crank's mathematical model.

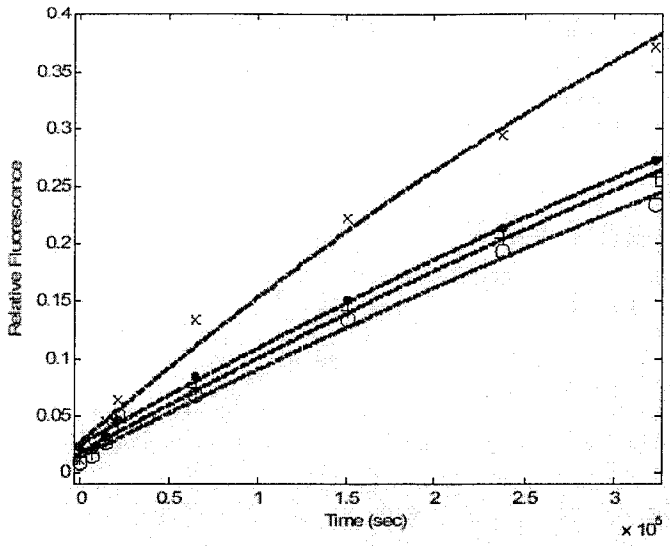

Figure 8.3(b). Leaching versus time for alginate microspheres. Captions include microspheres coated with one PAH/ alginate bilayer (×), one PAH/chondroitin sulfate bilayer (◦), one PAH/humic acid layer (+), and one PAH/dextran sulfate bilayer (•). Dashed lines indicate the fitted results obtained using Crank's mathematical model.

The leaching of the enzyme through the PEG amine and PEG bis(amine) coatings was very similar, with the total leaching for PEG bis(amine) being slightly higher than the PEG amine coating. The amine groups of the PEG derivatives can interact with the carboxyl groups on the alginate matrix, thus forming a complex. This interaction is expected to provide a smoother surface on the alginate matrix, generally improving its biocompatibility. Since the surface coverage of these coatings is related to the PEG chain length, the differences observed in the leaching of the enzyme may be related to the molar mass of the PEG used in this experiment. Leaching through chondroitin sulfate and humic acid coating was lower than the other materials, most probably due to the strong interaction between these coatings and PAH due to the presence of a number of reactive sites in these materials. Overall, the leaching observed for the cationic coatings was

higher than that for anionic coatings, possibly due the presence of an intermediate PAH layer for the anionic coatings. An exception to this leaching result was observed for microspheres coated with alginate. These results are consistent with the observations of Pommersheim et al.,[138] who assessed leaching from cytochrome C-loaded alginate microspheres coated with a multilayer membrane consisting of poly(*N*-vinylamine) and poly(acrylic acid). Generally, a decrease in protein loss was observed when at least two bilayers of the polyelectrolyte materials were used, while single coatings were not able to retain Cytochrome C. This decrease was attributed to a decrease in permeability of the films with additional layers. Another reason for this decrease might be the adsorption-desorption process reported by Kovacevic et al,[190] which showed that in solutions containing both weak polyelectrolytes with salt, the buildup of multilayers is modified and becomes an adsorption-desorption process, thus the resulting architecture has larger pores than the other coated microspheres, resulting in faster release. The leaching of glucose oxidase presented in the time-dependent release measurements are reorganized into a bar graph for direct comparison in Figure 8.4. The results shown are for the total leached amount at the end of four days (n = 3 measurements). The bar graph highlights the observations made with Figure 8.3. Microspheres coated with the anionic coatings (except alginate) are superior in terms of retaining the enzyme with less than 20% enzyme loss reported for all materials tested.

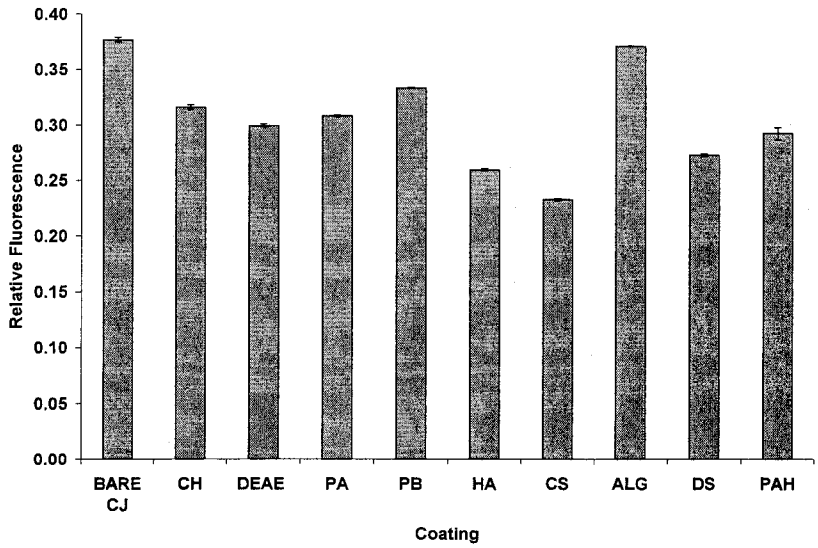

Figure 8.4. Leaching comparison for different polyelectrolyte materials – Monolayer coatings (captions include CH – chitosan, DEAE – DEAE dextran, PA – PEG amine, PB – PEG bis(amine), HA – humic acid, CS – chondroitin sulfate, ALG – alginate, DS – dextran sulfate, CJ – conjugated).

Similarly, the total leached amount for FITC-GOx for microspheres coated with combinations of cationic and anionic polyelectrolytes is plotted as a bar graph in Figure 8.5. Five different combinations of materials were used in this experiment, DEAE-dextran/humic acid (DE-HA), DEAE-dextran/chondroitin sulfate (DE-CS), chitosan/humic acid (CH-HA), chitosan/chondroitin sulfate (CH-CS), and chitosan/alginate (CH/Alg) to compare the effect of these combinations on total amount of enzyme leached at the end of four days. The leaching of the enzyme was less than 5% for the uncoated microspheres, while the leaching of the enzyme through DE-HA coatings dropped to less than 4% with the application of single bilayer.

Leaching studies on alginate gel beads coated with DEAE-Dextran has been investigated,[167] which explained that the DEAE-dextran has one DEAE group (or DEAE-DEAE group) per three glucose units, with the content in DEAE-DEAE group being two

times higher than that for the DEAE group. The tertiary amine on the DEAE group which has a pKa of ~9.2 was totally protonated at all pH of formation for the beads, and it could, therefore, interact with the carboxyl groups on the alginate. On the other hand, the quaternary amine on the DEAE-DEAE group (pKa of ~5.5) was not very accessible due to steric effects and therefore the interaction of this material was not strong enough.

The leaching for chitosan/alginate coatings was observed to be higher than the leaching for other materials, perhaps because at the pH of storage (pH 7.4), the chitosan ionization becomes lower (pKa of the chitosan amine group is ~6.3), and the membrane becomes less dense, leading to higher loss of the enzyme. On the other hand, the leaching of the enzyme through microspheres coated with chitosan/chondroitin sulfate was significantly lower than the other coating combinations used. This decrease may be due to the complex coacervation between the chitosan, chondroitin sulfate, and alginate leading to a reduction in the pore size of the membrane to provide better retention within the matrix.

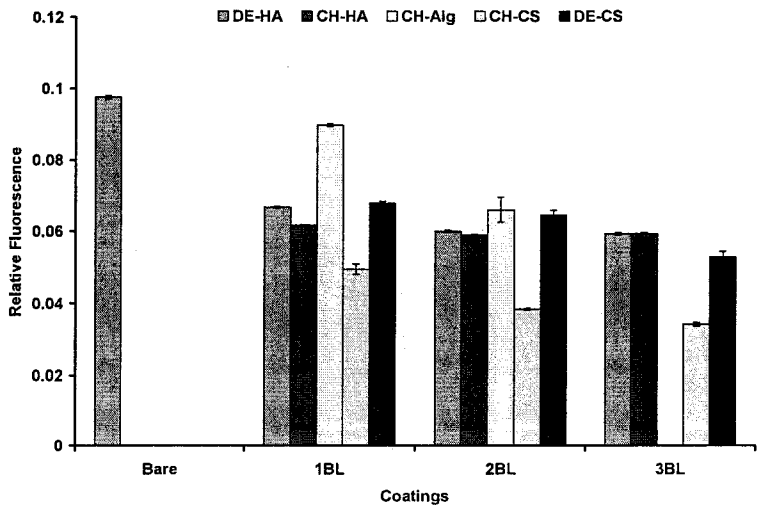

Figure 8.5. Leaching comparison for different polyelectrolyte materials – multilayer coatings.

The diffusion coefficients for the enzyme through alginate microspheres with different polyelectrolyte combinations are presented in Table 8.1. The diffusion coefficient results are similar to those presented in section 7.5 for the enzyme conjugated to alginate microspheres. The diffusion coefficient values for the enzyme leaching through coated microspheres is similar to that for uncoated microspheres because the conjugation of the enzyme was successful in immobilizing the enzyme within the alginate matrix, and the effect was due to the conjugation and not the coatings used.

Table 8.1. Diffusion coefficients for glucose oxidase in alginate microspheres coated with different polyelectrolyte nanofilms ($D_e \times 10^{-15}$ cm^2/sec).

Material	D_e
Conjugated uncoated microspheres	12.6
Chitosan coating (CH)	9.7
DEAE dextran coating (DE)	9.2
PEG amine coating (PA)	9.8
PEG bis(amine) coating (PB)	10.8
PAH/Alginate coating (ALG)	11.9
PAH/Dextran sulfate coating (DS)	8.2
PAH/Chondroitin sulfate coating (CS)	7.4
PAH/Humic acid coating (HA)	8

8.4.3 Activity and Stabilization of Encapsulated Glucose Oxidase in Conjugated Alginate Microspheres

In order to use the GOx-encapsulated alginate microspheres as practical glucose sensors, stable activity of the encapsulated enzyme must be realized. The enzyme activity results presented in section 7.5 showed that there was more than 90% activity retention in alginate microspheres at the end of four weeks. Since, similar conjugation techniques were used in this experiment, the retention in enzyme activity is expected to follow the same trends. As a baseline for further comparisons, the activity of conjugated uncoated and conjugated coated with cationic and anionic multilayers was assessed immediately following microsphere fabrication and following one, four, and twelve weeks of storage in phosphate buffer. The enzyme activity results are presented in Figure 8.6, with all activities normalized to total enzyme mass per sample as determined by Lowry assay. Similarly, the results for the activity experiment completed with the different combinations of coatings following fabrication and following one and four weeks of storage in phosphate buffer is presented in Figure 8.7.

It is instructive to begin the analysis by observing the activity of uncoated unconjugated microspheres over 12 weeks (Figure 8.6). After one week, the effective activity of the uncoated microspheres is decreased by approximately 78% from the initial value. Over the next 11 weeks, there is no further significant reduction in effective activity for the uncoated microspheres. Thus, while the activity of the uncoated microspheres is remarkably stable after the first week of wet storage, the process is far from efficient due to the large loss in effective activity over the first week. However, the enzyme activity for conjugated uncoated and conjugated coated microspheres

demonstrates more than 90% activity retention over 12 weeks. This retention is most likely due to enhanced stabilization of the enzyme with chemical conjugation techniques as already explained in section 7.5.

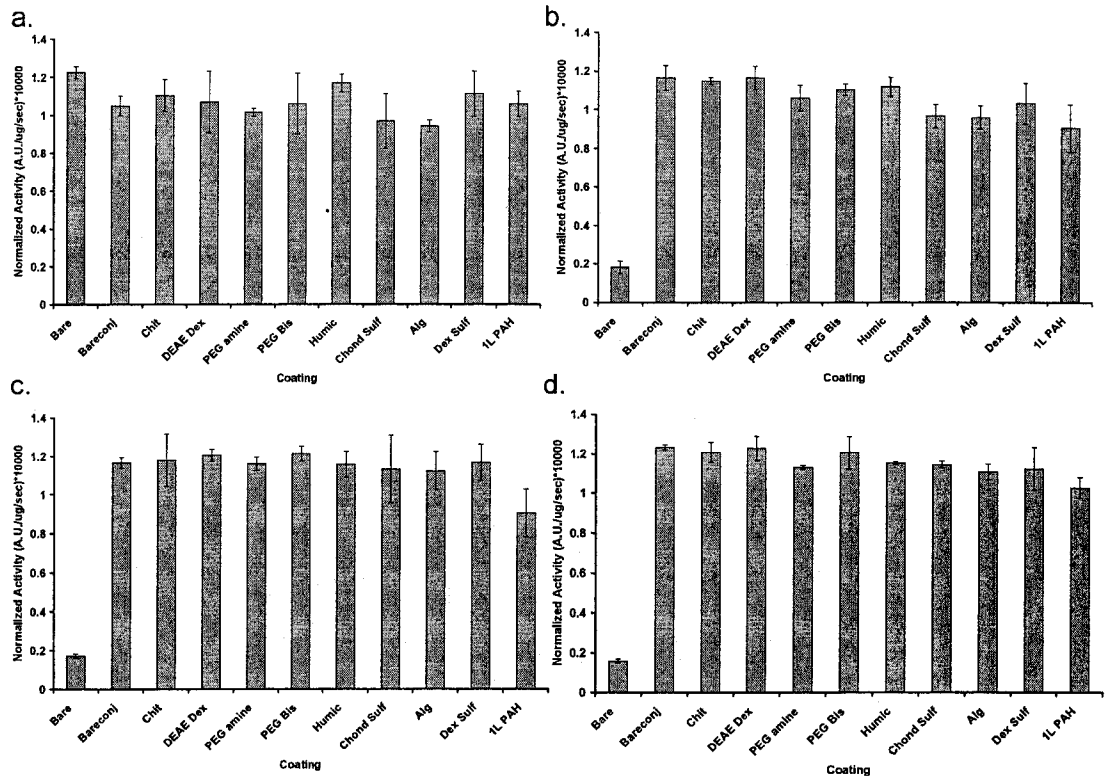

Figure 8.6. Comparison of coating on normalized activity over time of glucose oxidase inside alginate microspheres. (a) Activity of enzyme inside microspheres at week zero, (b) activity at week one, (c) activity at week four, and (d) activity at week 12. (Error bars ± one standard deviation, n=3.)

The enzyme activity results presented in Figure 8.7 show no significant change in activity for combinations of the coatings used at one week and four weeks of storage in the PBS solution, except for the chitosan-alginate multilayers, for which the enzyme activity was significantly lower than the enzyme activity for all other coatings used. These findings match the leaching results already explained in the previous section.

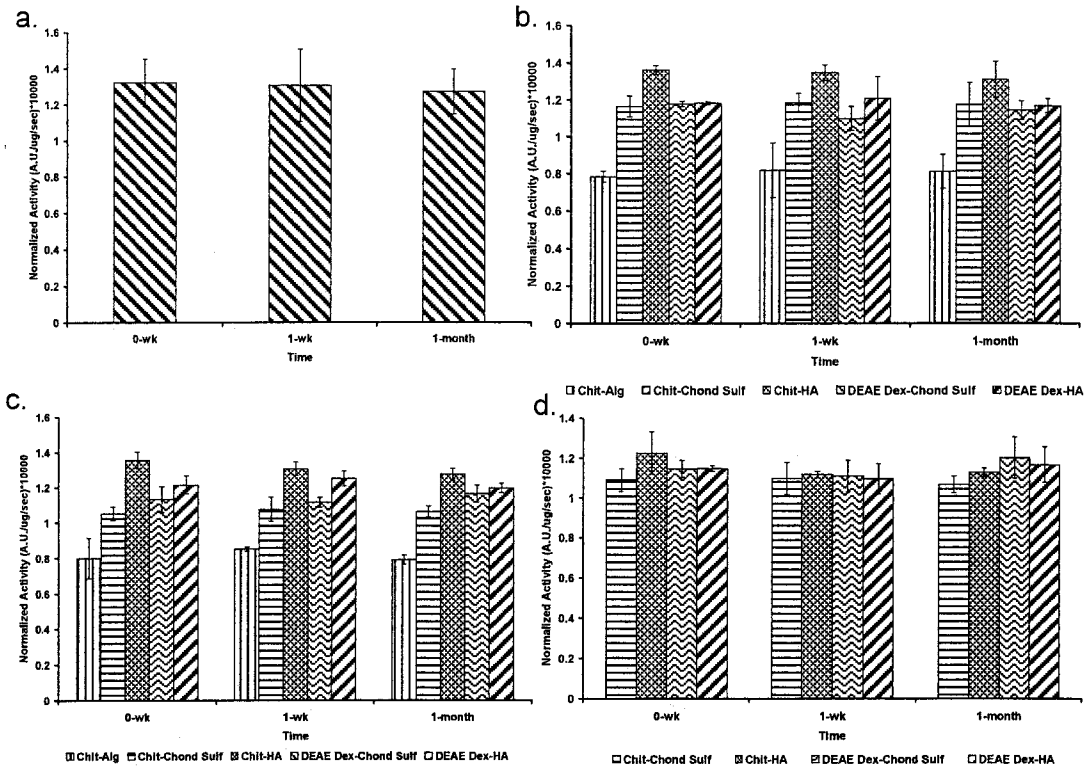

Figure 8.7. Comparison of coating on normalized activity over time of glucose oxidase inside alginate microspheres. (a) Activity of enzyme inside uncoated microspheres, (b) activity of enzyme inside one bilayer coated microspheres, (c) activity of enzyme inside two bilayer coated microspheres, and (d) activity of enzyme inside three bilayer coated microspheres. (Error bars ± one standard deviation, n=3.)

Overall, what is apparent from these findings is that the activity of encapsulated enzyme is significantly affected by the conjugation method used and not so much due to the materials used as coatings. The coating materials are applied to improve the biocompatibility of the implantable sensors. *In vitro* cytotoxicity experiments performed with these coating materials are more important in the context of this work. These tests are described in the following sections.

8.4.4 Cell Culture Studies

The *in vitro* studies examining cell behavior, cell viability and cellular activity conducted with NIH-3T3 mouse fibroblasts follow the protocols described in section 3.7. For the first part of this experiment, the cell behavior, viability and activity were assessed using cells grown on coated substrates.

8.4.4.1 Coated Substrates - Cell Behavior The cell behavior on 96-well assay plates coated with the polyelectrolyte materials are shown as brightfield and fluorescence images in Figure 8.8. The images were acquired at the end of 24 and 72 hours, culture period respectively, after the cells had been grown on the 96-well plates. The surface of the 96-well plates (tissue culture polystyrene [TCPS]) was chosen as the control in this experiment. The fibroblasts exhibited normal morphology with spreading on the control surface shown in Figure 8.8 (a). On the other hand, the cells on the wells coated with the polycationic polyelectrolyte materials (chitosan [CH], DEAE dextran [DE], PEG amine [PA], and PEG bis[amine] [PB]) did not present a normal fibroblast morphology and were more rounded in structure. The cells did not attach on these surfaces most likely due to the surface charge on the substrate presented to the cell surface.

One example of these observations is shown in Figure 8.8(c), for cells in contact with DE coated well plates. It can be seen that the cells did not attach to the substrate and were more rounded in structure. A small number of dead cells were observed floating in the medium. Finally, the cells on the wells coated with the polyanionic polyelectrolyte materials (alginate [ALG], chondroitin sulfate [CS], humic acid [HA], and dextran sulfate [DS]) seemed to spread and attach to the surface. A typical result is shown in Figure 8.8 (e), for cells in contact with CS coated well plates. The cells present a similar

morphology as observed for the TCPS substrate. The cell viability results from the live-dead assay kit are also presented in Figure 8.8 and will be discussed in the next section.

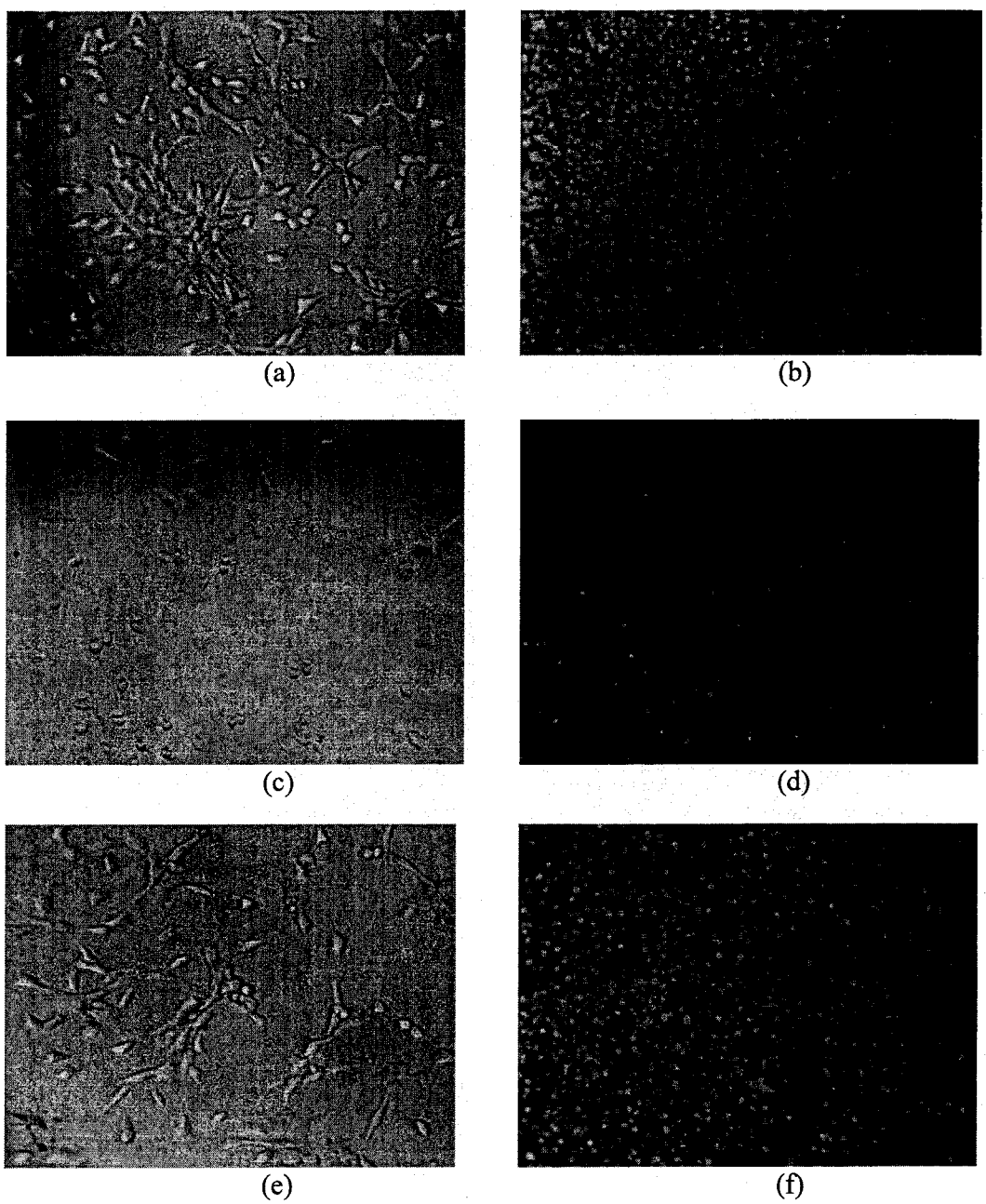

Figure 8.8. Brightfield image (at 24 hours) and fluorescence image (at 72 hours) for cells in contact with TCPS substrate (a & b), cells in contact with DE-coated substrate (c & d), and cells in contact with CS-coated substrate (e & f).

8.4.4.2 Coated Substrates – Cell Viability The cell viability experiments were conducted according to the protocol described in section 3.7, after cells were in contact with the coated substrates for 72 hours. The live cells show intense bright green fluorescence, while the dead cells are stained red. The fluorescence was recorded with a fluorescence plate reader, and the fluorescence intensity measurements were normalized to the fluorescence intensity recorded from the TCPS substrate after adjusting for the background fluorescence. Some of the images taken using the fluorescence microscope are shown in Figure 8.8 (b,d,f). The cells in contact with the TCPS substrate (control) which exhibited normal fibroblast morphology were stained green with the calcein dye. A large number of live cells were seen in Figure 8.8 (b) for the control. In contrast, a large number of dead cells were observed in Figure 8.8 (d), for the cells in contact with DE coated substrates for 72 hours. Finally, Figure 8.8 (f) contains a fluorescence image for cells in contact with CS coated substrate, which contains a large number of live cells and no dead cells, implying that some polyelectrolyte materials are conducive to cell attachment and therefore, promote cell viability compared to other polyelectrolyte materials.

The overall results for viability measurements are presented in a bar graph shown in Figure 8.9, which compares the percentage of live cells on different substrates to the cells grown on the control (taken as 100%). The data suggest that the wells coated with CS and HA were more favorable (significantly different) for the attachment and viability of the fibroblasts than the other materials used and were even an improvement over the control. Chondroitin sulfate is the predominant glycosaminoglycan found in cartilage and skin

and is associated with collagen in connective tissue and tendon *in vivo*.[199] For this reason, it is expected to have strong compatibility with cells.

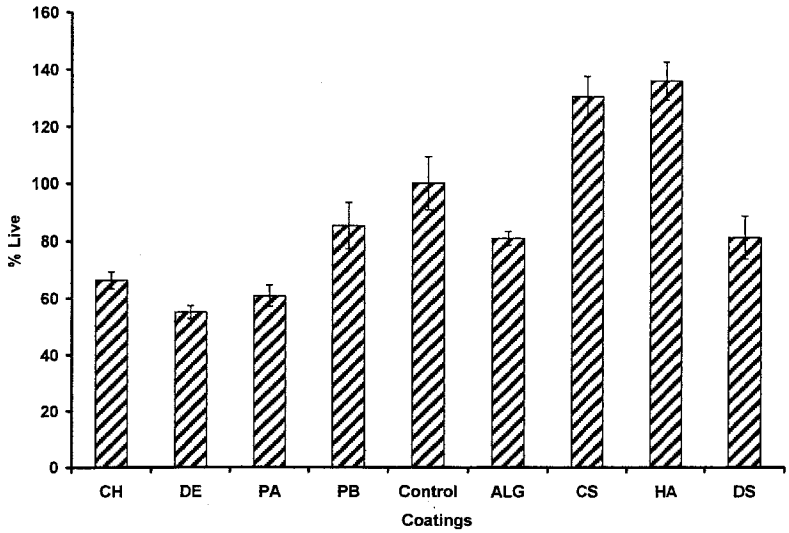

Figure 8.9. Cell viability using the live-dead assay. Results normalized to TCPS (control) substrate.

The experiments conducted with the live-dead viability assay suggested that chondroitin sulfate and humic acid coatings were superior to the other coatings used. To further establish the utility of these coating materials, a cell activity assay conducted according to the protocol described in section 3.7 has been described in the next section.

8.4.4.3 Coated Substrates – Cell Activity Cell activity on coated well plates was determined by the MTT assay, which is based on the mitochondrial conversion of the tetrazolium salt of 3-(4,5-dimethylthiazol-2-yl)-2,5-diphenyl-2H-tetrazolium bromide (MTT). This process yielded purple formazan crystals, which were subsequently dissolved in IPA to measure absorbance at 570nm. The result of this experiment has been plotted in a bar graph as a percentage of the cell activity observed for the control (Figure 8.10). The results of this experiment suggested that the cell activity for cells grown on

anionic substrates was higher than that for the TCPS substrate, further supporting the efficacy of these coatings for biocompatibility purposes. It is also possible that some polyelectrolyte materials are not conducive to cell attachment and therefore, the cellular activity is reduced for unattached cells. For this experiment, the cell activity observed for CS-coated well plate was significantly higher than the other materials.

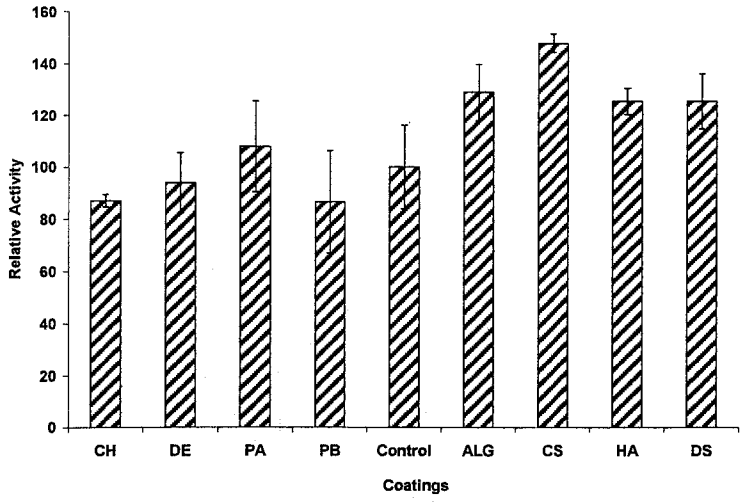

Figure 8.10. Cell activity using the MTT assay. Results normalized to TCPS (control) substrate.

The cell behavior, viability, and activity assays conducted with coated well plates suggest that anionic polyelectrolyte materials were superior to the cationic polyelectrolyte materials, although only results for chondroitin sulfate coating were found to be significantly different from other coating materials. This difference suggests that further tests are required to support the observations noted in this section. The next section covers the cell viability and activity assay results for cells in contact with microspheres coated with these polyelectrolyte materials.

8.4.4.4 Cell Contact with Microspheres – Cell Viability The cell viability experiments were conducted with alginate microspheres without GOx at the end of 24 hours after the microspheres were added to the cells. Some of the images for cell morphology taken at the end of this period are shown in Figure 8.11. The cells growing in the control well (TCPS substrate) displayed normal fibroblast morphology (Figure 8.11[a]), while the cells in contact with uncoated microspheres (Figure 8.11[b]) appeared to be proliferating (increasing in number) compared to the control substrate. These results exhibit the biocompatible nature of alginate coatings.

The cell morphology results for microspheres coated with chitosan and PEG amine (Figure 8.11[c-d]) contained more dead cells compared to the control substrate, implying that these coatings were not favorable for cell growth. These findings were in agreement with the morphology results for coated substrates, where it was observed that the cationic coatings demonstrated poor cell viability compared to anionic coatings. On the other hand, the microspheres coated with alginate as the outer coating displayed poor cell viability, as a number of dead cells were observed floating in the solution (Figure 8.11[e]). As discussed in the leaching section, this finding may be attributed to the poor coating properties of alginate, leading to large pores in the matrix through which the cells were exposed to the underlying PAH layer, which has been shown to be cytotoxic to cells. Chondroitin sulfate coating was shown to be biocompatible with cells (higher viability and activity compared to control) in the previous section. Similar results were observed for cells in contact with CS-coated microspheres in Figure 8.11(f); increased cell proliferation and network formation of cells were observed.

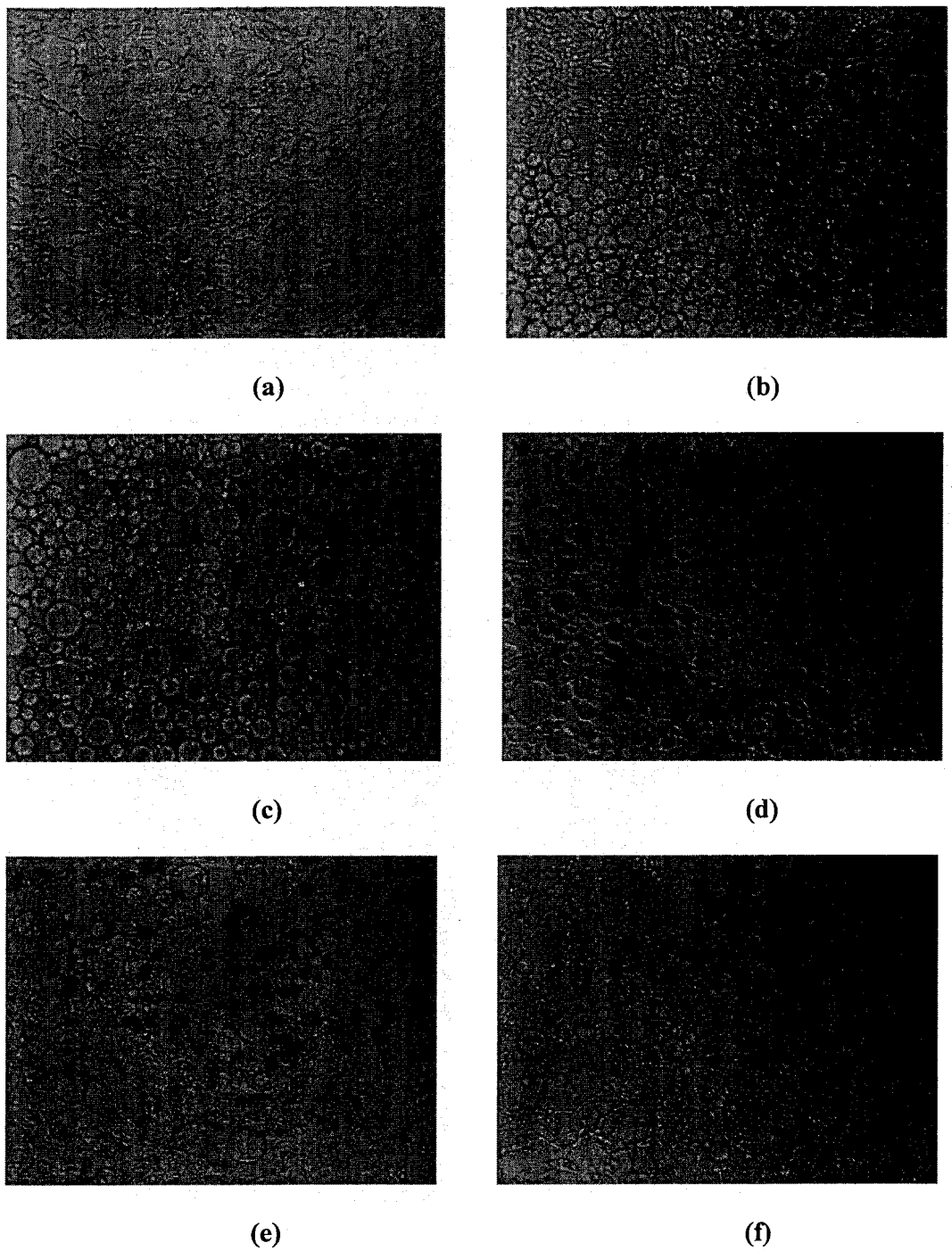

Figure 8.11. Brightfield images for cells in contact with microspheres without GOx at 24 hours for (a) control and wells with (b) uncoated, (c) CH-coated, (d) PA-coated, (e) ALG-coated, and (f) CS-coated microspheres.

These findings are reported in the bar graph shown in Figure 8.12, which compares the percentage of live cells for microspheres coated with polyelectrolyte materials at different concentrations on the microspheres to the TCPS substrate (control). Since the *in vivo* testing of the sensors coated with the different polyelectrolyte materials will involve using a fairly high concentration (>1nM) of the polyelectrolytes, it was important to gauge the effect of high concentrations of these polyelectrolyte materials using the *in vitro* cytotoxicity tests described in this experiment. The maximum concentration achieved with DE and DS coatings on alginate microspheres was 0.6nM; therefore, 1nM concentration was not tested for these materials. Uncoated microspheres at all concentrations exhibited superior cell viability, as more than 125% of live cells were detected at all the concentrations tested. On the other hand, significant differences were found between chondroitin sulfate, humic acid, and PEG bis(amine) with all the other coatings at all concentrations. Microspheres coated with chitosan, DEAE dextran, PEG amine, alginate and dextran sulfate expressed poor cell viability (<50% live cells) compared to the control at high concentrations.

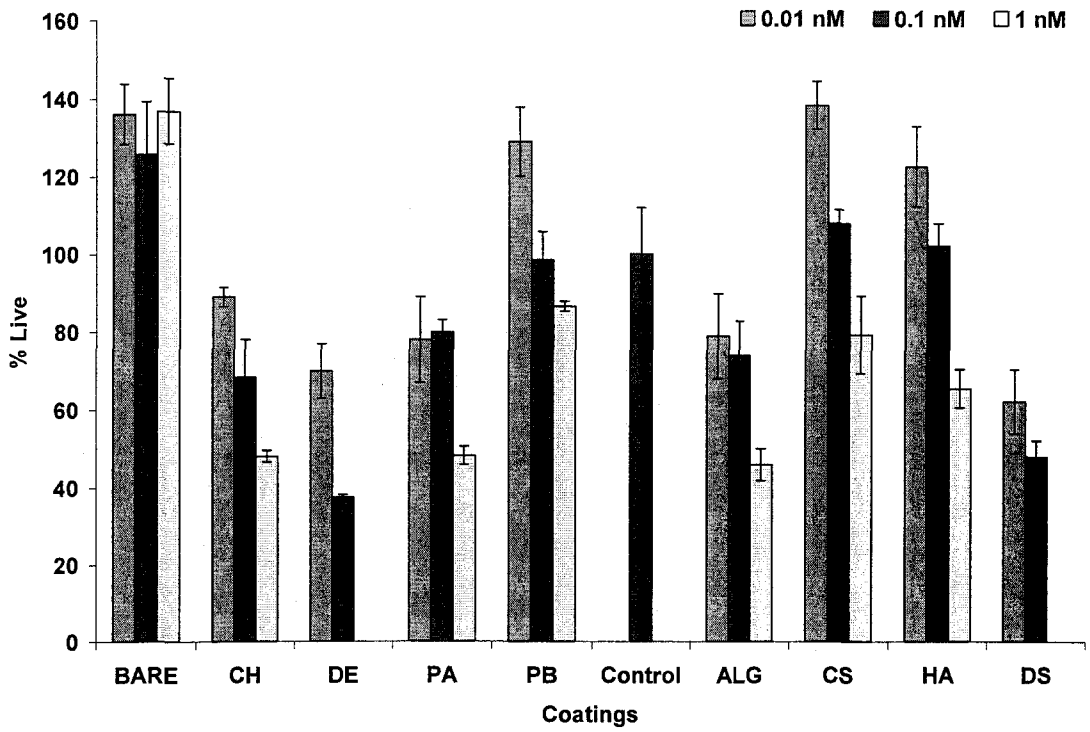

Figure 8.12. Live-dead assay results for cell contact with microspheres normalized to TCPS control substrate (bare microspheres have been diluted 10-times and 100-times from the concentrated suspension).

After the cell behavior and viability experiments were completed, the cell proliferation assay was conducted using the MTT assay kit to determine the number of active cells at the end of 24 and 72 hours after the cells were in contact with the microspheres. These experiments are described in the next section.

8.4.4.5 Cell Contact with Microspheres – Cell Proliferation The cell behavior was assessed before conducting the cell activity assay. Some of the brightfield images taken before adding the assay reagents are shown in Figure 8.13. As noted in the previous section, uncoated alginate microspheres (Figure 8.13[a]) exhibited superior cell viability at the end of 72 hours, which agrees with the observations at 24 hours. There were a

large number of dead cells observed for cells in contact with alginate coated microspheres (Figure 8.13[e]). The cells in contact with CS-coated microspheres were proliferating and forming networks as shown in Figure 8.13 (f).

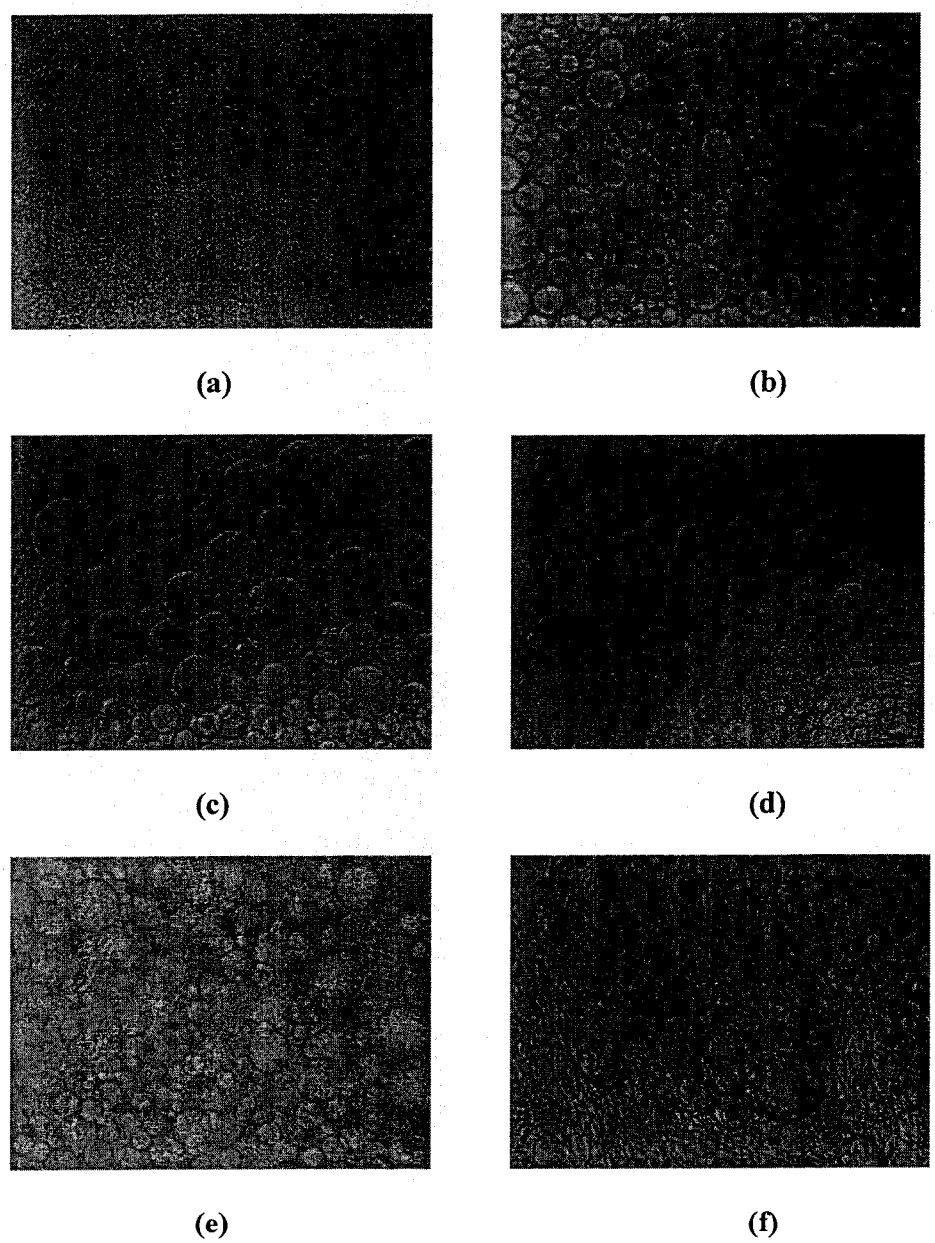

Figure 8.13. Brightfield images for cells in contact with microspheres without GOx at 72 hours for (a) control and wells with (b) uncoated, (c) CH-coated, (d) PA-coated, (e) ALG-coated, and (f) CS-coated microspheres.

The number of active cells for each coating at each time period was calculated by using a standard curve constructed with MTT assay conducted on known cell numbers as described in section 3.7. The active cell numbers at the end of 24 and 72 hours are presented in Figure 8.14 (a) and (b) respectively, which is plotted as a bar graph to aid in better understanding of the results. At 24 hours for high concentrations, there were insignificant differences between control, uncoated microspheres, and microspheres coated with CS, HA and PB (approximately 12000 cells), while ALG coating contained the lowest cell number (~6000 cells). There were approximately 8000 cells observed for CH and PA coatings. At lower concentrations, though, CS reported the highest cell number (~20,000 cells) compared to ~12000 cells for the control substrate. DE and DS coatings had the same cell numbers as the control at lower concentrations. At 72 hours, much lower cell numbers were reported for DE and DS coatings (~25,000 cells) compared to ~50,000 cells for the control. These results suggested that DE and DS coatings were not suitable for cell proliferation. Finally, at higher concentrations, HA, CS, CH, PA, and PB coatings had ~30-50,000 cells compared to 50,000 cells for the control and were therefore, found to be superior to other coatings towards cell proliferation and growth. In summary, the cell viability and activity experiments performed with 96-well assay plates coated with the different polyelectrolyte materials suggested that the anionic coatings were favorable to cell growth, with chondroitin sulfate and humic acid coatings being superior to the other coatings. For the experiments conducted with microspheres (no GOx inside), the uncoated microspheres exhibited superior cell viability with more than 125% of live cells (compared to the control) detected at all the concentrations tested. Microspheres coated with chitosan, DEAE

dextran, PEG amine and dextran sulfate exhibited poor cell viability (<50% live cells) compared to the control at high concentrations. Finally, chondrotin sulfate, PEG bis(amine) and humic acid were found to be favorable to cell growth at high concentrations with more than 75% cell viability at high concentrations.

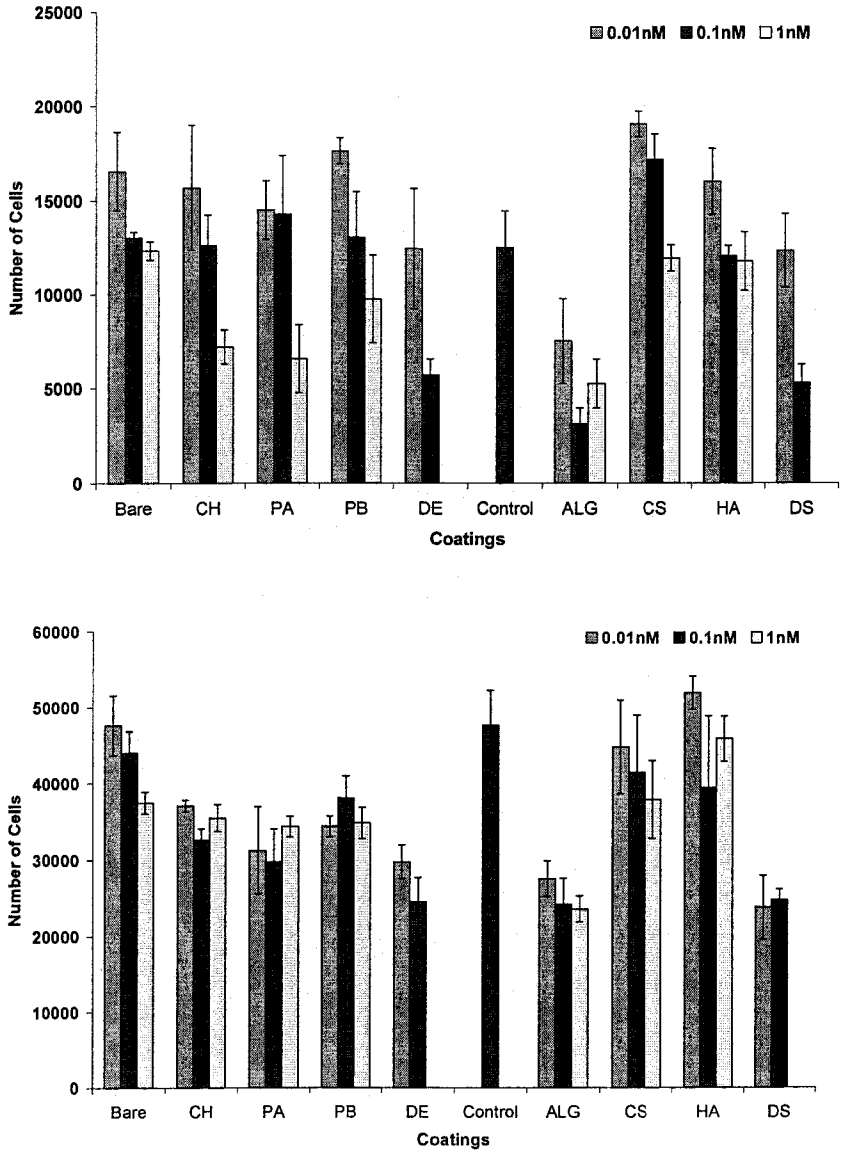

Figure 8.14. (a) Cell proliferation at 24 hours for microspheres without GOx, (b) cell proliferation at 72 hours for microspheres without GOx (bare microspheres have been diluted 10-times and 100-times from the concentrated suspension).

Since it is difficult to quantify the results obtained using the live-dead and activity assays together, a biocompatibility index (BI) was calculated which scaled the live-dead results and the MTT assay results to the TCPS control and averaged them to get a value, which then allow the assays be compared together. For example, a BI greater than one implies that the coatings are superior to TCPS, while a BI less than one suggests the opposite. Figure 8.15 displays the graph for the BI versus polyelectrolyte materials at 0.1nM concentrations.

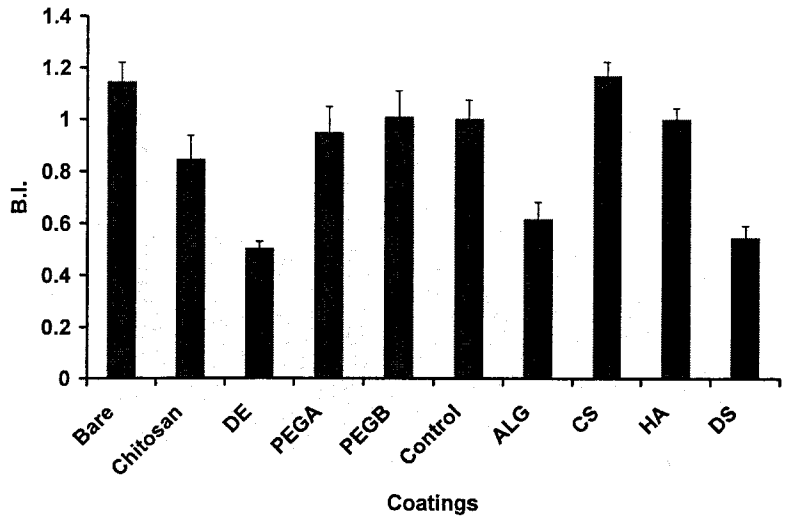

Figure 8.15. Biocompatibility Index (BI) versus polyelectrolyte materials.

From the graph, it is evident that BARE, CS, HA, PA, PB, and chitosan coatings are superior to DE, DS and ALG coatings, when compared to the TCPS control. At higher concentrations, though, PA is also eliminated. In conclusion, microspheres coated with chitosan, PEG bis(amine), chondroitin sulfate and humic acid are found to be suitable for *in vivo* testing, while microspheres coated with alginate, DEAE dextran and dextran sulfate, which exhibited poor cell viability and cell activity are not recommended.

CHAPTER 9

CONCLUSIONS AND FUTURE WORK

Alginate-based hydrogels have several unique properties that have enabled them to be used as a matrix for the entrapment of a variety of enzymes, proteins, and cells for applications in bioprocessing, drug delivery, and chemical sensing. However, control over release rates or to achieve stable encapsulation, remains a difficult goal, especially for small particles with high surface-area-to-volume ratios, therefore, the major objectives of this project were to develop stable entrapment procedures for enzymes using nanoengineered ultrathin coating technologies on alginate matrices towards implantable glucose sensors.

In the first part of this work, the potential to limit diffusion of dextran entrapped in alginate spheres with nanofilm coatings was assessed. Dextran was chosen because it has been traditionally used in diffusion studies, it is available in different molecular weights and it has same surface charge as glucose oxidase at physiological pH. Alginate microspheres were fabricated using an emulsification process, and dextran was encapsulated in the gel phase by mixing with the alginate in solution. The exterior surface was then modified with polyelectrolyte coatings using the layer-by-layer self assembly technique. Leaching studies to assess retention of dextran with varying molecular weight confirmed that the application of multilayer thin films to the alginate microspheres was effective in reducing leaching rate and total loss of the encapsulated material from the

microspheres. For the best case, the rate of release for dextran of 2 MDa molecular weight decreased from 1%/hour in bare microspheres to 0.1%/hour in polyelectrolyte-coated microspheres. Diffusion coefficient values for the release of dextran from alginate microspheres were also calculated, and only {PAH/PSS} coatings were found to significantly affect the diffusion coefficient values from alginate microspheres.

The experimental results obtained for the release of dextran from alginate microspheres were then used to choose the coating materials for the stable encapsulation of glucose oxidase enzyme inside alginate microspheres. Different crosslinking techniques (photocrosslinking and chemical conjugation) were also assessed in order to achieve stable encapsulation of the enzyme. Glucose oxidase was encapsulated in alginate microspheres using similar techniques as shown for the encapsulation of dextran. Polyelectrolyte nanofilm coatings of different composition and thickness were then deposited on the microspheres and the loss of enzyme was monitored over one week. The total loss of encapsulated material was reduced to less than 25% and 15% with the application of single {PAH/PSS} and crosslinked {PAH/PAA} coatings, respectively, in comparison to at least 45% loss observed with uncoated and {PDDA/PSS}-coated microspheres. The activity of the encapsulated enzyme was also tested over three months, and it was found that {PAH/PSS} and crosslinked {PAH/PAA}-coated spheres retained more than 84% and 60% of their initial activity, respectively, after three months, whereas uncoated and {PDDA/PSS}-coated microspheres retained less than 20% of initial activity after three months.

In the next part, the nanoassembly and photocrosslinking of diazo-resin (DAR) coatings on small alginate microspheres for stable enzyme entrapment was described.

Uncoated spheres exhibited rapid loss of activity, retaining only 20% of initial activity after one week, and a dramatic reduction in effective activity over 24 weeks, whereas the uncrosslinked and crosslinked {DAR/PSS}-coated spheres retained more than 50% of their initial activity after four weeks, which remained stable even after 24 weeks for the two and three bilayer films. The experimental results suggested that the application of {DAR/PSS} multilayer thin films was effective in reducing loss of the encapsulated enzyme compared to bare microspheres, as well as increasing retention of enzymatic activity. The findings exhibit that enzyme immobilization and stabilization can be achieved by using simple modifications to the layer-by-layer self-assembly technique and show that crosslinked {DAR/PSS} films may be used to decrease leaching of enzyme from alginate microspheres and protect the spheres from degradation, without adversely influencing effective activity in longer-term applications for enzyme based bioreactors and biosensors.

The leaching and activity results obtained using the coatings described suggested that a combination of the methods used, involving chemical conjugation and {PAH/PSS} multilayers was expected to provide enhanced retention of the enzyme. The next experiment involved the stabilization of the enzyme accomplished using chemical conjugation techniques. The leaching results for microspheres conjugated with the enzyme suggested that the enzyme was stably encapsulated inside the microspheres with less than 20% leaching of the enzyme over five days. Finally, the activity results demonstrated the effectiveness of the chemical conjugation, as more than 90% enzyme activity was preserved in all cases over one month of testing. This method was then selected for all future experiments.

In the last section, novel biocompatible materials were used to coat the alginate microspheres to improve biocompatibility for long term biosensor use. The enzyme was crosslinked to the alginate matrix using the conjugation technique and leaching and activity studies were conducted. The experimental results suggested improved retention of the enzyme over time, most likely due to the chemical crosslinking. *In vitro* cytotoxicity tests were completed using 3T3 cells to determine the "optimum" coating material towards biosensor use. Of all the materials tested, chondroitin sulfate, humic acid, PEG bis(amine), and chitosan coatings were found to be suitable for testing on sensors *in-vivo*. The experimental results from the *in vitro* cytotoxicity studies have been incorporated in an ongoing work which involves testing the cytotoxicity of the alginate-based glucose sensors in rats.

The novel aspect of this work was to present a stable encapsulation technique for glucose oxidase enzyme, using modifications to the existing fabrication and self-assembly technique, towards long term biosensor use. The experimental results obtained in this dissertation can be potentially used to encapsulate proteins, enzymes, growth factors, drugs etc., in polymer matrices and ultrathin film coatings can then be used to achieve stable encapsulation or controlled release over time. Also, the biocompatibility work conducted as part of this dissertation pointed out several coatings that can be used to modify the surface properties of implants in order to make them suitable for *in vivo* use. Finally, a design of an "optimum" alginate based-glucose sensor is presented here.

For the design, the fabrication of the alginate microspheres, in the size range 50-60μm diameter will be accomplished using the overhead stirrer with the emulsification technique. To achieve ~20mM glucose oxidase concentration in the alginate

microspheres, 50mg of glucose oxidase enzyme will be mixed in the alginate aqueous phase before making the microspheres. The chemical conjugation technique will ensure stable encapsulation of the enzyme. The oxygen sensitive fluorophore will then be incorporated in the uncoated alginate microspheres using precipitation technique. After this, {PAH/PSS} nanofilm coatings (in 0.25M $CaCl_2$) will be applied to introduce the reference dye for the glucose sensing measurements as well as to provide a diffusion barrier to the substrates. Finally, an outer coating of chondroitin sulfate will be assembled to tailor the biocompatibility of the sensors. The microspheres can be stored at 4°C in pH 7.4 0.01M PBS buffer to ensure maximum retention of enzyme activity over time. For the design presented, it is expected that there will be less than 5% leaching of the enzyme over long term and more than 95% activity retention over three months. Future work will involve making more uniform microspheres for better characterization of the glucose sensing properties and testing these sensors *in vivo*. These results can therefore be useful in tailoring the transport properties of alginate and other hydrogel microspheres and will ultimately find use in encapsulating and protecting the sensor chemistry towards the fabrication of implantable glucose sensors.

REFERENCES

[1] NDFS. Centers for Disease Control and Prevention: National diabetes fact sheet: general information and national estimates on diabetes in the United States, 2003. Rev ed. Atlanta, GA: U.S. Department of Health and Human Services, Centers for Disease Control and Prevention.

[2] WHO. Diabetics Action Now: an Initiative of the World Health Organization and the International Diabetes Federation. 2004. WHO, Geneva, Switzerland.

[3] J C Pickup, F Hussain, N D Evans, N Sachedina. In vivo glucose monitoring: the clinical reality and promise. 2004. Biosensors and Bioelectronics, in press.

[4] D M Nathan. Long-term complications of diabetes mellitus. 1993. New England Journal of Medicine 328, 1676-1685.

[5] Diabetes Control and Complications Trial Research Group. The effect of intensive treatment of diabetes on the development and progression of long term complications in insulin dependent diabetes. 1993. New England Journal of Medicine, 329, 977-986.

[6] American Diabetes Association. Self monitoring of blood glucose. 1994. Diabetes Care, 17, 81-86.

[7] R A Peura. Chemical biosensors. Medical Instrumentation: Application and Design. 1998. 3rd ed. J G Webster, ed. John Wiley and Sons, Inc: New York.

[8] T Koschinsky, L Heinemann. Sensors for glucose monitoring: technical and clinical aspects. 2001. Diabetes Metabolic Research Reviews, 17, 113-123.

[9] Y. Wickramasinghe, Y Yang, S A Spencer. Current problems and potential techniques in in-vivo glucose monitoring. 2004. Journal of Fluorescence, 14, 513-520.

[10] N Sachedina, J C Pickup. Performance assessment of the Medtronic-Minimed continuous glucose monitoring system and its use for measurement of glycaemic control in type 1 diabetic subjects. 2003. Diabetes Medicine, 20, 1012-1015.

[11] J A Tamada, S Garg, L Jovanovic, K R Pitzer, S Fermi, R O Potts. Non-invasive glucose monitoring. Comprehensive clinical results. 1999. JAMA 282, 1839-1844.

[12] A Maran, C Crepaldi, A Tiengo. Continuous subcutaneous glucose monitoring in diabetic patients. A multicenter study. 2002. Diabetes Care, 25, 347-352.

[13] W Kerner. Implantable glucose sensors: Present status and future developments. 2001. Experimental and Clinical Endocrinology and Diabetes,109, S341-S346.

[14] E A Moschou, B V Sharma, S K Deo, S Daunert. Fluorescence glucose detection: Advances toward the ideal *in vivo* biosensor. 2004. Journal of Fluorescence, 14, 535-547.

[15] J. C. Pickup, F. Hussain, N. D. Evans, O. J. Rolinski, D. J. S. Birch. Fluorescence-based glucose sensors. 2004. Biosensors and Bioelectronics. in press.

[16] S Weiss. Fluorescence spectroscopy of single molecules. 1999. Science, 283, 1676-1683.

[17] H Fang, G Kaur, B Wang. Progress in Boronic Acid-Based Fluorescent Glucose Sensors. 2004. Journal of Fluorescence, 14, 481-489.

[18] J D Newman, A P F Turner. Home blood glucose biosensors: a commercial perspective. 2005. Biosensors and Bioelectronics, in press.

[19] R Ballerstadt, R Ehwald. Suitability of aqueous dispersions of dextran and Concanavalin A for glucose sensing in different variants of the affinity sensor. 1994. Biosensors and Bioelectronics, 9, 557-567.

[20] J Slavik. Fluorescent Probes in Cellular and Molecular Biology. 1994. CRC Press: Boca Raton.

[21] R J Russell, M V Pishko, C G Gefrides, M J McShane, G L Coté. A Fluorescence-Based Glucose Biosensor using Concanavalin A and Dextran Encapsulated in a Poly(ethylene glycol) Hydrogel. 1999. Analytical Chemistry, 71, 3126-3132.

[22] M J McShane, R J Russell, M V Pishko, G L Coté. Towards minimally-invasive glucose monitoring using implanted fluorescent microspheres. 2000. IEEE Engineering in Medicine and Biology Magazine, 19, 36-45.

[23] M J McShane. Potential for glucose monitoring with nanoengineered fluorescent biosensors. 2002. Diabetes Technology and Therapeutics, 4, 533-538.

[24] M J McShane. Microcapsules as "Smart Tattoo" Glucose Sensors: Engineering Systems with Enzymes and Glucose-Binding Elements. 2005. Submitted for Topics in Fluorescence, Vol 10, Glucose Sensing.

[25] M J McShane, S Rastegar, M Pishko, G L Coté. Monte Carlo Modeling for Implantable Fluorescent Analyte Sensors. 2000. IEEE Transactions on Biomedical Engineering, 47, 624-632.

[26] R J Russell, M V Pishko, C C Gefrides, G L Coté. A fluorescent glucose assay using poly-l-lysine and calcium alginate microencapsulated TRITC-Succinyl-Concavalin A and FITC-Dextran. 1998. Proceedings of the 20th Annual International Conference of the IEEE Engineering in Medicine and Biology Society, 20, 2858-2861.

[27] S N Thennadil, J L Rennert, B J Wenzel, K H Hazen, T L Ruchti, M B Block. Comparison of Glucose Concentration in Interstitial Fluid, and Capillary and Venous Blood During Rapid Changes in Blood Glucose Levels. 2001. Diabetes Technology and Therapeutics, 3, 357-365.

[28] R A Copeland. 2000. Enzymes: A Practical Introduction to Structure, Mechanism and Data Analysis, Wiley-VCH, Inc.

[29] V V Karnati, X Gao, S Gao, W Yang, W Ni, S Sankar, B Wang. A glucose-selective fluorescence sensor based on boronic acid-diol recongnition. 2002. Biorganic Medicinal and Chemistry Letters, 12, 3373-3377.

[30] T D James, K R A S Sandanayake, R Iguchi, S Shinkai. Novel saccharide-photoinduced electron transfer sensors based on the interaction of boronic acid and amine. 1995. Journal of Americal Chemical Society, 117, 8982-8987.

[31] H Eggert, J Frederiksen, C Morin, J C Norrid. A new glucose-selective fluorescence bisboronic acid. First report of strong a-furanose complexation in aqueous solution at physiological pH. 1999. Journal of Organic Chemistry, 64, 3846-3852.

[32] N DiCesare, J R Lakowicz. Evaluation of two synthetic glucose probes for fluorescence-lifetime based sensing. 2001. Analytical Biochemistry, 294, 154-160.

[33] R Badugu, J R Lakowicz, C D Geddes. A glucose sensing contact lens: A non invasive technique for continuous physiological glucose monitoring. 2003. Journal of Fluorescence, 13, 371-374.

[34] V Scognamiglio, M Staiano, M Rossi, S D'Auria. Protein-Based Biosensors for Diabetic Patients. 2004. Journal of Fluorescence, 14, 491-498.

[35] L L Salins, R A Ware, C M Ensor, S Daunert. A novel reagentless sensing system for measuring glucose based on the galactose/glucose-binding protein. 2001. Analytical Biochemistry, 294, 19-26.

[36] L Tolosa, I Gryczynski, L R Eichhorn, J D Dattelbaum, F N Castellano, G Rao, J R Lakowicz. Glucose sensor for low cost lifetime based sensing using a genetically engineered protein. 1999. Analytical Biochemistry, 267, 114-120.

[37] K Ye, J S Schultz. Genetic engineering of an allostrically based glucose indicator protein for continuous glucose monitoring by fluorescence resonance energy transfer. 2004. Analytical Chemistry, 75, 3451-3459.

[38] J D Newman, A P F Turner. 2004. Biosensors for Monitoring Glucose, Sensors in Medicine and Health Care, Wiley-VCH Verlag GmbH & Co. KGaA, Weinheim.

[39] G S Wilson, Y Hu. Enzyme-Based Biosensors for *in vivo* Measurements. 2000. Chemical Reviews, 100, 2693-2704.

[40] R Wilson, A P F Turner. Glucose oxidase: an ideal enzyme. 1992. Biosensors and Bielectronics, 7, 165-185.

[41] S D'Auria, P Herman, M Rossi, J R Lakowicz. The fluorescence emission of the apo-glucose oxidase from *Aspergillus niger* as probe to estimate glucose concentrations. 1999. Biochemical and Biophysical Research Communications, 263, 550-553.

[42] S D'Auria, N Di Cesare, Z Gryczynski, M Gryczynski, M Rossi, J R Lakowicz. A thermophilic apoglucose dehydrogenase as non consuming glucose sensor. 2000. Biochemical and Biophysical Research Communications, 274, 727-731.

[43] H Xu, J W Aylott, R Kopelman. Fluorescent nano-PEBBLE sensors designed for intracellular glucose imaging. 2002. Analyst, 41, 1471-1477.

[44] S W Klang, J W Kuan, S S Kuan, G G Guilbaut. Measurement of glucose in plasma, with use of immobilized glucose oxidase and peroxidase. 1976. Clinical Chemistry, 22, 1378-1382.

[45] V Sanz, J Galban, S de Marcos, J R Castillo. Fluorometric sensors based on chemically modified enzymes: Glucose determination in drinks. 2003. Talanta, 60, 415-423.

[46] G N Reeke, J W Becker, G M Edelman. The covalent and three-dimensional structure of Concanavalin A. 1975. J Biological Chemistry, 250, 1525-1547.

[47] S.Mansouri, J.S.Schultz. A miniature optical glucose sensor based on affinity binding. 1984. Biotechnology, 885-890.

[48] J.S.Schultz, G.Sims. Affinity sensors for individual metabolites. 1979. Biotechnology and Bioengineering Symposium, 9, 65-71.

[49] D.L.Meadows, J.S.Schultz. Miniature fiber optic sensor based on fluorescence energy transfer. 1992. Proceedings of the SPIE, 1648, 202-211.

[50] D.L.Meadows, J.S.Schultz. Design, manufacture and characterization of an optical fiber glucose affinity sensor based on an homogeneous fluorescence energy transfer assay system. 1993. Analytica Chimica Acta, 280, 21-30, 1993.

[51] R.Ballerstadt, J.S.Schultz. Competitive-binding assay method based on fluorescence quenching of ligands held in close proximity by a multivalent receptor. 1993. Analytica Chimica Acta, 345, 203-207.

[52] L.Tolosa, H.Szmacinski, G.Rao, J.R.Lakowicz. Lifetime-Based Sensing of Glucose Using Energy Transfer with a Long Lifetime Donor. 1997. Analytical Biochemistry, 250, 102-108.

[53] L.Tolosa, H. Malak, G.Rao, J.R.Lakowicz. Optical assay for glucose based on the luminescnence decay time of the long wavelength dye Cy5™. 1997. Sensors and Actuators B, 45, 93-99.

[54] J.R.Lakowicz, B.Maliwal. Optical sensing of glucose using phase-modulation fluorimetry. 1993. Analytica Chimica Acta, 271, 155-164.

[55] O.J.Rolinski, D.J.S.Birch, L.McCartney, J.C.Pickup. Molecular distribution sensing in a fluorescence resonance energy transfer based affinity assay for glucose. 2001. Spectrochimica Acta - Part A: Molecular and Biomolecular Spectroscopy. 57, 11, 2245-2254.

[56] D.J.S.Birch, O.J.Rolinski. Fluorescence resonance energy transfer sensors. 2001. Resources Chemical Intermediates, 27, 425-446.

[57] O J Rolinski, D J S Birch, L J McCartney, J C Pickup. Fluorescence resonance energy transfer from allophycocyanin to malachite green. 1999. Chemical Physics Letters, 309, 395-401.

[58] O J Rolinski, D J S Birch, J L McCartney, J C Pickup. A time resolved near infrared fluorescence assay for glucose: opportunities for transdermal sensing. 2000a. Journal of Photochemistry and Photobiology, B 54, 26-34.

[59] B.L.Ibey, M.A.Meledeo, V. A.Gant, V.Yadavalli, M.V.Pishko, G.L.Cote. *In vivo* monitoring of blood glucose using poly(ethylene glycol) microspheres. 2003. Proceeding of SPIE, 4965, 1-6.

[60] S Chinnayelka, M J McShane. Glucose-Sensitive Nanoassemblies Comprising Affinity-Binding Complexes Trapped in Fuzzy Microshells. 2004. Journal of Fluorescence, 14, 585-595.

[61] S Chinnayelka, M J McShane. Resonance Energy Transfer Nanobiosensors Based on Affinity Binding between Apo-Enzyme and it Substrate. 2004. Biomacromolecules, 5, 1657-1661.

[62] W S J Bennet, T A Steitz. Structure of the complex between yeast hexokinase and glucose: Structure determination and refinement at 3.5°A resolution. 1980. Journal of Molecular Biology, 140, 183-209.

[63] R C McDonald, T A Steitz, D M Engelman. Yeast hexokinase in solution exhibits a large conformational change upon binding glucose or glucose 6-phosphate. 1979. Biochemistry, 18, 338-342.

[64] F. Hussain, D. J. S. Birch, J. C. Pickup. Glucose sensing based on the intrinsic fluorescence of sol-gel immobilized yeast hexokinase. 2005. Analytical Biochemistry, in press.

[65] W C W Chan, D J Maxwell, X Gao, R E Bailey, M Han, S Nie. Luminescent quantum dots for multiplexed biological detection. 2002. Current Opinions in Biotechnology, 13, 40-46.

[66] C Batich, F Vaghefi. Process for Microencapsulating Cells, US Patent # 6242230 B1, Jun 5 2001.

[67] S Slomkowski, T Basinska, B Miksa. New Types of Microspheres and Microsphere-related Materials for Medical Diagnostics. 2002. Polymers for Advanced Technologies, 13, 906-918.

[68] W R Gombotz, S F Wee. Protein release from alginate matrices. 1998. Advanced Drug Delivery Reviews, 31, 267-285

[69] J G Garces. Microcapsules and Processes for making the same using various polymers and chitosans, US Patent # 6733790 B1, May 11, 2004.

[70] M N V Ravi Kumar. Nano and Microparticles as Controlled Drug Delivery Devices. 2000. Journal of Pharmacy and Pharmaceutical Sciences, 3, 234-258.

[71] C Perez, I C Castellanos, H R Constantino, W Al-Azzam, K Griebenow. Recent trends in stabilizing protein structure upon encapsulation and release from bioerodible polymers. 2002. Journal of Pharmacy and Pharmacology, 54, 301-313.

[72] S Zhou, X Deng, M Yuan, X Li. Investigation on Preparation and Protein Release of Biodegradable Polymer Microspheres as Drug-Delivery System. 2002. Journal of Applied Polymer Science, 84, 778-784.

[73] S Wang, M Yoshimoto, K Fukunaga, K Nakao. Optimal Covalent Immobilization of Glucose Oxidase-Containing Liposomes for Highly Stable Biocatalyst in Bioreactor. 2003. Biotechnology and Bioengineering, 83, 444-453.

[74] E M D'Urso, G Fortier. Albumin-poly(ethylene glycol) hydrogel as matrix for enzyme immobilization: Biochemical characterization of crosslinked acid phosphatase. 1996. Enzyme and Microbial Technology, 18, 482-488.

[75] Q Hussain, J Iqbal, M Saleemuddin. Entrapment of Concanavalin A-Glycoenzyme Complexes in Calcium Alginate Gels. 1985. Biotechnology and Bioengineering. 27, 1102-1107.

[76] W K Chui, L S C Wan. Prolonged retention of crosslinked trypsin in calcium alginate microspheres. 1997. Journal of Microencapsulation, 14, 51-61.

[77] Y M Lvov. Thin Film Nanofabrication by Alternate Adsorption of Polyions, Nanoparticles, and Proteins. 2003. Handbook of Surfaces and Interfaces of Materials, edited by H S Nalwa, Volume 3: Nanostructured Materials, Micelles and Colloids. Academic Press.

[78] K Sankaran, S S Godbole, S F D'Souza. Preparation of spray-dried, sugar-free egg powder using glucose oxidase and catalase coimmobilized on cotton cloth. 1989. Enzyme and Microbial Technology, 11, 617-619.

[79] J W Vanderhoff, C X Lu, C C Lee, C-Chun Tsai. Process for the Preparation of Aqueous Dispersions of Particles of Water Soluble Polymers and the Particles Obtained, US Patent # 6214331 B1, Apr 10, 2001.

[80] O Smidsrod, G Skjak-Braek. Alginate as immobilization matrix for cells. 1990. TIBTECH, 8, 71-77.

[81] A Kikuchi, M Kawabuchi, M Sugihara, Y Sakurai, T Okano. Pulsed Dextran release from calcium-alginate gel beads. 1997. Journal of Controlled Release, 47, 21-29.

[82] B L Strand, O Gaserod, B Kulseng, T Espevik, G Skjak Braek. Alginate-polylysine-alginate microcapsules: effect of size reduction on capsule properties. 2002. Journal of Microencapsulation. 19, 615-630.

[83] B Thu, P Bruheim, T Espevik, O Smidsrod, P Soon-Shiong, G Skhak-Braek. Alginate polycation microcapsules I. Interaction between alginate and polycation. 1996. Biomaterials, 17, 1031-1040.

[84] O Gaserod, A Sanned, G Skjak-Braek. Microcapsules of alginate-chitosan II. A study of capsule stability and permeability. 1999. Biomaterials, 20, 773-783.

[85] Lin-Shu Liu, Shu-Qin Liu, S Y Ng, M Froix, T Ohno, J Heller. Controlled release of interleukin-2 for tumour immunotherapy using alginate/chitosan porous microspheres. 1997. Journal of Controlled Release, 43, 65-74.

[86] B Amsden, N Turner. Diffusion Characteristics of Calcium Alginate Gels. 1999. Biotechnology and Bioengineering. 65, 605-610.

[87] G Decher, J D Hong and J Schmitt. Buildup of ultrathin multilayer films by a self-assembly process: III. Consecutively alternating adsorption of anionic and cationic polyelectrolytes on charged surfaces. 1992. Thin Solid Films, 210, 831-835.

[88] G B Sukhorukov, E Donath, S Davis, H Lichtenfield, F Caruso, V I Popov, and H Mohwald. Stepwise Polyelectrolyte Assembly on Particle Surfaces: a Novel Approach to Colloid Design. 1998. Polymer Advanced Techniques, 9, 759-767.

[89] F Lim, A M Sun. Microencapsulated islets as bioartificial endocrine pancreas. 1980. Science, 210, 908-910.

[90] P Aslani, R A Kennedy. Studies on diffusion in alginate gels. I. Effects of crosslinking with calcium or zinc ions on diffusion of acetaminophen. 1996. Journal of Controlled Release, 42, 75-82.

[91] M Kierstan, C Bucke. The immobilization of Microbial Cells, Subcellular Organelles, and Enzymes in Calcium Alginate Gels. 1997. Biotechnology and Bioengineering 19, 387-397.

[92] F A Goosen, G O'Shea, G Gharapetian, S Chou, and A Sun. Optimization of microencapsulation parameters: Semi permeable microcapsules as a bioartificial pancreas. 1985. Biotechnology and Bioengineering, 27, 146-150.

[93] D S Seifert, J A Phillips. Production of small monodispersed alginate beads for cell immobilization. 1997. Biotechnology Progress, 13, 562-568.

[94] L S C Wan, P W S Heng, L W Chan. Drug encapsulation in alginate microspheres by emulsification. 1992. Journal of Microencapsulation, 9, 309-316.

[95] L S C Wan, P W S Heng, L W Chen. Surfactant effects on alginate microspheres. 1994. International Journal of Pharmaceutics, 103, 267-275.

[96] L S C Wan, P W S Heng, L W Chen. Influence of hydrophile-lipophile balance on alginate microspheres. 1993. International Journal of Pharmaceutics, 95, 77-83.

[97] L W Chan, P W S Heng. Effect of aldehydes and methods of cross-linking on properties of calcium alginate microspheres prepared by emulsification. 2002. Biomaterials, 23, 1319-1326.

[98] P W S Heng, L S C Wan, T W Wong. Formation of alginate microspheres produced using emulsification techniques. 2003. Journal of Microencapsulation, 20, 401-414.

[99] L W Chan, L T Lim, P W S Heng. Microencapsulation of oils using sodium alginate. 2000. Journal of Microencapsulation, 17, 757-766.

[100] P W Heng, L W Chan, C V Liew, T Y Ng. Effect of tabletting compaction pressure on alginate microspheres. 2000. Journal of Microencapsulation, 17, 553-564.

[101] K Landfester, M Antonietti. 2003. Colloids and Colloid Assemblies, Edited by Frank Caruso, Wiley-VCH Verlag GmbH and Co. KGaA, Weinheim, Germany.

[102] R Razdan, P V Devarajan. Microemulsions – A review. 2003. Indian Drugs, 40, 139-146.

[103] L W Chan, P W S Heng, L S C Wan. Effect of cellulose derivatives on alginate microspheres prepared by emulsification. 1997. Journal of Microencapsulation, 14, 409-420.

[104] L W Chan, P W S Heng. Effects of poly(vinylyrrolidone) and ethyl cellulose on alginate microspheres prepared by emulsification. 1998. Journal of Microencapsulation, 15, 545-555.

[105] D Lemoine, F Wauters, S Bouchend'homme, V Preat. Preparation and characterization of alginate microspheres containing a model antigen. 1998. International Journal of Pharmaceutics, 176, 9-19.

[106] D Poncelet, R Lencki, C Beaullieu, J P Halle, R J Neufeld, A Fournier. Production of alginate beads by emulsification/internal gelation. I. Methodology. 1992. Applied Microbiology and Biotechnology, 38, 39-45.

[107] D Poncelet, B Poncelet De Smet, C Beaullieu, M L Huguet, A Fournier, R J Neufeld. Production of alginate beads by emulsification/internal gelation. II. Physiochemistry. 1995. Applied Microbiology and Biotechnology, 43, 644-650.

[108] L W Chan, H Y Lee, P W S Heng. Production of alginate microspheres by internal gelation using an emulsification technique. 2002. International Journal of Pharmaceutics, 242, 259-262.

[109] G Fundueanu, C Nastruzzi, A Carpov, J Desbrieres, M Rinaudo. Physico-chemical characterization of Ca-alginate microparticles produced with different methods. 1999. Biomaterials, 20, 1427-1435.

[110] C Charcosset, I Limayem, H Fessi. The membrane emulsification process – a review. 2004. Journal of Chemical Technology and Biotechnology. 79, 209-218.

[111] J-O You, S-B Park, H-Y Park, S Haam, C-H Chung, W-S Kim. Preparation of regular sized Ca-alginate microspheres using membrane emulsification method. 2001. Journal of Microencapsulation, 18, 521-532.

[112] S Sugiura, M Nakajima, J Tong, H Nabetani, M Seki. Preparation of monodispersed solid lipid microspheres using a microchannel emulsification technique. 2000. Journal of Colloid and Interface Science, 227, 95-103.

[113] S Sugiura, M Nakajima, S Iwamoto, M Seki. Interfacial tension driven monodispersed droplet formation from microfabricated channel array. 2001. Langmuir, 17, 5562-5566.

[114] S Sugiura, M Nakajima, M Seki. Effect of channel structure on microchannel emulsification. 2002. Langmuir, 18, 5708-5712.

[115] S Sugiura, M Nakajima, M Seki. Prediction of droplet diameter for microchannel emulsification. 2002. Langmuir, 18, 3854-3859.

[116] S Sugiura, M Nakajima, M Seki. Preparation of monodispersed polymeric microspheres over 50μm employing microchannel emulsification. 2002. Industrial Engineering and Chemical Research, 41, 4043-4047.

[117] S Sugiura, T Oda, Y Izumida, Y Aoyagi, M Satake, A Ochiai, N Ohkohchi, M Nakajima. Size control of calcium alginate beads containing living cells using micro-nozzle array. 2005. Biomaterials, 26, 3327-3331.

[118] J F Liang, Y T Li, V C Yang. Biomedical application of immobilized enzymes. 2000. Journal of Pharmaceutical Sciences, 89, 979-990.

[119] E Taqieddin, M Amiji. Enzyme immobilization in novel alginate-chitosan core shell microcapsules. 2004. Biomaterials, 25, 1937-1945.

[120] J E Gregor, E Fenton, G Brokenshire, P Van Den Brink, B O'Sullivan. Interactions of Calcium and Aluminum ions with Alginate. 1996. Water Research, 30, 1319-1324.

[121] L W Chan, Y Jin and P W S Heng. Cross-linking mechanisms of calcium and zinc in production of alginate microspheres. 2002. International Journal of Pharmaceutics, 242, 255-258.

[122] A Blandino, M Macias, D Cantero. Immobilization of glucose oxidase within calcium alginate gel capsules. 2001. Process Biochemistry, 36, 601-606.

[123] A Blandino, M Macias, D Cantero. Glucose oxidase release from calcium alginate gel capsules. 2000. Enzyme and Microbial Technology, 27, 319-324.

[124] A Blandino, M Macias, D Cantero. Formation of calcium alginate gel capsules: Influence of sodium alginate and $CaCl_2$ concentration on gelation kinetics. 1999. Journal of Bioscience and Bioengineering, 88, 686-689.

[125] A Dashevsky. Protein loss by microencapsulation of an enzyme (lactase) in alginate beads. 1998. International Journal of Pharmaceutics, 161, 1-5.

[126] A R DeGroot, R J Neufeld. Encapsulation of urease in alginate beads and protection from a-chymotrypsin with chitosan membranes. 2001. Enzyme and Microbial Technology, 29, 321-327.

[127] A Blandino, M Macias, D Cantero. Calcium alginate gel as encapsulation matrix for coimmobilized enzyme systems. 2003. Applied Biochemistry and Biotechnology, 110, 53-60.

[128] G Coppi, V Iannuccelli, E Leo, M T Bernabei, R Cameroni. Protein immobilization in crosslinked alginate microparticles. 2002. Journal of Microencapsulation, 19, 37-44.

[129] L Zhang, J Guo, X Peng, Y Jin. Preparation and release behavior of carboxymethylated chitosan/alginate microspheres encapsulating BSA. 2004. Journal of Applied Polymer Science, 92, 878-882.

[130] H Tanaka, M Matsumura, I A Veliky. Diffusion characteristics of substrates in Ca-alginate gel beads. 1984. Biotechnology and Bioengineering, 26, 53-58.

[131] E Favre, M Leonard, A Laurent, E Dellacherie. Diffusion of polyethylene glycols in calcium alginate hydrogels. 2001. Colloids and Surfaces A: Physiochemical and Engineering Aspects, 194, 197-206.

[132] A Martinsen, I Storro, G Skjak-Braek. Alginate as Immobilization Material III. Diffusional Properties. 1992. Biotechnology and Bioengineering, 39, 186-194.

[133] A Kikuchi, M Kawabuchi, A Watanabe, M Sugihara, Y Sakurai, T Okano. Effect of Ca^{+2}-alginate gel dissolution on release of dextran with different molecular weights. 1999. Journal of Controlled Release, 58, 21-28.

[134] R M Iskakov, A Kikuchi, T Okano. Time-programmed pulsatile release of dextran from calcium alginate gel beads coated with carboxy-n-propylacrylamide copolymers. 2002. Journal of Controlled Release, 80, 57-68.

[135] P de Vos, B De Haan and R Van Schilfgaarde. Effect of the alginate composition on the biocompatibility of alginate-polylysine microcapsules. 1997. Biomaterials, 18, 273-278.

[136] R Robitaille, J-Francois Pariseau, F A Leblond, M Lamoureux, Y Lepage, J-Pierre Halle. Studies on small (<350μm) alginate-poly-l-lysine mirocapsules III. Biocompatibility of smaller versus standard microcapsules. 1999. Journal of Biomedical Materials Research, 44, 116-120.

[137] P de Vos, C G Hoogmoed, H J Busscher. Chemistry and biocompatibility of alginate-PLL capsules for immunoprotection of mammalian cells. 2002. Journal of Biomedical Materials Research, 60, 252-259.

[138] P Rilling, T Walter, R Pommersheim, W Vogt. Encapsulation of cytochrome C by multilayer microcapsules. A model for improved enzyme immobilization. 1997. Journal of Membrane Science, 129, 283-287

[139] A Gaumann, M Laudes, B Jacob, R Pommersheim, C Laue, W Vogt, J Schrezenmeir. Effect of media composition on long term *in vitro* stability of barium alginate and polyacrylic acid multilayers. 2000. Biomaterials, 21, 1911-1917.

[140] S Schneider, P J Feilen, V Slotty, D Kampfner, S Preuss, S Berger, J Beyer, R Pommersheim. Multilayer capsules: a promising microencapsulation system for transplantation of pancreatic islets. 2001. Biomaterials, 22, 1961-1970.

[141] R Pommersheim, J Schrezenmeir. Immobilization of enzymes by multilayer microcapsules. 1994. Macromolecular Chemical Physics, 195, 1557-1567.

[142] A Gaumann, M Laudes, B Jacob, R Pommersheim, C Laue, W Vogt, J Schrezenmeir. Xenotransplantation of parathyroids in rats using Barium Alginate and polyacrylic acid multilayer microcapsules. 2001. Experience in Toxicology and Pathology, 53, 35-43.

[143] S Leporatti, A Voigt, R Mitlohner, E Donath, H Mohwald, G Sukhorukov. Scanning Force Microscopy Investigation of Polyelectrolyte Nano- and Microcapsule Wall Texture. 2000. Langmuir, 16, 4059-4063.

[144] J Chen, L Huang, L Ying, G Luo, X Zhao, W Cao. Self-Assembly ultrathin films based on diazoresins. 1999. Langmuir, 15, 7208-7212.

[145] T Cao, L Wei, S Yang, M Zhang, C Huang, W Cao. Self-Assembly and Photovoltaic Property of Covalent-Attached Multilayer Film Based on Highly Sulfonated Polyaniline and Diazoresin. 2002. Langmuir, 18, 750-753.

[146] J Sun, T Wu, B Zou, X Zhang, J Shen. Stable Entrapment of Small Molecules Bearing Sulfonate Groups in Multilayer Assemblies. 2001. Langmuir, 17, 4035-4041.

[147] P Y Vuillaume, M A Jonas, A Laschewsky. Ordered Polyelectrolyte "Multilayers". 5. Photo-Cross-Linking of Hybrid Films Containing an Unsaturated and Hydrophobized Poly(diallylammonium) Salt and Exfoliated Clay. 2002. Macromolecules, 35, 5004-5012.

[148] J J Harris, P M DeRose, M L Bruening. Synthesis of passivating, nylon like coatings through cross-linking of ultrathin polyelectrolyte films. 1999. Journal of Americal Chemical Society, 121, 1978-1979.

[149] J Dai, A W Jenson, D K Mohanty, J Erndt, M L Bruening. Controlling the permeability of multilayered polyelectrolyte films through derivatization, cross-linking, and hydrolysis. 2001. Langmuir, 17, 931-937

[150] B J Lee, T Kunitake. Two-Dimensional Polymer Networks of Maleic Acid Copolymers and Poly(allylamine) by the Langmuir-Blodgett Technique. 1994. Langmuir, 10, 557-562.

[151] D Beyer, T M Bohanon, W Knoll, H Ringsdorf. Surface Modification via Reactive Polymer Interlayers. 1996. Langmuir, 12, 2514-2518.

[152] M J McShane, J Q Brown, K B Guice, Y M Lvov. Polyelectrolyte microshells as carriers for fluorescent sensors: Loading and sensing properties of a Ruthenium-based oxygen sensor. 2002. Journal of Nanoscience and Nanotechnology, 2, 1-6.

[153] J Q Brown, R Srivastava,M J McShane. Encapsulation of glucose oxidase and an oxygen-quenched fluorophore in polyelectrolyte-coated calcium alginate microspheres as optical glucose sensor systems. 2005. Biosensors and Bioelectronics, in press.

[154] N Wisniewski, W M Reichert. Methods for reducing biosensor membrane biofouling. 2000. Colloids and Surfaces B, 18,197-219.

[155] N Wisniewski, F Moussy, W M Reichert. Characterization of implantable biosensor membrane biofouling. 2000. Journal of Analytical Chemistry, 366, 611-621.

[156] M H Schoenfisch, K A Mowery, M V Rader, N Baliga, J A Wahr, M E Meyerhoff. 2000. Analytical Chemistry, 72, 1119-1126.

[157] Y Murata, E Miyamoto, S Kawashima. Additive effect of chondroitin sulfate and chitosan on drug release from calcium induced alginate gel beads. 1996. Journal of Controlled Release, 38, 101-108.

[158] C Lee, I Chu. Characterization of modified alginate-poly-l-lyisne microcapsules. 1997. Artificial Organs, 21, 1002-1006.

[159] C Picart, J Mutterer, L Richert, Y Luo, G D Prestwich, P Schaaf, J C Voegel, P Lavalle. Molecular basis for the explanation of the exponential growth of polyelectrolyte multilayers. 2002. Proceedings of the National Academy of Science. 99, 12531-34.

[160] L Richert, P Lavalle, E Payan, X S Zheng, G D Prestwich, J F Stoltz, P Schaaf, J -C Voegel, C Picart. Layer by Layer Buildup of Polysaccharide Films: Physical Chemistry and Cellular Adhesion Aspects. 2004. Langmuir, 20, 448-452.

[161] F Boulmedais, V Ball, P Schwinte, B Frisch, P Schaaf, J -C Voegel. Buildup of Exponentially Growing Multilayer Polypeptide Films with Internal Secondary Structure. 2003. Langmuir, 19, 440-444.

[162] P Lavalle, C Gergely, J F G Cuisinier, G Decher, P Schaaf, J –C Voegel, C Picart. Comparison of the Structure of Polyelectrolyte Multilayer Films Exhibiting a Linear and an Exponential Growth Regime: An in Situ Atomic Force Microscopy Study. 2002. Macromolecules, 35, 4458-4464.

[163] F Boulmedais, M Bozonnet, P Schwinté, J -C Voegel, P Schaaf. Multilayered Polypeptide Films: Secondary Structures and Effect of Various Stresses. 2003. Langmuir, 19, 9873-9882.

[164] K Y Lee, D J Mooney. Hydrogels for Tissue Engineering. 2001. Chemical Reviews, 101, 1869 -1880.

[165] E Brynda, M Houska. Multiple alternating molecular layers of albumin and heparin on solid surfaces of medical devices. 1996. Journal of Colloids and Interface Science, 183, 18-24.

[166] J M Harris. 1992. Poly(ethylene glycol) Chemistry: Biotechnical and Biomedical Applications; Ed.; Plenum: New York,

[167] M L Huguet, R J Neufeld, E Dellacherie. Calcium alginate beads coated with polycationic polymers; Comparison of chitosan and DEAE-Dextran. 1996. Process Biochemistry, 31, 347-353.

[168] J D Mendelsohn, S Y Yang, J A Hiller, A I Hochbaum, M F Rubner. Rational design of cytophilic and cytophobic polyelectrolyte multilayer thin films. 2003. Biomacromolecules, 4, 96-106.

[169] L Richert, Ph Lavalle, D Vautier, B Senger, J.-F Stolz, P Schaaf, J.-C Voegel, C Picart. Cell interactions with polyelectrolyte multilayer films. 2002. Biomacromolecules, 3, 1170-1178.

[170] L Richert, F Boulmedais, Ph Lavalle, J Mutterer, E Ferreux, G Decher, P Schaaf, J.-C Voegel, C Picart. Improvement of stability and cell adhesion properties of polyelectrolyte multilayer films by chemical crosslinking. 2004. Biomacromolecules, 5, 284-294.

[171] M L Amirpour, P Ghosh, W M Lackowski, R M Crooks, M V Pishko. 2001. Analytical Chemistry, 73, 1560-1566.

[172] N P Huang, R Michel, J Voros, M Textor, R Hofer, A Rossi, D L Elbert, J A Hubbel, N D Spencer. Poly(L-lysine)-g-poly(ethylene glycol) layers on metal oxide surfaces: Surface-Analytical characterization and resistance to serum and fibrinogen adsorption. 2001. Langmuir, 17, 489-498.

[173] J-Ping Chen, I-Ming Chu, M-Yi Shiao, B R-Sea Hsu, S-Huei Fu. Microencapsulation of islets in PEG-Amine modified alginate-PLL-alginate microcapsules for constructing bioartificial pancreas. 1998. Journal of Fermentation and Bioengineering, 86, 185-190.

[174] A S Sawhney, C P Pathak, J A Hubbel. Interfacial photopolymerization of poly(ethylene glycol)-based hydrogels upon alginate-poly(l-lysine) microcapsules for enhanced biocompatibility. 1993. Biomaterials, 14, 1008-1016.

[175] A S Sawhney, J A Hubbel. Poly(ethylene oxide)-graft-poly(L-lysine) copolymers to enhance the biocompatibility of poly(L-lysine)-alginate microcapsules membranes. 1992. Biomaterials, 13, 863-870.

[176] P de Vos, C G Van Hoogmoed, B J De Haan, H J Busscher. Tissue responses against immunoisolating alginate-PLL capsules in the immediate posttransplant period. 2002. Journal of Biomedical Materials Research, 62, 430-437.

[177] C M Bunger, B Tiefenbach, A Jahnke, C Gerlach, Th Freier, K P Schmitz, U T Hopt, W Schareck, E Klar, P de Vos. Deletion of the tissue response against alginate-pll capsules by temporary release of co-encapsulated steroids. 2005. Biomaterials, in press.

[178] C D Scott, C A Woodward, J E Thompson. Solute diffusion in biocatalyst gel beads containing biocatalysts and other additives. 1989. Enzyme and Microbial Technology, 11, 258-263.

[179] Y Chai, L-He Mei, D-Qiang Lin, S-Jing Yao. Diffusion coefficients in intrahollow calcium alginate microcapsules. 2004. Journal of Chemical Engineering Data. 49, 475-478.

[180] R P Haugland. 2003. Handbook of Fluorescence Probes and Research Products. Molecular Probes Handbook. Ninth Edition: 11-13.

[181] G L Peterson. A simplification of the protein assay method of Lowry et al. which is more generally applicable. 1977. Analytical Biochemistry, 83, 346-356.

[182] K Andrieux, P Lesieur, S Lesieur, M Ollivon, C Grabielle-Madelmont. Characterization of Fluorescein Isothiocyanate-Dextrans used in Vesicle Permeability Studies. 2002. Analytical Chemistry, 74, 5217-5226.

[183] R A McAloney, M Sinyor, V Dudnik, M C Goh. Atomic force microscopy studies of salt effects on polyelectrolyte multilayer film morphology. 2001. Langmuir, 17, 6655-6663.

[184] H Zhu, R Srivastava, M J McShane. Spontaneous loading of positively charged macromolecules into alginate templated polyelectrolyte multilayer capsules. 2005. accepted in Biomacromolecules.

[185] S Leporatti, AVoigt, R Mitlohner, E Donath, M Mohwald, G Sukhorukov. Scanning Force Microscopy Investigation of Polyelectrolyte Nano- and Microcapsule Wall Texture. 2000. Langmuir, 16, 4059-4063.

[186] C Lee, I Chu. Characterization of modified alginate-poly-l-lysine microcapsules. 1997. Artificial Organs 21, 1002-1006.

[187] G T Hermanson. Bioconjugate techniques, G T Hermanson Ed.; Academic Press: San Diego 169-176, 1996.

[188] S Sugawara, T Imai, M Otagiri. The controlled release of prednisolone using alginate gel. 1994. Pharmaceutical Research, 11, 272–277.

[189] S Shiraishi, T Imai, M Otagiri. Controlled-release preparation of indomethacin using calcium alginate gel. 1993. Biological and Pharmaceutical Bulletin, 16, 1164–1168.

[190] D Kovacevic, S van der Burgh, A de Keizer, M A Stuart Cohen. Specific ionic effects on weak polyelectrolyte multilayer formation. 2003. Journal of Physical Chemistry B, 107, 7998-8002.

[191] J Shen, J Sun, T Wu, F Liu, Z Wang, X Zhang. Covalently Attached Multilayer Assemblies by Sequential Adsorption of Polycationic Diazo-Resins and Polyanionic Poly(acrylic acid). 2000. Langmuir, 16, 4620-4624.

[192] H Zhu, M J McShane. Macromolecule Encapsulation in Diazoresin-Based Hollow Polyelectrolyte Microcapsules. 2005. Langmuir, 21, 424-430.

[193] G B Sukhorukov, E Donath, H Lichtenfeld, E Knippel, M Knippel, A Budde, H Möhwald. Layer-by-layer self assembly of polyelectrolytes on colloidal particles. 1998. Colloids and Surfaces A: Physicochemical and Engineering Aspects, 137, 253-266.

[194] http://chem.ch.huji.ac.il/~eugeniik/edc.htm

[195] Y W Cho, Y N Cho, S H Chung, G Yoo, S W Ko. Water-soluble chitin as a wound healing accelerator. 1999. Biomaterials, 20, 2139-2145.

[196] J K F Suh, H W T Matthew. Porous chitosan scaffolds for tissue engineering. 1999. Biomaterials, 20, 1133-1142.

[197] T A Becker, D A Kipke, T Brandon. Calcium alginate gel: A biocompatible and mechanically stable polymer for endovascular embolization. 2001. Journal of Biomedical Materials Research, 54, 76-86.

[198] J H Lee, H B Lee, J D Andrade. Blood compatibility of polyethylene oxide surfaces. 1995. Progress in Polymer Science, 20, 1043-47.

[199] S Mizuguchi, T Uyama, H Kitagawa, K H Nomura, K Dejima, K Gengyo-Ando, S Nitani, K Sugahara, K Nomura. Chondroitin proteoglycans are involved in cell division of Caenorhabditis elegans. 2003. Nature, 423, 443-448.

[200] J Drobnik. Hyaluronan in drug delivery. 1991. Advanced Drug Delivery Reviews, 1991, 7, 295-308.

[201] J E Scott. Collagen-proteoglycan interactions. Localization of proteoglycans in tendon by electron microscopy. 1980. Biochemical Journal, 187, 887-891.

[202] http://www.dextran.dk

[203] I Galeska, T Hickey, F Moussy, D Kreutzer, F Papadimitrakopoulos. Characterization and Biocompatibility Studies of Novel Humic Acids Based Films as Membrane Material for an Implantable Glucose Sensor. 2001. Biomacromolecules, 2, 1249-1255.